Insights into function of transcription factor Ap-2δ: target genes and interaction partners

Thesis

Submitted for a Doctoral Degree
in Natural Sciences (Dr. rer. nat.) to the
Faculty of Mathematics and Natural Sciences
Rheinische Friedrich-Wilhelms-University of Bonn

Submitted by

Katrin Hesse

from

Attendorn

Bonn, July 2011

With authorization of the Faculty of Mathematics and Natural Sciences of the Rheinische Friedrich-Wilhelms-University of Bonn

The study presented here was conducted at the Institute of Pathology of the University Hospital Bonn.

First Referee (Thesis Advisor):	Prof. Dr. Reinhard Büttner
Second Referee:	Prof. Dr. Michael Hoch
Third Referee:	Prof. Dr. Hubert Schorle
Fourth Referee:	PD Dr. Gerhild van Echten-Deckert

PhD defense: December 21, 2011

Year of publication: 2012

Declaration

I solemnly declare that the work submitted here is the result of my own investigation, except where otherwise stated. This work has not been submitted to any other university or institute towards the partial fulfillment of any degree.

Katrin Hesse; Author

Summary

The Ap-2 transcription factors comprise a family of closely-related sequence-specific DNA-binding proteins that play pivotal and non-redundant roles in regulating gene expression during development, differentiation, and tumorigenesis. In mammals, five members of the Ap-2 family have been identified (Ap-2α-ε). The Ap-2 family members share a highly conserved basic DNA-binding domain and a carboxy-terminal helix-span-helix motif mediating DNA binding and dimerization. The N-terminus is more divergent although certain critical residues in the transactivation domain are conserved. Ap-2δ is considered the most divergent family member because within its transactivation domain Ap-2δ lacks those critical amino acids that are important for transcriptional activity suggesting that Ap-2δ may interact with a different set of coactivators and target genes.

According to the restricted Ap-2δ expression in posterior and dorsal midbrain, Ap-2δ knockout mice exhibited enhanced apoptotic cell death in the posterior midbrain resulting in the complete loss of this structure at the newborn state. Affimetrix GeneChip technology on RNA from posterior midbrains of wildtype and Ap-2δ-deficient mice was employed to identify de novo Ap-2δ targets from the posterior midbrain region. The set of potential candidates enclosed the transcription factors Pitx2, Mef2c, Bhlhb4 and Pou4f3. Moreover, in a luciferase reporter assay, Ap-2δ positively mediated activation of the *Bhlhb4* and *Pou4f3* promoters. This study also revealed that Ap-2δ specifically binds to regulatory sites located in the promoter regions of the *Bhlhb4* and *Pou4f3* genomic loci. Electrophoretic mobility shift assays (EMSA) confirmed the direct binding of Ap-2δ to an Ap-2δ-specific consensus sequence within the *Pou4f3* promoter. Consistently, Ap-2δ occupied the promoters of *Pou4f3* and *Bhlhb4* also *in vivo* as demonstrated with chromatin immunoprecipitation (ChIP) assays, identifying these genes as direct targets of Ap-2δ. In addition, Ap-2δ

ablation resulted in the downregulation of known Pou4f3 target genes in the posterior midbrain. In summary, the data presented here denote the regulatory activity of Ap-2δ on midbrain-expressed transcription factors as essential for the development of the posterior midbrain.

In the second part of this study, the transcription factor Nfatc2 was identified as a new binding partner for Ap-2δ using a yeast-two hybrid assay. Nfatc2 is a widely expressed, calcium-regulated transcription factor and a key mediator of gene transcription. The interaction of Nfatc2 with Ap-2δ was confirmed in *in vitro* GST pulldown assays. Co-immunoprecipitations were used to establish an interaction in mammalian cells. Furthermore, both transcription factors co-localized in the nucleus after activation of Nfatc2. Quantitative real-time PCR was employed to analyze the synergistical action of Nfatc2 and Ap-2δ on downstream targets. The newly identified targets *Atm*, *Egr3*, and *Mtss1* were found to be downregulated after overexpression of Ap-2δ and ectopic expression of Nfatc2 in Neuro2a cells. Consistently, downregulation of *Tcfap2d* by siRNA increased transcript levels of these targets indicating for the first time that Ap-2δ also exerts a repressive function. Using ChIP assays, *Atm*, *Egr3*, and *Mtss1* were identified as direct targets because Ap-2δ and Nfatc2 occupied the promoter of these genes. Taken together, this work demonstrates that Ap-2δ together with Nfatc2 can function as a transcriptional repressor and plays an important role in the synergistical regulation of neuronal gene expression.

Table of contents

List of abbreviations

Ap-2	activating enhancer binding protein-2
APS	ammoniumperoxodisulfate
Atm	ataxia-telangiectasia mutated
ATP	adenosine triphosphate
Bdnf	brain-derived neurotrophic factor
Bhlhb4	Class B basic helix-loop-helix protein 4
bp	base pairs
BSA	bovine serum albumin
Calb2	calbindin 2
cDNA	complementary DNA
ChIP	chromatin immunoprecipitation
CsA	Cyclosporin A
Cxcl12	chemokine (C-X-C motif) ligand 12
DAPI	4'-6-Diamidino-2-phenylindole
DMEM	dulbecco's modified eagle medium
DMSO	dimethyl sulfoxide
DNAse	desoxyribonuclease
dNTP	deoxynucleotidetriphosphate
DTT	dithiothreitol
EDTA	ethylenediaminetetraacetic acid
E. coli	*Escherichia coli*
Egr3	early growth response protein 3
ES	embryonic stem (cells)
FCS	fetal calf serum
Fgf3	fibroblast growth factor 3
FoxG1	forkhead-box protein G1
g	gram
HA	hemagglutinin
Hjurp	holliday junction recognition protein
HRP	horseradish peroxidase
Ig	immunoglobulin
IPTG	isopropyl-β-D-thiogalactopyranoside
kb	kilobases
kDa	kilodalton
L	liter
LB	*Luria Bertani*
Lhx3	LIM/homeobox protein 3
luc	gene encoding luciferase
m	milli
M	mol L^{-1}
Mef2c	myocyte enhancer factor 2
Mops	3-(N-Morpholino)propanesulfonic acid
mRNA	messenger RNA
mt	mutant
Mtss1	metastasis suppressor protein 1
Myh8	myosin, heavy polypeptide 8, skeletal muscle, perinatal
Neuro2a	mouse neuroblastoma cell line
Ndst4	N-deacetylase/N-sulfotransferase (heparin glucosaminyl) 4

Nfatc2	nuclear factor of activated T cells, cytoplasmic 2
NLS	nuclear localization signal
NSCs	neural stem cells
OD	optical density
PAGE	polyacrylamide gelelectrophoresis
PBS	phosphate-buffered saline
PCR	polymerase chain reaction
PFA	paraformaldehyde
Pitx2	paired-like homeodomain transcription factor 2
Pou4f3	POU domain class IV transcription factor 3
PVDF	polyvinyliden fluoride
qRT-PCR	quantitative real-time polymerase chain reaction
Rdh9	retinol dehydrogenase 9
Rgs4	regulator of G-protein signaling 4
Rnase	ribonuclease
rpm	revolutions per minute
SDS	sodium dodecyl sulfate
siRNA	short interference ribonucleic acid
Slap	Scr-like adaptor protein
TAD	transactivation domain
Tcfap2d	transcription factor activating enhancer binding protein-2δ (gene name)
Temed	N,N,N',N'-tetramethylethylendiamine
Tris	Tris-(hydroxymethyl)-aminomethane
TSS	transcription start site
U	unit
UDG	uracil DNA glycosylase
UV	ultra violet
wt	wildtype
µ	micro
+/+	wildtype
-/-	knockout
%	percent
°C	temperature in degree Celsius
α	alpha
β	beta
γ	gamma
δ	delta
ε	epsilon

1. Introduction

1.1. The family of Ap-2 transcription factors

The Ap-2 transcription factor family (Ensembl family ENSF00000001105) consists of sequence-specific DNA-binding proteins that have been implicated in orchestrating gene expression in the process of development, differentiation, and tumorigenesis. Using affinity chromatography, Ap-2α was the first identified family member and was isolated as a nuclear protein of 52 kDa from HeLa cells (Williams et al., 1988). Up to date, five members of the Ap-2 family have been identified in humans and mice: Ap-2α, Ap-2β, Ap-2γ, Ap-2δ and Ap-2ε which are all encoded by separate genes (murine gene names *Tcfap2a*-*Tcfap2e*). Homologs of Ap-2 have also been found in other species. The single *Drosophila melanogaster* and the two *Caenorhabditis elegans* Ap-2 proteins show the weakest phylogenetic relationship with vertebrate Ap-2 transcription factors (for review see (Eckert et al., 2005)). Nevertheless, their presence suggests an evolutionary conservation of Ap-2 proteins.

1.1.1. Structure of Ap-2 proteins

The Ap-2 family members share a common, characteristic domain structure (Fig. 1). Highly conserved are a basically charged DNA-binding domain and a carboxy-terminal dimerization domain. The latter consists of two putative amphipathic alpha helices separated by a large intervening span region of approximately 80 amino acids. This helix-span-helix motif is characteristic for Ap-2 proteins and, together with the basic domain, mediates DNA binding and dimerization (Williams and Tjian, 1991b). The proline and glutamine-rich N-terminus is less conserved although a PY motif and other critical residues in this domain are shared. Due to fine-mutational analyses of the human Ap-2α N-terminus, the activation motif was assigned to amino

acids 52-107. Within this sequence, fewer than 36 residues are identical or similar among the Ap-2 proteins and are therefore thought to play an essential role for transcriptional activity (Wankhade et al., 2000). Ap-2δ is considered the most divergent family member because within its transactivation domain (TAD) those critical amino acids are missing. This suggests that coactivators and target genes interacting with Ap-2δ might be distinct from the candidates already known for other Ap-2 proteins.

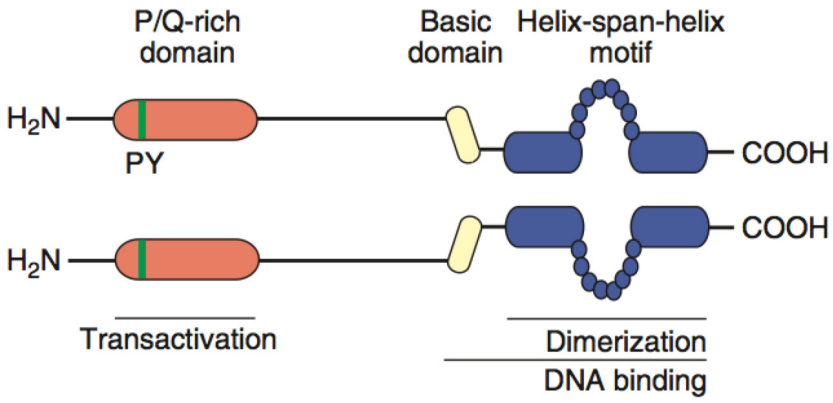

Figure 1: Homodimeric domain structure of Ap-2α protein. The transactivation domain (red) contains a conserved PY motif (green) and is followed by a basic domain (yellow) and the characteristic helix-span-helix motif (blue) that mediate DNA binding and dimerization (Eckert et al., 2005) .

Homo- and heterodimer formation as well as integrity of the basic region are essential for DNA binding (Williams and Tjian, 1991a, 1991b). Ap-2 dimers bind DNA at highly conserved GC-rich consensus sequences present in many cis-regulatory regions of cellular and viral promoters and enhancers (Imagawa et al., 1987; Mitchell et al., 1987; Williams et al., 1988). The sequences 5'-GCCN$_{3/4}$GGC-3' and 5'-GCCN$_{3/4}$GGG-3' were shown to be ideal binding sites for Ap-2 transcription factors (Mohibullah et al., 1999). However, Ap-2 binding to a 5'-CCCCAGGC-3' site in the SV40 enhancer element demonstrates that Ap-2 proteins can bind GC-rich regions of different compositions (Mitchell et al., 1987). Also, isotype-dependent dimers vary

considerably in binding site affinities. Zhao et al. (2001) could show that Ap-2δ preferentially binds the specific variation of the GC motif 5'-GCCTGAGGC-3' providing the first example of target sequence specificity among the Ap-2 family (Zhao et al., 2003). Therefore, a number of specifically composed Ap-2/DNA complexes may be present in tissues depending on the expression of different Ap-2 isoforms.

1.1.2. Murine Tcfap2 genes

Expression studies of *Tcfap2* genes during mouse embryogenesis revealed that *Tcfap2a*, *Tcfap2b*, and *Tcfap2c* show an overlapping expression pattern first detected in neural crest cells and their derivatives (Chazaud et al., 1996; Mitchell et al., 1991; Moser et al., 1995; Moser et al., 1997). Furthermore, they are coexpressed in many structures of the peripheral and central nervous system, facial and limb mesenchyme, various epithelia and the extraembryonic trophectoderm. Strikingly, *Tcfap2d* and *Tcfap2e* expressions deviate from this pattern. *Tcfap2d* was observed in the central nervous system, the retina and the developing heart (Zhao et al., 2003). *Tcfap2e* was detected in neural tissue and cells of the olfactory bulb (Wang et al., 2004).

1.1.2.1. Ap-2α

AP-2α was the first characterized family member and was identified as a nuclear protein due to its ability to bind to the viral SV40 promoter and the human metallothionein IIa promoter (Mitchell et al., 1987).

Tcfap2a is expressed at day E8.5 in neural folds and head mesenchyme of neural crest cell origin. During development, *Tcfap2a* expression persists in neural crest derivatives like the dorsal root ganglion and facial and branchial arch mesenchyme.

Appreciable *Tcfap2a* signals also occur in epidermal ectoderm, limb bud mesenchyme, mesometanephric regions, and a lateral portion of the CNS. In adult mouse tissue, *Tcfap2a* mRNA was observed at low levels in the kidney, cerebellum, spleen and thymus (Mitchell et al., 1991). Another group also detected *Tcfap2a* expression in adult skin, eye, and prostate (Moser et al., 1995).

Two groups independently from each other disrupted the *Tcfap2a* gene in mice by targeted mutation of either exon 5 or 6, respectively (Schorle et al., 1996; Zhang et al., 1996). These mice had multiple congenital defects and died perinatally. They exhibited cranio-abdominoschisis and severe dismorphogenesis of the face, skull, sensory organs and the cranial ganglia. A failure of cranial neural tube closure was observed between E9 and E9.5. In wildtype animals, neural folds are apposed and fused over most of the spinal and cranial region at that time. However, in knockout mice, cranial neural folds remained widely separated over their entire rostral-caudal axis, resulting in exencephaly. Wildtype and mutant embryos displayed a similar staining of migratory neural crest cells indicating that neural crest cells are able to migrate and differentiate into derivatives of the facial mesenchyme. TUNEL staining revealed coincided increased apoptosis in the trigeminal ganglia and the midbrain, anterior hindbrain and proximal mesenchyme of the first branchial arch resulting in underdeveloped or missing cranial ganglia (Schorle et al., 1996; Zhang et al., 1996).

1.1.2.2. Ap-2β

The murine cDNA encoding the second Ap-2 transcription factor, Ap-2β, was first cloned and characterized by Moser et al. (Moser et al., 1995). Ap-2β shared an overall identity of 76% with Ap-2α and exhibited similar DNA binding and transactivation abilities. During embryonic development, *Tcfap2b* mRNA was detected between E11.5 and 17.5. Around E13.5 and E15.5, strong signals for

Tcfap2b were observed in many neural tissues especially the midbrain and the spinal cord. Expression overlapped with regions of developing sensory neurons. Furthermore, *Tcfap2b* mRNA was detected in facial mesenchyme like the olfactory epithelium and the first branchial pouch, and to a lesser extent, also in peripheral tissues such as the kidney and skin. Transcript levels decreased significantly after birth but were still abundant in the eye, skin, and kidney and at lower levels in the prostate, thymus, and brain (Moser et al., 1995).

Generation of *Tcfap2b* null mice revealed a role for Ap-2β in programming cell survival in renal epithelial cells (Moser et al., 1997). *Tcfap2b*-/- mice completed embryogenesis but died at postnatal days 1 and 2 due to polycystic kidney disease. Kidney development occured normally, but at the end of embryogenesis expression of bcl-X_L, bcl-w, and bcl-2 was downregulated resulting in massive apoptotic death of collecting duct and distal tubular epithelia (Moser et al., 1997).

The autosomal dominant disorder Char syndrome is characterized by patent ductus arteriosus, facial dysmorphism and hand anomalies. Char syndrome was linked to the genomic critical region on chromosome 6p12-p21 which encodes the human *TFAP2B* gene. Two families inheriting Char syndrome were then analyzed for mutations in the *TFAP2B* gene. Indeed, the substitution of an alanine by aspartic acid at codon 264 and the substitution of an arginine by cysteine at codon 289 were identified in all affected individuals of the family. These missense mutations altering conserved residues were not observed in any unaffected family members (Satoda et al., 2000). The protein resulting from the mutations was impaired in its ability to bind to a consensus AP-2 target DNA sequence despite proper dimerization. Dimerization of mutant with wildtype AP-2β reduced transactivation of gene expression indicating a dominant negative mechanism. These findings identified the first genetic cause for

Char syndrome and assigned an essential role for AP-2β in ductal, facial and limb development (Satoda et al., 2000).

1.1.2.3. Ap-2γ

The *Tcfap2c* gene was identified as an immediate-early retinoic acid-induced gene in murine P19 embryonal carcinoma cells (Oulad-Abdelghani et al., 1996). Like Ap-2α and Ap-2β, the Ap-2γ protein is able to form a complex with the Ap-2 recognition sequence $GCCN_3GGC$ and activate transcription from an Ap-2 binding site containing reporter.

As early as E7.0, *Tcfap2c* signals were observed in extraembryonic tissue. Strong signals were derived from the lining of the extraplacental cavity and in the chorion as well as from trophoblast giant cells (Chazaud et al., 1996). *Tcfap2c* was also expressed in the innermost cells of the decidua.

At E7.5, *Tcfap2c* expression was detected in the boundary region between neural plate and surface ectoderm. *Tcfap2c* transcripts were also present in premigratory and migrating neural crest cells until E8.5. Moreover, *Tcfap2c* was expressed in facial mesenchyme, limb buds, the presumptive cortical region of the forebrain vesicles and the urogenital system (E9.5 – E11.5). Interestingly, *Tcfap2c* transcripts were abundant in primordial germ cells in the genital ridges. However, this expression seemed to be transient as mRNA levels could no longer be detected in the fetal ovary by E14.5 – E15.5 (Chazaud et al., 1996). *Tcfap2c* expression in adult mouse tissue is clearly tissue-specific because significant signals were only detected in lungs, ovary and testis. In addition to that, *Tcfap2c* is expressed in most squamous epithelia, several exocrine glands and in the inner nuclear and ganglion cell layer of the retina (Oulad-Abdelghani et al., 1996).

To dissect the function of Ap-2γ, *Tcfap2c* knockout mice were generated. This genotype resulted in embryonic lethality and assigns Ap-2γ an essential role during early embryogenesis. Ap-2γ deficiency led to reduced proliferation in extraembryonal ectoderm and in the ectoplacental cone. As a consequence, the embryo could not be sufficiently supplied with nutrients and died (Werling and Schorle, 2002). To overcome embryonic lethality, a conditional *Tcfap2c* mouse mutant was generated which enables the spatial and temporal deletion of both *Tcfap2c* alleles (Werling and Schorle, 2002) by circumventing the placenta phenotype. The analysis of those null mutants suggests a role for Ap-2γ in germ cell development as Ap-2γ-deficient mice were sterile and had lost their germ cells (Weber et al., 2011).

1.1.2.4. Ap-2δ

The mouse *Tcfap2d* gene was cloned and characterized by Zhao and collegues in 2001 (Zhao et al., 2001). During positional cloning studies for Char syndrome on the *Tcfap2b* genomic locus, a novel *Tcfap2* gene was identified residing 40 kb from the 3' end of the *Tcfap2b* gene. The cDNA derived from 8 exons included 1788 bp and encoded a protein (designated Ap-2δ) of 452 amino acids that gave an estimated molecular weight of 49.5 kDa. This gene was highly homologous to previously identified *Tcfap2* genes in its DNA binding and dimerization mediating C-terminus but differed significantly from other Ap-2 members in the transactivation domain. The PY motif and other residues critical for transactivation are not conserved in the Ap-2δ transactivation domain. In particular, four residues in the basic binding region which are completely conserved among all other Ap-2 proteins differ in Ap-2δ (Asp^{209}, Leu^{210}, Lys^{235}, and Ile^{252}).

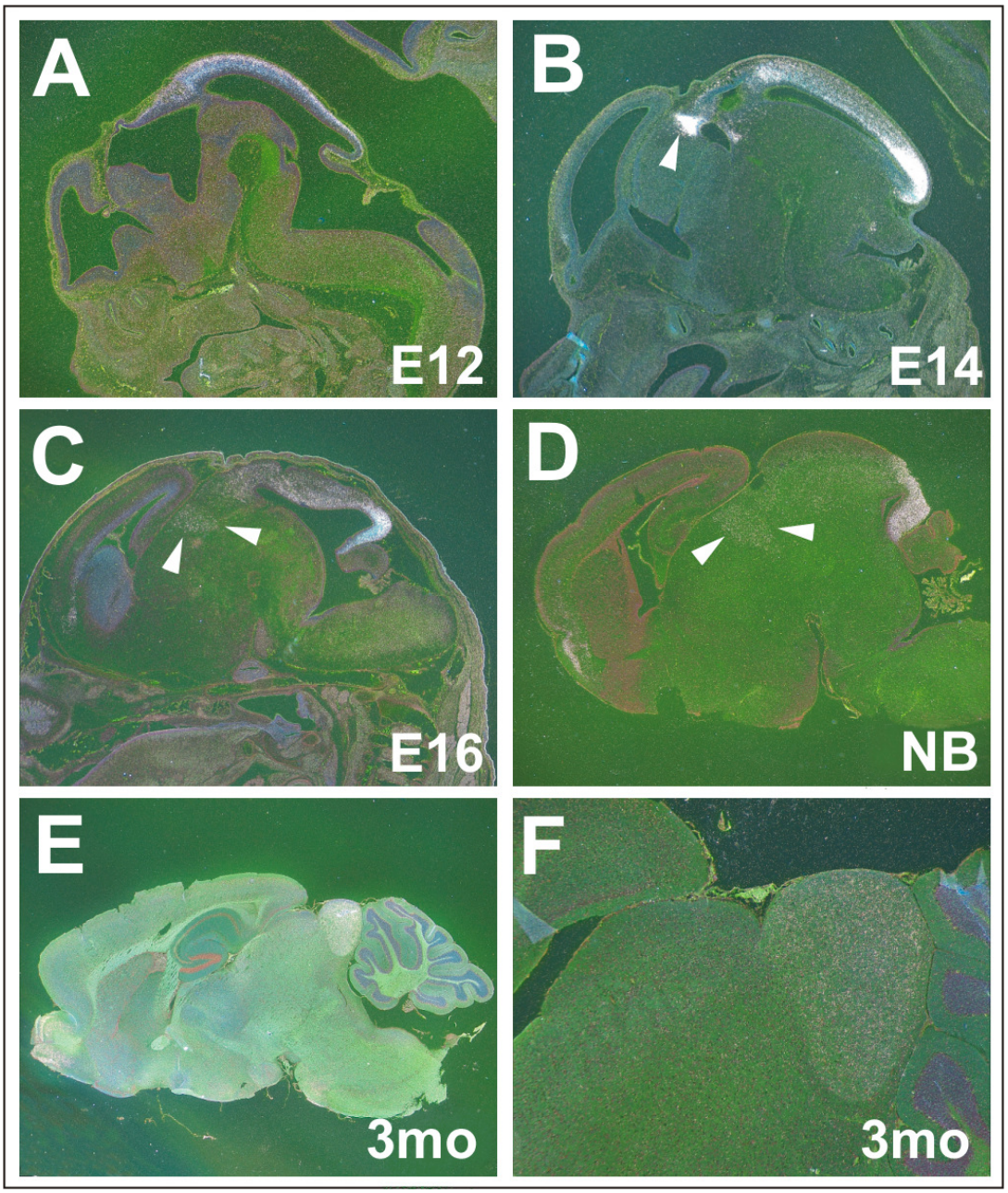

Markus Moser

Figure 2: *Tcfap2d* expression during development and in the postnatal brain.
Tcfap2d expression was analyzed using radioactive in situ hybridization with a *Tcfap2d*-specific probe at different developmental stages: whole embryos (E12-E16; A-C), isolated brains (D-F) of newborns (NB; D) and three months old mice (3 mo; E, F). Expression can be observed in the posterior mesencephalon (A-F) and the dorsal thalamus (A-D; white arrows B-D) (Hesse et al., 2011).

Tcfap2d shows a spatially restricted expression pattern with a predominant expression in the fore- and midbrain. The first detection of *Tcfap2d* occurs on E9.5 in the central nervous system and the myocardium (Zhao et al., 2003). In situ hybridization on sagittal sections of mouse embryos and isolated brains of newborns and 3 months old mice, respectively, localized *Tcfap2d* to the mesencephalic tectum

and the dorsal diencephalon at E12.5 and E14.5 (Fig. 2). During development, *Tcfap2d* exhibits a dynamic expression in that it shifts towards the posterior midbrain. This shift in expression is completed at the newborn stage. The dorsal aspect of the midbrain is comprised by the anterior colliculi superior and the posterior colliculi inferior. In the adult brain, *Tcfap2d* can be predominantly detected in the posterior structure, the colliculi inferior. *Tcfap2d* is also weakly expressed in the dorsal thalamus and the forebrain. This expression persists during embryogenesis and adulthood (Fig. 2) (Hesse et al., 2011). In contrast to the other three *Tcfap2* genes which are all expressed in neural crest cells in the neural fold and head mesenchyme, *Tcfap2d* expression cannot be detected in these tissues. From E13.5 to E16.5, *Tcfap2d* signals also persist in the inner nuclear layer of the retina (Zhao et al., 2003). In summary, *Tcfap2d* shows the most restricted and divergent expression pattern of *Tcfap2* genes; it is not expressed in neural crest cells but is present in the developing heart and retina.

1.1.2.5. Ap-2ε

The fifth and most recent identified member of the Ap-2 family is AP-2ε which consists of the typical modular structure with its highly conserved C-terminal DNA binding and dimerization domain as well as conserved proline and critical amino acid residues in the activation domain (Feng and Williams, 2003; Wang et al., 2004). During embryogenesis, *Tcfap2e* expression can be observed from E7.5 throughout all later embryonic stages until birth. It is restricted to neural tissues such as the midbrain, hindbrain and olfactory bulb. Within the olfactory bulb, *Tcfap2e* expression becomes refined to the projection neurons and the mitral and tufted cellls. In line with the expression pattern, Feng and collegues reported a defective olfactory bulb architecture in *Tcfap2e* null mice. The mitral cell layer was disorganized and the

adjacent internal plexiform layer was absent. Despite these findings, Ap-2ε-deficient mice could discriminate a variety of odors and were viable and fertile (Feng et al., 2009). The data imply that Ap-2ε is required for the establishment of appropriate neuronal lamination in the olfactory bulb.

1.1.3. Regulation of Ap-2 proteins

Early analysis of the human *TCFAP2* genomic locus revealed that typical sequence motifs for basal transcription factors such as TATA, CCAAT or SP-1 boxes are absent in the *TCFAP2* promoter (Bauer et al, 1994). Yet, an initiator element and an octamer binding site close to the transcriptional start site were reported to be indespensable for basal promoter activity (Creaser et al, 1996). Interestingly, AP-2 consensus binding sequences were identified that confer positive autoregulation. Transfection with an AP-2α expression plasmid increased promoter activity of a construct containing a partial *TCFAP2* fragment including the AP-2 consensus site (position -336) (Bauer et al., 1994). Extended *TCFAP2A* promoter studies revealed that the transcription factor BTEB-1 represents an even stronger activator of the *TCFAP2* promoter than AP-2 itself. Furthermore, the zinc finger protein AP-2rep was isolated as a negative regulator conferring strong transcriptional repression of the *TCFAP2A* gene (Imhof et al., 1999).

Besides these genomic elements that mediate regulation of *TCFAP2* transcripts, AP-2 proteins are mainly influenced by second messengers, posttranslational modifications, and protein interactions. Park and Kim could demonstrate that an AP-2 binding site is required for cAMP activation in the insulin induction of acetyl-CoA carboxylase (ACC) gene expression. They could further show that cAMP-dependent protein kinase can phosphorylate AP-2α *in vitro* and *in vivo* without affecting its binding activity (Park and Kim, 1993). A few years later, Garcia et al. reported that

also the APOE (apolipoprotein E) promoter stimulation by cAMP is mediated by AP-2α. Protein kinase A phosphorylation of AP-2α at Ser^{239} did not affect DNA binding but enhanced the activatory properties of AP-2α (Garcia et al., 1999). Transcriptional activation mediated by AP-2 can also be induced by another signal transduction pathway, the phorbol-ester and diacylglycerol-activated protein kinase C (Imagawa et al., 1987). Besides the stimulation by forskolin via the cAMP pathway, the stimulation by the phorbol ester tumor promoter 12-O-tetradecanoyl-phorbol-3-acetate (TPA) also activated a reporter containing a pentameric repeat of an AP-2 binding site derived from the SV40 enhancer. These data implicate that cAMP modulates AP-2 activity by PKA-induced phosphorylation and furthermore that phorbol esters can activate AP-2 transactivation involving protein kinase C.

Human AP-2α transcriptional acitvation was shown to be dually regulated by poly(ADP-ribose) polymerase 1 (PARP-1). Interaction with the automodification/BRCT (breast cancer suscepitibility gene 1 C-terminal) region of PARP-1 increased AP-2 activity. In contrast, the C-terminal catalytic domain of PARP-1 strongly interacted with and poly(ADP-ribosyl)ated AP-2α thereby negatively affecting AP-2α transcription (Li et al., 2004).

The HER-2/neu proto-oncogene is overexpressed in approximately one fourth of mammary carcinomas (King et al., 1985; King et al., 1989). AP-2 proteins participate in HER-2/neu mediated mammary carcinogenesis in that they bind to the HER-2/neu promoter and efficiently activate transcription (Bosher et al., 1996; Vernimmen et al., 2003). HER-2 positive breast cancer cell lines concurrently overexpress AP-2α or AP-2γ. This strict correlation suggests that the deregulation of AP-2 proteins is the preceding pathological event. Li et al. could show that the increased abundance of AP-2 in HER-2/neu mammary carcinomas is due to high stability of the protein. The high stability results from reduced ubiquitination of AP-2 in HER2 positive tumor

tissues compared to HER2 negative tissues (Li et al., 2006). These data indicate that defective ubiquitin-dependent proteasomal degradation pathways may be a major cause of increased AP-2 and HER-2/neu levels in breast cancer.

Other than defective ubiquitination, sumoylation also increases protein stability representing another possible reason for increased AP-2 half-lives in tumors (Muller et al., 2001). Using a two-hybrid screen, the SUMO-conjugating enzyme UBC9 was identified to interact with the C-terminus of AP-2. Furthermore, AP-2 is sumoylated *in vivo* at Lys^{10} leading to reduced transactivatory potential (Eloranta and Hurst, 2002). Interestingly, this site of sumoylation is not conserved in the divergent transactivation domain of AP-2δ whereas the proposed region of interaction with UBC9 is conserved.

Another mechanism of regulating AP-2α was proposed by Nyormoi and collegues in 2001. They demonstrated that the apoptosis-inducer TNF-α downregulated the expression of AP-2α and AP-2γ in breast cancer cells (Nyormoi et al., 2001). Moreover, recombinant caspase studies suggested that AP-2α is cleaved by caspase 6. Cleavage of AP-2α *in vivo* led to AP-2α degradation and loss of DNA binding activity indicating that AP-2α is a critical component during TNF-α induced apoptosis.

Protein interactions can also negatively regulate AP-2 activation by displacing AP-2 proteins from their binding sites. For example, Nuclear Factor 1 (NF-1) and AP-2 bind mutually exclusive to the same region of the hGH promoter as AP-2 binding only occurs if NF-1 binding is prevented (Courtois et al., 1990). Mercurio and Karin described another case where AP-2 was replaced by another DNA binding factor. AP-2 and AP-3 competed for binding to the SV40 core sequence in which the binding sites for both proteins are overlapping (Mercurio and Karin, 1989). In a very recent report, the interaction between AP-2 and potassium channel tetramerization domain-containing 1 (KCTD1) at the N-termini of both proteins was described. This

interaction significantly repressed AP-2α-mediated transactivation (Ding et al., 2009). Taken together, these data define different means to posttranslationally regulate AP-2 activity.

1.1.4. Initiation of AP-2-mediated transcription via interaction partners

AP-2 proteins positively or negatively regulate transcription of target genes by cooperation with other transcription factors or coactivators which augment building a link to the basal transcriptional machinery.

Two members of the CITED family, CITED2 and CITED4, have been shown to physically interact with and coactivate AP-2α, AP-2β, and AP-2γ by linking them to p300 and CBP (Bamforth et al., 2001; Braganca et al., 2003; Braganca et al., 2002). p300 and CBP exert an intrinsic histone acetyltransferase activity. The transfer of acetyl groups to histone tails results in the relaxation of tightly packed heterochromatin and renders DNA more accessible to transcription factors. Despite the presence of conserved residues at the N- and C-termini of the two CITED proteins, CITED2 mediates binding and transactivation of AP-2 proteins through its C-terminus whereas residues 2-20 of the N-terminus as well as the C-terminus are essential for co-activation by CITED4. Moreover, Cited2 and Ap-2 occupied the murine Pitx2c promoter *in vivo* and cooperatively transactivated this promoter in transient transfection assays (Bamforth et al., 2004).

AP-2α has been implicated in the regulation of the hamster histone H3.2 gene together with the transcription factor YY1. It was shown to interact with the N-terminus of YY1 through its DNA binding and dimerization domain. Although AP-2α and YY1 can independently bind to AP-2 and YY1 binding sites in the hamster H3.2 promoter, they were both found in a complex that binds to the AP-2 binding sites (Wu and Lee, 2001) indicating a modulation of AP-2 activity by physical interaction with

YY1. YY1 and AP-2 binding sites were also found in the galactocerebrosidase (GALC) gene and gave rise to the assumption that AP-2 and YY1 are involved the transcriptional suppression of the GALC gene (Beier and Gorogh, 2005).

1.1.5. Interaction with tumor suppressors

The tumor suppressor RB encoded by the retinoblastoma gene has been shown to restrict cell proliferation, promote cell differentiation, and promote apoptosis by acting as either a positive or negative regulator of transcription (for review see (Harbour and Dean, 2000; Lipinski and Jacks, 1999; Wang, 1997)). In the context of epithelial differentiation, it activates the *E-cadherin* gene by directly binding to AP-2 *in vivo* and acting synergistically with it (Batsche et al., 1998b). Similarly, the positive regulation of the *BCL-2* gene by RB also requires the interaction with AP-2 in the same cells (Decary et al., 2002). Both proteins bind to the same sequences within the *E-cadherin* and *BCL-2* promoters suggesting that a complex containing these two proteins cooperatively activates gene transcription in epithelial cells. Interestingly, *E-cadherin* and *BCL-2* promoters were found to be highly acetylated when bound by RB and AP-2 linking activation again to the association of AP-2 with the coactivator p300 that exhibits acetyltransferase activity (Decary et al., 2002). Activation of *BCL-2* by AP-2 is in line with the observation of apoptotic cell death with downregulation of bcl-2 in the absence of Ap-2β in knockout mice (Moser et al., 1997). In contrast, repression of the *bcl-2* gene was reported by Wajapeyee and collegues during Ap-2α-elicited apoptosis. Adenoviral- or chemotherapy-induced overexpressed Ap-2α binds to a more proximal binding site in the *bcl-2* promoter and reduced *Bcl-2* gene transcription via a bax/cytochrome c/Apaf1/caspase-9-dependent mitochondrial pathway (Wajapeyee et al., 2006).

A direct protein-protein interaction with AP-2α and AP-2γ was also demonstrated for another tumor suppressor protein, p53. Interaction of AP-2 with p53 augmented the transactivation of a p53-responsive promoter. Moreover, AP-2 and p53 bind *in vivo* to the $p21^{Waf1/CIP1}$ promoter at a p53 binding site and p53-mediated induction of p21 mRNA is supported by the association of AP-2 to p53. AP-2 was able to induce G_1 and G_2 cell cycle arrest only in the presence of p53 (McPherson et al., 2002). These results may explain the tumor suppressor function ascribed to AP-2 in breast cancer, colon cancer, and malignant melanoma (Gee et al., 1999; Karjalainen et al., 1998; Ropponen et al., 2001).

1.1.6. Ash2l represents an interaction partner for Ap-2δ

Up to date, only one interaction partner has been described for Ap-2δ. Using a yeast two-hybrid screen, the trithorax superfamily member Ash2l was identified to bind exclusively to the TAD of Ap-2δ and synergistically activate Ap-2δ-mediated gene expression in a dose-dependent manner. Ap-2δ was shown to associate with endogenous Ash2l and Alr, a member of the MLL family of histone lysine methyltransferases. This complex is able to methylate lysine 4 of histone 3 (H3K4). Intriguingly, Ap-2δ is essential for the recruitment of Ash2l and Alr to the *Hoxc8* locus and formation of this complex leads to H3K4 trimethylation and subsequent gene activation (Tan et al., 2008). Using microarray analysis, gene expression profiles were produced from Ap-2δ and Ash2l-deficient Neuro2a cells. By this approach, *Fgfr3* was identified as a direct transcriptional target of the Ap-2δ-Ash2l complex. Similar to the *Hoxc8* locus, Ap-2δ is also responsible for the recruitment of the Ash2l-containing complex to the *Fgfr3* promoter resulting in H3K4 trimethylation (Tan et al., 2009). The data provide for the first time evidence that Ap-2δ has a functional role in recruiting histone methyltransferases to specifc gene loci in a spatiotemporal manner.

Owing to the highly restricted expression pattern of Ap-2δ and its sequence-specific DNA binding properties, these findings present a mechanism how MLL family members achieve specificity despite their global expression patterns (Tan et al., 2008).

1.2. The family of NFAT transcription factors

The nuclear factor of activated T cells (NFAT) family of transcription factors plays pivotal roles in many vertebrate developmental events as diverse as immune responses, axonal outgrowth, cardiac and lung morphogenesis and neural crest diversification (Crabtree and Olson, 2002; Graef et al., 2001; Macian, 2005).

Five family members have been currently idenitified and are named NFATc1/2/c, NFATc2/1/p, NFATc3/4/x, NFATc4/3, and NFAT5/TonEBP (Graef et al., 2001; Macian, 2005; Rao et al., 1997). Structural analysis of these proteins revealed a highly conserved DNA binding domain that shares a homology of approximately 70% among NFATc proteins (Serfling et al., 2004). This domain is also called “Rel homology region” (RHR) due to its structural similarity to the DNA binding domain of Rel/Nf-κb family transcription factors.

Figure 3: Structure of NFAT proteins. NFAT proteins are composed of a highly conserved DNA binding region also termed Rel homology region (RHR) and a less conserved Nfat homology region (NHR) that contains a N-terminal transactivation domain (TAD) and the regulatoty region with calcineurin docking site and SRR and SP motifs. SRR = serine rich region, SP = serine proline phosphorylation motif, NLS = nuclear localization signal (Mancini and Toker, 2009)

NFATc1-4 furthermore share a strong TAD located at the N-terminus followed by the NFAT homology region which contains regulatory elements. The latter comprises elements relevant for proper NFAT function including several serine rich regions (SRR), serine-proline phosphorylation motifs, a calcineurin docking site, and a nuclear localization signal (NLS) (Fig. 3).

1.2.1. Calcium-calcineurin-NFAT signaling pathway

NFAT activation is elicited by a rise in intracellular calcium levels initiated by cell surface receptors that stimulate activation of phospholipase Cγ (PLCγ). Activated PLC enzymes initiate release of calcium from the endoplasmic reticulum. In response, calcium-release activated calcium channels (CRAC) are opened which confer a sustained calcium signal. Calcium is bound by calmodulin which activates the serine/threonine phosphatase calcineurin (Clipstone and Crabtree, 1992; Hogan et al., 2003; Jain et al., 1993).

In resting cells, NFAT is located in a highly phosphorylated state in the cytoplasm (Fig. 4). It only shows a weak affinity for DNA binding (Viola et al., 2005). Upon rise in intracellular calcium levels and subsequent calcineurin activation, calcineurin binds to NFAT within the regulatory domain and dephosphorylates up to 18 serine residues. This evokes a conformational change which masks a nuclear export signal (NES) and exposes the NLS promoting translocalization to the nucleus and an increase in DNA binding affinity (Beals et al., 1997; Okamura et al., 2004). Calcineurin also maintains NFAT in a dephosphorylated state in the nucleus (Zhu and McKeon, 1999). Nuclear localization is temporally restricted and counteracted by several kinases such as glycogen synthase kinase 3 (GSK-3) (Neal and Clipstone, 2001), casein kinase 1 (CK1) (Okamura et al., 2004), and tyrosine-phosphorylation regulated

kinases (DYRK) (Gwack et al., 2006) that sequentially rephosphorylate the serine residues.

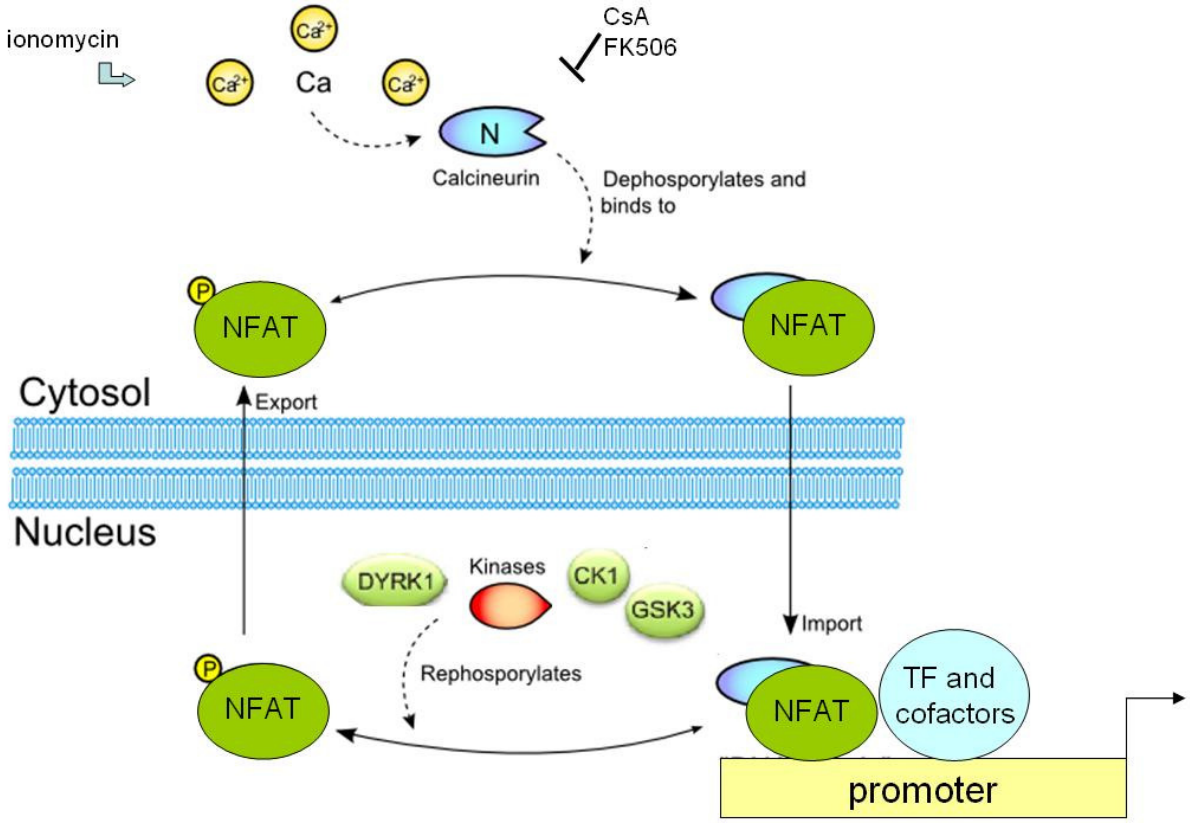

Figure 4: Calcineurin-NFAT-signaling. Increased intracellular calcium activates calcineurin which dephosphorylates Nfat promoting nuclear entry. In the nucleus, Nfat binds to DNA together with other transcription factors and coactivators to initiate transcription of target genes. This function is counteracted by Nfat kinases such as GSK-3, CK1 and DYRK that rephosphorylate Nfat resulting in nuclear exit. Calcineurin activity can be inhibited by the immunosuppressive drugs CsA and FK506. (Modified from Cooling et al, 2009)

Thus, NFAT loses its DNA binding affinity and is transported out of the nucleus into the cytoplasm. GSK-3 and DYRK-1 act as export kinases, whereas CK1 can function as both export and maintenance kinase. DYRK-2 phosphorylates NFAT in the cytoplasm and acts as a maintenance kinase. In summary, NFAT activation relies on the balance between calcineurin-mediated dephosphorylation and NFAT-kinase-regulated rephosphorylation.

Calcineurin-NFAT signalling represents a target for immunosuppressive drugs such as cyclosporin A (CsA) and FK506. These drugs block nuclear localization of NFAT by inhibiting calcineurin phosphatase activity. CsA and FK506 bind at subnanomolar affinity to the intracellular proteins cyclophilin and FKBP, respectively. This drug/protein composite surface then binds to calcineurin, thereby inhibiting substrate access (Liu et al., 1991).

NFAT5 is the most divergent family member. It has a distinct domain structure as it does not contain a calcineurin docking site and thus is calcium and calcineurin-insensitive (Lopez-Rodriguez et al., 1999). Its activation is regulated via osmotic pressure (Lee and Park, 2006).

In addition to phosphorylation, NFAT acitivity is also modulated by other posttranscriptional modifications. Sumoylation of NFAT proteins represents another means of NFAT regulation as it results in nuclear retention of the transcription factor (Nayak et al., 2009; Terui et al., 2004). In breast cancer cells, NFAT1 has also been shown to be ubiqitinated by the E3 ubiqitinin ligase murine double minute 2 (MDM2) that targets the transcription factor for degradation (Yoeli-Lerner et al., 2005). These data demonstrate the complexity of the mechanisms required for NFAT activation.

1.2.2. Knockout animal studies of Nfat

Targeted disruption of *Nfat* genes has defined roles in development of the cardiovascular, musculoskeleton, and nervous system with complicated immunological phenotypes. The resulting phenotypes suggest redundancy but also isoform-specific differences among *Nfatc1-4* (Table 1).

Nfatc1 null mice are embryonically lethal with defects in cardiac valve formation (de la Pompa et al., 1998; Ranger et al., 1998). *Nfatc2*-deficient mice suffer from

hyperproliferation of splenic B and T cells and display dysregulation of chondrogenesis (Ranger et al., 1998; Xanthoudakis et al., 1996).

Table 1: Phenotypes of *Nfat* knockout mice (modified from Crabtree and Olson, 2002; Kiani et al., 2000)

Nfat protein	Phenotype of knockout mice
Nfatc1/2/c	Embryonic lethality (heart valve defect) Lymphocytes produce less IL-4
Nfatc2/1/p	Immune hyperactivation and allergic responses, suppression of chondrogenesis
Nfatc3/4/x	Defect in positive selection of thymocytes, hyperproliferation of lymphocytes
Nfatc4/3	Viable and fertile, no apparent defects
c1 + c2	Failure of T cell and immune response gene activation
c2 + c3	Spontaneous Th1 differentiation, excessive allergic response
c3 + c4	Lethal vascular patterning defects
Nfat5/TonEBP	Knockouts not reported yet, Nfat5 is not implicated in regulation of conventional Nfat target genes

Nfatc3 knockout mice exhibit defects in myogenesis as well as reduced thymocyte numbers (Amasaki et al., 2002; Oukka et al., 1998). Mice with a targeted disruption of *Nfatc4* appear to be developmentally normal (Graef et al., 2001). More pronounced phenotypes are evident when more than one Nfat isoform is deleted. Double mutant mice for *Nfatc1* and *Nfatc2* show an impaired activation of cytokine genes because no IL-2, IL-4 and TNF-a were produced (Peng et al., 2001). *Nfatc2/Nfatc3* knockout mice display spontaneous differentiation into Th2 cells as well as severe allergic responses with extremely high levels of IgE (Ranger et al., 1998). *Nfatc3/Nfatc4* null

mice have profound defects in angiogenesis characterized by vessel instability and disorganization which result in embryonic lethality at approximately E11.5 (Graef et al., 2001).

1.2.3. Regulation of target genes via interaction with other transcription factors

NFAT family members have been shown to regulate transcription through the cooperative binding to DNA sites in concert with other transcription factors. Interaction of transcription factors stimulated via distinct signaling pathways constitutes an important mechanism to integrate these signals and elicit cellular response. NFAT proteins do so by cooperation with AP-1 transcription factors. Whereas NFAT proteins are regulated by calcium and calcineurin, AP-1 proteins are regulated by other pathways including MAPkinase/PKC and Ras. NFAT and AP-1 proteins cooperate in promoter/enhancer regions of several genes in immune cells (reviewed in Rao et al., 1997). Most of the known binding sites in these genes are composite Nfat/Ap-1 DNA elements which are composed of a Nfat binding sequence (GGAAA) adjacent to an often weak Ap-1 site. The resulting ternary protein complex consists of one Nfat monomer and one homo- or heterodimer produced by the AP-1 proteins fos and jun (Macian, 2005).

Several studies have also shown the cooperate activation of gene transcription by Nfat and Sp-1 proteins. These two transcription factors are responsible for FasL gene activation in IL-2 treated T cells. The critical region for this regulation contains an Sp-1 as well as an Nfat binding site which are partially overlapping. Mutation of either binding site reduced FasL promoter activity (Xiao et al., 1999). Nfat and Sp-1 also physically interact in mammalian cells in a calcineurin-dependent manner as interaction upon treatment with CsA could no longer be observed (Santini et al., 2001). Because Sp-1 factors are not sensitive to calcium or calcineurin treatment,

calcineurin controls Nfat proteins that bind to Sp-1, thereby enhancing Sp-1 transactivating abilities at the $p21^{WAF1/CIP1}$ promoter in keratinocytes leading to differentiation (Santini et al., 2001).

1.3. Aim of this study

The murine cDNA encoding Ap-2δ was isolated in 2001 by Zhao and collegues (Zhao et al., 2001). In contrast to other Ap-2 proteins, Ap-2δ lacks a conserved PY motif and several other critical residues in the transactivation domain which are thought to be important for the activatory potential of Ap-2 proteins. Ap-2δ is mainly expressed in the midbrain, the myocardium and the retina. During development, Ap-2δ expression shows a dynamic shift from the mesencephalic tectum and the dorsal diencephalon to the posterior part of the midbrain, the colliculus inferior.

The genetic disruption of the *Tcfap2d* gene revealed the absence of the colliculus inferior in Ap-2δ-deficient mice. Loss of Ap-2δ results in the degradation of this structure due to massive apoptosis indicating an essential role for Ap-2δ in the maintenance and further maturation of the posterior midbrain.

1. To understand Ap-2δ-dependent control of the posterior midbrain, one aim of the present study was to identify Ap-2δ specific target genes *in vivo* that are involved in the formation of this brain structure. Microarray analyses revealed genes that were differentially regulated in the posterior midbrain of Ap-2δ-deficient mice compared to wildtype controls. With the help of different biochemical and cellular assays, the contribution of Ap-2δ to the activation of these altered genes was examined.

2. Although Ap-2δ lacks critical motifs in the transactivation domain that are conserved in other Ap-2 proteins, Ap-2δ does not exhibit a reduced transactivation potential compared to other isoforms. The divergent transactivation domain furthermore implicates an involvement of other coactivators and interaction partners than those known for other Ap-2 family members. A yeast-two hybrid screen identified the transcription factors Nfatc2 and FoxG1 as putative interaction partners of Ap-2δ. In the present work,

these interactions were characterized by *in vitro* and *in vivo* assays. In addition, the synergistical activation of target genes by both transcription factors was analyzed.

2. Materials and Methods

2.1. Material

2.1.1. Chemicals

Chemicals	Manufacturer	Location
2-Propanol	Merck	Darmstadt
Acetic acid	Merck	Darmstadt
Acrylamide (Rotiphorese Gel 30)	Carl Roth GmbH	Karlsruhe
Agar	Merck	Darmstadt
Agarose	Sigma Aldrich	St. Louis, USA
Ammonium peroxisulfate (APS)	Carl Roth GmbH	Karlsruhe
Ampicillin	Carl Roth GmbH	Karlsruhe
β-mercaptoethanol	Sigma Aldrich	St. Louis, USA
Bovine serum albumin (BSA)	Sigma Aldrich	St. Louis, USA
Calcium chloride	Merck	Darmstadt
Chloroform	Merck	Darmstadt
Complete Mini	Roche Diagnostics	Mannheim
Dimethyl sulfoxide (DMSO)	Sigma Aldrich	St. Louis, USA
dNTPs	Invitrogen	Karlsruhe
Dulbecco´s MEM	Invitrogen	Karlsruhe
Dynabeads®	Invitrogen	Karlsruhe
ECL reagent	Perbio	Bonn
Ethanol	Merck	Darmstadt
Ethidium bromide	Sigma Aldrich	St. Louis, USA
Ethylenediaminetetraacetic acid	Merck	Darmstadt
Exacta Cruz B™	Santa Cruz	Heidelberg
Fetal calf serum	Invitrogen	Karlsruhe
Glycerol	Sigma Aldrich	St. Louis, USA
Glycine	Sigma Aldrich	St. Louis, USA
HEPES	Sigma Aldrich	St. Louis, USA
Hoechst 33342	Invitrogen	Karlsruhe
Horse radish peroxidase (HRP)	Sigma Aldrich	St. Louis, USA
Isopropanol	Sigma Aldrich	St. Louis, USA
IPTG	Merck	Darmstadt
Lipofectamine™	Invitrogen	Karlsruhe
Luciferin	Roche	Pensheim
Methanol	Merck	Darmstadt
Non-fat dry milk	Merck	Darmstadt
NP-40	Calbiochem	Darmstadt
Penicillin/Streptomycin	Invitrogen	Karlsruhe
Paraformaldehyde	Merck	Darmstadt
Potassium chloride	Merck	Darmstadt
RNase-Out™	Invitrogen	Karlsruhe
Roti®-load 4x concentrate	Carl Roth	Karlsruhe
Salmon sperm DNA	Invitrogen	Karlsruhe
Sodium acetate	Merck	Darmstadt
Sodium chloride	Merck	Darmstadt

Sodium dodecyl sulfate (SDS)	Merck	Darmstadt
Skim milk powder	Sigma Aldrich	St. Louis, USA
TEMED	Bio Rad	Hercules, USA
Trishydroxymethylaminomethane (Tris)	Merck	Darmstadt
Triton-X100	Sigma Aldrich	St. Louis, USA
TRIzol® Reagent	Invitrogen	Karlsruhe
Tween-20	Sigma Aldrich	St. Louis, USA

2.1.2. Apparatus

Apparatus	Manufacturer	Location
Abiprism 7900HT	Applied Biosystems	Foster City, USA
Bacteria shaker Innova 4000	New Brunswick Scientific	Nürtingen
Centrifuges 5415D	Eppendorf	Hamburg
Centrifuges 5417R	Eppendorf	Hamburg
ELISA Reader ELx800	BioTek Instruments	Winooski, USA
Hoefer Dual Gel Caster	Amersham Bioscience	Freiburg
Luminometer Centro	Berthold Technologies	Bad Wildbad
Magnetic stirrer	Ika-Combimag RCT, IKA-Werke GmbH	Staufen
Membrane pump	M72C, Vacubrand GmbH & Co	Wertheim
Microscope Axioscop50	Zeiss	Oberkochen
	Leica	Wetzlar
Millipore-Pelicon Filtration device	Millipore	Molsheim, France
Nano Drop	Peqlab Biotechnologie	Erlangen
pH-meter	MP 220, Mettler Toledo	Greifensee, Switzerland
Pipettes	Gilson Pipetman	Langenfeld
	Eppendorf	Hamburg
Power supplies E143	Consort	Turnhout, Belgien
Shakers	Series 25 New Brunswick Scientific CO., Inc.	Edison, USA
	Multitron, Infors AG	Bottmingen, Switzerland
Sterile bench	Biohazard, Gelaire	Mailand, Italy
	Heraeus-Christ	Hanau
Thermocycler	Analytik Jena	Jena
Thermomixer compact	Eppendorf	Hamburg
TransBlot Semi-Dry Transfer	Bio- Rad	Hercules, USA
UV-imaging system	Intas UV system	Göttingen
UV-transilluminator	Biometra	Göttingen

2.1.3. Consumables

Consumables	Manufacturer	Location
1.5 ml tubes	Sarstedt	Nümbrecht
2 ml tubes	Sarstedt	Nümbrecht
200 µl PCR tubes	Axygen	Union City, USA
12-well cell culture plates	Costar	Lowell, USA
6-well cell culture plates	Costar	Lowell, USA
10 cm cell culture dishes	Costar	Lowell, USA
75T cell culture plates	Costar	Lowell, USA
96-well LB luminometer plates	Nunc	Wiesbaden
Autoradiography film	Kodak	New Haven, USA
Cryo Tubes™	Nunc	Wiesbaden
Falcon 2052	Costar	Lowell, USA
Petri dishes	Costar	Lowell, USA
PVDF transfer membrane	Roth	Karlsruhe

2.1.4. Kits

Kits	Manufacturer	Location
NucleoBond Xtra Maxi Plus	Macherey-Nagel	Düren
Zymoclean Gel DNA recovery kit	Zymo Research	Freiburg
High Pure PCR purification kit	Roche	Penzberg
SYBR® Green *Taq* PCR Mix™	Invitrogen	Karlsruhe
TOPO TA cloning®	Invitrogen	Karlsruhe
Exacta Cruz Immunoprecipitation kit	Santa Cruz	Heidelberg

2.1.5. Enzymes and markers

Enzyme	Manufacturer	Location
DNA 100 bp laddder	Invitrogen	Karlsruhe
DNA 1 kb ladder	Invitrogen	Karlsruhe
Prestained SDS-PAGE standard	Invitrogen	Karlsruhe
DNase I	NEB	Schwalbach
RNase	NEB	Schwalbach
Platinum Taq High Fidelity Polymerase	Invitrogen	Karlsruhe
Klenow	Invitrogen	Karlsruhe
Proteinase K	Merck	Darmstadt
Restriction endonucleases	NEB	Schwalbach

RNAseOUT	Invitrogen	Karlsruhe
Shrimp Alkaline Phosphatase	New England BioLabs	Frankfurt
SuperScript III Reverse Transcriptase	Invitrogen	Karlsbad
T4 DNA ligase	Invitrogen	Karlsruhe
Trypsin EDTA (0.25% / 0.02%)	Invitrogen	Karlsruhe

2.1.6. Antibodies

Antibodies	Manufacturer	Location
Rabbit polyclonal Ap-2δ antiserum	PD Dr. Markus Moser	Martinsried
Mouse monoclonal Nfatc2 antibody	abcam	Cambridge, UK
Mouse monoclonal HA.11 antibody (hemagglutinin tag)	Covance	Emeryville, USA
Rabbit polyclonal histone H3 antibody	abcam	Cambridge, UK
Mouse-monoclonal ß-Actin antibody (AC15)	Sigma Aldrich	St. Louis, USA
Mouse IgG antibody	Diagenode	Liège, Belgium
Rabbit IgG antibody	Diagenode	Liège, Belgium
Goat polyclonal antibody anti-rabbit HRP conjugate	Dako	Glostrup, Denmark
Goat polyclonal antibody anti-mouse HRP conjugate	Dako	Glostrup, Denmark
Alexa Fluor 594 goat anti-mouse IgG	Invitrogen	Karlsruhe
Alexa Fluor 488 goat anti-rabbit IgG	invitrogen	Karlsruhe

2.1.7. Vectors

Vector	Insert	Source
pCMX-PL1		Umesono et al., 1991
pCMX-mAp-2δ	mAp-2δ cDNA	PD Dr. M. Moser, Martinsried
pCMX-HA-mAp-2δ	mAp-2δ cDNA, N-terminal HA-tag	this work
pCMX-Flag-mAp-2δ	mAp-2δ cDNA, N-terminal Flag-tag	this work
pCMX-HA-mNfatc2	mNfatc2 cDNA, N-terminal HA-tag	this work
pCMX-HA-mFoxG1	mFoxG1 cDNA, N-terminal HA-tag	this work
pGl3-basic	luciferase reporter	Promega, Mannheim
pGl3-Bhlhb4 -300bp	300 bp mBhlhb4 promoter	this work

	fragment	
pGl3-Bhlhb4 -1.8kb	1.8 kb mBhlhb4 promoter fragment	this work
pGl3-Pou4f3-2.6kb	2.6 kb mPou4f3 promoter fragment	this work
pSG5		Stratagene, Amsterdam
pSG5-mAp-2δ	mAp-2δ cDNA	this work
pSG5-HA-mAp-2δ	mAp-2δ cDNA, N-terminal HA-tag	this work
pGEX-3x		Amersham, GE Healthcare, München
pGEX-3x-mAp-2δ TAD	mAp-2δ TAD	PD Dr. M. Moser, Martinsried
pGEX-3x-GST		PD Dr. Jutta Kirfel, Bonn
pCR®II-TOPO		Invitrogen, Karlsruhe

2.1.8. Primers and oligonucleotides

qRT-PCR primers	**5'-3'**
Tcfap2d	F: TCATGTCAACTACCTTTCCCG
	R: GAACTCGTAATGGAAGGACTGG
Pou4f3	F: AACCCAAATTCTCCAGCCTAC
	R: GCGAGGTAGAAGTGCAGG
Bdnf	F: GCCCAACGAAGAAAACCATAAG
	R: AGGAGGCTCCAAAGGCACTT
Calbindin2	F: GATGGGAAAATTGAGATGGCG
	R: AGTATGGTCTGGGTGTACTCC
Lhx3	F: ACTACGAAACAGCCAAGCAG
	R: CAGTCTCTTTTCCTTAGCCCG
Nfatc2	F: ACGGGAGTGACCGTCAAA
	R: GGAGGGAGGTCCTGAAAACT
Atm	F: GGACTCCAGCTTTAAAGATAAAGAGA
	R: TGCAGGGTTTTCTAAGCAAGT
c-Fos	F: GGGGCAAAGTAGAGCAGCTA
	R: AGCTCCCTCCTCCGATTC
Egr3	F: CAATCTGTACCCCGAGGAGA
	R: CCGATGTCCATCACATTCTCT
Itpr1	F: ACCGGAAGCTGAGAACTCC
	R: TGGTCTTCCAGTTGCCTCA
Mtss1	F: AGCTGCAGAAGAAGGCAAAA
	R: TTTCCTCCAACAGGAGGTATTT
ChIP primers	**5'-3'**
Bhlhb4-300 bp	F: AGAAATGGCAGTTGAGGGG
	R: AATCAGAGGGGACCTGCTG
Bhlhb4-1.8 kb	F: TCTCTTCCTAGCCTCCCACA
	R: GCTGTTCAGGGGAGTCTGTC
Pou4f3-2.6 kb	F: TGACCATTGCTAGTGGACCTT
	R: CCAATGCGGTTCA ACAGAC
Atm bs1	F: TAGCAGCTGGTTCTGTACGC
	R: GGTTGTGGCCAGAGAGGAC
Atm bs2	F: TTCTTGCTCTCATCCCTTCC

	R: TAGCCGAGGAAGGACTGGTT
Egr3 bs1	F: CCCAATTGCCTGGCTCTC
	R: GCGGTGTGAGCCTAGCTG
Egr3 bs2	F: AAACTGAGGGGAGGGAAGAG
	R: GGGAACTTGCATCTCTCAGG
ITPR1 bs1	F: TAGATGGGAGGCAGGAAGTG
	R: TGTCCATGCTGTCTGGAATC
ITPR1 bs2	F: TCAGACACAAGTTCGCAACC
	R: GCTTATATAGGCCGGGAAGC
ITPR1 bs3	F: CTAACCCCTCTCCTGGTCCT
	R: CACCAAAGCCACCAAGAACT
Mtss1 bs1	F: AAAAATGCCCGGAGAAGACT
	R: GCTGCCCTTTTTCGTTCTCT
Mtss1 bs2	F: CCGCCTCCTTTTTACTCCTG
	R: CTCTGCACGCCTCTCAGC
Mtss1 bs3	F: CGGATCTGTTGAGGCAGACT
	R: GGTTTTCTGGTGCTCAGAGG
Mtss1 bs4	F: AAGCACTCCACCCCAAACC
	R: CGGCTGCTCTGACCTCG
Oligonucleotides for EMSA	**5'-3'**
Zhao	F: GAACTGACCGCCTGAGGCGCGTGTGCA
	R: TGCACACGCGCCTCAGGCGGTCAGTT
Pou wt	F: TTTCTAGGGGCCTGAGGGAAGTAGTGG
	R: CCACTACTTCCCTCAGGCCC
Pou mt1	F: TTTCTAGGGGCCAGTGGGAAGTAGTGG
	R: CCACTACTTCCCACTGGCCC
Pou mt2	F: TTTCTAGGGGCCGTTGGGAAGTAGTGG
	R: CCACTACTTCCCAACGGCCC
Bhlhb4	F: CGCGGAACCTGAGGGCGCTTT
	R: GCCTTGGACTCCCGCGAAA

2.1.9. siRNA oligonucleotides

siRNA	Manufacturer	Location
All stars negative control siRNA	Qiagen	Hilden
mAp-2δ siRNA	Ambion	Austin, USA
Block-iT^{TM} fluorescent control siRNA	Invitrogen	Karlsruhe

2.1.10 Media, buffers, and solutions

2.1.10.1. Cell culture and bacterial growth media

Media, buffers, solutions	Composition
Cell culture medium	Dulbecco's Modified Eagle Medium with 4.5 g/L D-Glucose, 10 % FCS, 2 mM L-Glutamine, 100 U/mL penicillin, 100 µg/mL streptomycin
1x trypsin/EDTA	500 mg/L trypsin, 200 mg/L EDTA in 1x HBS
LB medium	10 g tryptone 5 g yeast extract 10 g NaCl ad 1 L H_2O
LB plates	15 g bacto agar 10 g tryptone 5 g yeast extract 10 g NaCl ad 1 L H_2O
Ampicillin stock solution	100 mg/mL in H_2O

2.1.10.2. Nucleic acid analysis

Buffer	Composition
Buffer 1 (lysis)	50 mM Tris-HCl pH 8.0 10 mM EDTA
Buffer 2 (denaturation)	200 mM NaOH 1% SDS
Buffer 3 (neutralization)	3 M KAc pH 5.5
DNA loading buffer	50% glycerol 50% H_2O spatula point bromophenolblue spatula point xylenecyanol 0.5x TAE
50x TAE	2 M Tris(hydroymethyl)aminomethane 1 M NaAc 50 mM EDTA
10x TBE	890 mM Tris 890 mM boric acid 20 mM (Na_2)-EDTA
20x MOPS	800 mM MOPS 200 mM NaAc 20 mM EDTA
2x BES	50 mM BES 280 mM NaCl 1.5 mM $Na_2HPO_4x2H_2O$ pH 6.96

2.1.10.3. Immunoblotting and protein assays

Buffer	Composition
RIPA buffer	150 mM NaCl 0.5 % Na-deoxycholate 1 % NP-40 0.1 % SDS 50 mM Tris pH 7.5 1 tablet Complete Mini (protease inhibitor, Roche, Penzberg)/10 ml buffer
5x Laemmli Running buffer	25 mM Tris 250 mM glycine 0.1 % SDS
Transfer buffer	48 mM Tris 39 mM glycine 1.3 mM SDS 5% methanol
PBST	0.01% Tween-20 in PBS
Co-IP Lysis buffer	20 mM Tris-HCl pH 8 137 mM NaCl 10% glycerol 1% NP-40 2 mM EDTA before use add protease inhibitor
Coomassie solution	0.1% Coomassie brilliant blue 50% methanol 7% acetic acid
Destain solution	50% methanol 7% acetic acid
Luciferase Lysis buffer	125 mM Tris pH 7.8 10 mM EDTA 100 mM DTT 50% glycerol 5% Triton X-100
Luciferase Assay buffer	20 mM Tricine 1.07 mM $(MgCO_3)_4$ 2.67 mM $MgSo_4$ 0.1 mM EDTA 33.3 mM DTT 0.27 mM Coenzyme A 0.47 mM Luciferin 0.53 mM ATP
Pulldown interaction buffer	20 mM Hepes pH 7.7 75mM KCl 0.1 mM EDTA 25 mM $MgCl_2$ 10 mM DTT 0.15% NP-40
EMSA binding buffer	10 mM Tris pH 7.5 1 mM $MgCl_2$ 50 mM NaCl 0.5 mM EDTA 0.5 mM DTT

	4% glycerol 0.05 mg/ml poly (dI-dC)

2.1.10.4. Chromatin immunoprecipitation

Buffer	Composition
SDS lysis buffer	50 mM Tris 10 mM EDTA 0.1 % SDS
Dilution buffer	16.7 mM Tris 167 mM NaCl 1.2 mM EDTA 0.01 % SDS 1.1 % Triton X-100
TE buffer	10 mM Tris 1 mM EDTA
Wash buffer	0.01% Tween 20 in TE buffer
Elution buffer	20 mM Tris 5 mM EDTA 50 mM NaCl 1% SDS

2.1.11. Bacterial strains

Bacteria (*E. coli* strains)	Genotype
DH5α	F-, φ80*lac*ZΔM15, Δ(*lac*ZYA-*arg*F)U169, *rec*A1, *end*A1, *hsd*R17(rk-, mk+), *pho*A, *sup*E44, *thi*-1, *gyr*A96, *rel*A1 and *ton*A
TOP10	F-, *mcr*A, Δ(*mrr-hsd*RMS-*mcr*BC), Φ80*lac*ZΔM15, Δ*lac*X74, *rec*A1, *ara*D139, Δ(*araleu*)7697, *gal*U, *gal*K, *rps*L, (StrR),*end*A1 and *nup*G
BL21	F^-, ompT, $hsdS_B$ (r_B^- m_B^-), gal, dcm

2.1.12. Cell lines

Cell line	Description
Neuro2a	mouse neuroblastoma cell line
NIH/3T3	mouse embryonic fibroblast cell line

2.2. Methods

2.2.1. Cell Culture

Neuro2a and NIH/3T3 cells were cultured as an adherent monolayer in Dulbecco's Modified Eagle Medium supplemented with 10% fetal calf serum and 1% glutamine and penicillin/streptomycin in a humidified atmosphere with 5% CO_2 at 37°C. The adherent cells were removed from cell culture dishes with a 1x trypsin/ethylenediaminetetraacetic acid (EDTA) solution (10% 10x trypsin/EDTA + 90% PBS) incubated for 3 minutes at 37°C and split 1-2 times per week in a ratio of 1:5–1:10.

2.2.1.1. Cryo-conservation of cells

To be able to revert to a constant cell population in case of need, cells were conserved at -196°C in liquid nitrogen. Cells were supplied with freezing medium (FCS with 10% dimethyl sulfoxide (DMSO)) and stored at -80°C or –196°C (long term storage) in 1 ml aliquots containing 1 - 3 x 10^6 cells.

2.2.1.2. Transient transfection using calcium phosphate

Transient transfection assays were carried out using the standard calcium phosphate coprecipitation technique. One day prior to transfection, cells were split to reach 70-80% confluency. Total DNA amounts were equalized using salmon sperm carrier DNA and mixed with calcium chloride. BES-buffered saline was then allowed to form complexes with the DNA-calcium chloride solution resulting in a fine precipitate of positively charged calcium and negatively charged phosphate. This suspension of precipitates was added to the culture medium and taken up by the cells.

2.2.1.3. Transient transfection using Lipofectamine™

One day prior to transfection, cells were split to reach 70-80% confluency. Transfections were carried out according to the manufacturer's instructions in serum-free medium. DNA and lipofectamine were added in a ratio of 1:2.5 (µg:µl) to the cells. For siRNA transfections, cells were incubated with 60 nM siRNA directed against Ap-2δ or control siRNA complexed with 4 µl lipofectamine for 72 hours before harvesting.

2.2.2. Molecular biology

2.2.2.1. Generation of chemically competent bacteria

E. coli Top 10 were inoculated into 5 ml of LB medium and grown overnight at 37°C and 200 rpm. On the next day, this culture was used to inoculate 200 ml LB medium and grown to an optical density (OD) 600 of 0.2 – 0.4. The bacterial suspension was cooled down and centrifuged at 2500 rpm for 5 min at 4°C. The pellet was resuspended in 100 ml 50 mM $CaCl_2$ and incubated on ice for 20 min. After sedimentation, the pellet was resuspended in 20 ml 50 mM $CaCl_2$ containing 15 % glycerol and stored in 100 µl aliquots at -80°C.

2.2.2.2. Transformation of chemically competent bacteria

Competent bacteria were thawed on ice. After addition of the transforming DNA (5 µl of the ligation or 0.1 – 10 ng plasmid DNA, respectively), the bacteria were incubated on ice for 30 minutes before they were subjected to a heat-shock at 42°C for 30 seconds. The bacteria were then incubated in 500 µl SOC medium in a thermocycler at 37°C for one hour. After sedimentation, the bacteria were resuspended in 50 µl of the remaining medium and either inoculated in liquid LB medium and 100 µg/ml ampicillin or plated on LB agar plates (LB medium containing 1% agar and 100 µg/ml ampicillin). The transformed bacteria grew overnight into visible colonies.

2.2.2.3. Isolation of plasmid DNA

Plasmid DNA extraction was based on alkaline lysis. Cultures of 2 ml LB inoculated with a colony from an agar plate were grown overnight at 37°C and 200 rpm. Each pellet was lysed in 300 µl Buffer 1 and denatured in 300 µl Buffer 2. After neutralization with 300 µl Buffer 3, bacterial suspension was centrifuged and DNA was precipitated using isopropanol. Then the DNA pellet was washed with 70% ethanol and air-dried. The DNA was solved in 30 µl 10 mM Tris-HCl, pH 8.5 and subjected to restriction analysis.
For larger amounts of plasmid DNA, overnight cultures of 100 ml LB inoculated with a colony from an agar plate or a recently prepared transformation were grown at 37°C and 200 rpm. After sedimentation of the bacteria, the plasmid DNA was extracted via

anion exchange using the Nucleobond Xtra Maxi Plus Kit according to the manufacturer's protocol.

2.2.2.4. Isolation of genomic DNA from cultivated cells

Cultivated cells were trypsinized and pelletized at 1000 rpm for 5 minutes. The pellet was lysed in 500 µl lysis buffer containing proteinase K and vortexed thoroughly. The lysis was performed overnight at 56°C on a thermocycler. DNA was precipitated by the addition of 500 µl isopropanol. The precipitated DNA was sedimented at 13,000 rpm for 30 minutes at 4°C and subsequently washed with 70% ethanol for 15 minutes at 13,000 rpm to clean the pellet from residual ethanol or salts. After air-drying the pellet for 10 minutes, the DNA was solved in 50 - 200 µl 10 mM Tris, pH 8.5 (+ RNase 100 µg/ml)). For efficient solving, the resuspended DNA was incubated overnight at 37°C on a thermomixer.

2.2.2.5. Restriction hydrolysis

DNA was digested using restriction endonucleases from New England Biolabs. The reaction conditions included the enzyme-specific NEB buffers and 1% BSA as well as incubation under recommended temperatures. Plasmid DNA was digested with 2 - 5 U enzymes/µg DNA for 1 - 5 hours and analysed via agarose gel electrophoresis.

2.2.2.6. Purification of DNA

The purification of DNA from primers after PCR or from reagents after restriction hydrolysis was carried out using the High Pure PCR Purification Kit. Briefly, DNA was mixed with a high salt concentration buffer and bound to a silica membrane while contaminants passed through the column. Impurities were washed away by an ethanol-containing buffer and bound DNA was eluted using low salt concentration buffer.

2.2.2.7. Dephosphorylation

After plasmid restriction, the plasmid has two compatible ends that can self-ligate. In order to minimize religation and to increase cloning efficiency, 5'-ends of the plasmid were dephosphorylated so that only inserts with the essential 5'-phosphate ends can ligate with the plasmid. Dephosphorylation was performed using 2 units of shrimp

alkaline phosphatase for 1 μg of linearised plasmid. After 2 hours of incubation at 37°C, the enzyme was inactivated at 65°C for 15 minutes. The DNA was then purified from salts and proteins using the High Pure PCR Purification Kit.

2.2.2.8. Generation of blunt ends

DNA polymerase subunit, the Klenow fragment, catalyzes 5'->3' synthesis from primed single-stranded DNA in the presence of dNTP's. For the fill-in of recessed 3' termini, 0.3-1 µg of endonuclease-hydrolyzed DNA were incubated with New England BioLabs buffer 1, 100 µM dNTP's and 10 U of DNA polymerase I (Klenow) for 15 min at 25°C. After that, the reaction was terminated by the addition of 10 mM EDTA, heat-inactivated for 20 min at 75°C and purified using the PCR Purification Kit.

2.2.2.9. Ligation

For the alignment of two compatible DNA strands, the enzyme ligase connects the 5'-phosphate end of one strand with the 3'-OH end of the other strand. Purified DNA fragments were mixed with 2 µl 10x ligase buffer und 400 units ligase in a final volume of 20 µl and incubated at 16°C overnight.
PCR products were ligated into plasmids using the TOPO® TA cloning kit. The ligation was performed according to the manufacturer's instructions.

2.2.2.10. Agarose gel electrophoresis

DNA fragments were separated according to size using agarose gel electrophoresis. Within an electrical field, DNA moves to the anode due to its negatively charged phosphate backbone. The velocity of movement is inversely proportional to the logarithm of the molecular weight of the DNA fragment. By the addition of the intercalating dye ethidium bromide, DNA was visualized under short wave UV light (254 nm). The size of the DNA fragments was determined from a parallely loaded, defined migration standards.

Gels were prepared with 0.8 – 2 % (m/v) agarose solved by boiling in 1 x TAE buffer and supplied with ethidium bromide (1:10,000; c = 10 mg mL^{-1}). Gels were subjected to electrophoresis at 80 volts for 1-2 hours in 1 x TAE.

2.2.2.11. Isolation of DNA fragments

For the isolation of DNA fragments after restriction hydrolysis, DNA was separated according to size on an agarose gel. DNA was visualized under longwave UV light and the desired band was excised with a scalpel. The DNA was recoverd from the agarose block using the Zymoclean Gel DNA Recovery Kit according to the manufacturer's protocol. Agarose was melted at 50°C under slightly acidic conditions and bound to a silica membrane. Agarose was removed with a washing step and DNA was eluted under alkaline conditions.

2.2.2.12. Photometric quantification of DNA

The concentration of a DNA solution was determined with a photometer at a wavelength of 260 nm. An optical density (OD) of 1 equals a DNA concentration of 50 μg mL^{-1}. The OD $ratio_{260/280}$ determines the purity of the DNA where a ratio of > 1.8 defines pure DNA. A lower ratio indicates contaminations with proteins because aromatic amino acids absorb light at 280 nm.

2.2.2.13. Amplification of DNA fragments

DNA fragments were specifically amplified using the polymerase chain reaction (PCR, Mullis et al.,1986). A typical reaction contained 200 ng template DNA, 1x High Fidelity PCR buffer, 0.2 mM dNTP's, 2 mM $MgSO_4$, 0.2 µM each primer and 1 U Platinum Taq High Fidelity Polymerase. The PCR was performed in a PCR thermocycler under conditions summarized in Table 1.

Table 2: PCR cycling conditions

Cycle step	Temperature	Time	# of cycles
Initial denaturation	94°C	2 min	1
Denaturation	94°C	30 sec	30
Annealing	60°C	30 sec	
Extension	72°C	1 min/kb	
Storage	4°C	infinite	

1.1.1.1. Isolation of RNA

Total RNA was isolated with the help of Trizol® Reagent. Pellets of trypsinized cells grown to 80-90% confluency in a 6-well plate were resuspended in 0.5 ml Trizol and incubated for 5 min at room temperature and for 1 min at 30°C. Then, 200 µl of chloroform was added, vortexed for 15 sec and incubated for 2 min. The reaction was centrifuged for 15 min at 13,000 rpm and 4°C. After that, the colorless upper aqueous phase containing the RNA was transferred to a fresh tube and RNA was precipitated by adding 500 µl isopropanol. Samples were incubated for 10 min at room temperature and then centrifuged for 10 min at 13,000 rpm and 4°C. The pellet was washed with 1 ml 70% ethanol and centrifuged for 5 min at 7,500 rpm and 4°C. Subsequently, the RNA pellet was air-dried for 5-10 min and redissolved in 50 µl DEPC-treated water. Finally, RNA was incubated for 10 min at 55-60°C and stored in aliquots at -80°C.

2.2.2.14. RNA gel electrophoresis

Agarose gel (1.2%) was prepared using Mops buffer and 5% formaldehyde. Prior to electrophoresis, RNA was boiled with 10 µl FDP and 2 µl loading buffer in a total volume of 20 µl. Gels were subjected to electrophoresis at 100 volts for 30 min in 1 x Mops.

2.2.2.15. cDNA synthesis

Total RNA was isolated with the help of Trizol Reagent (see Isolation of RNA) and cDNA synthesis was performed using the SuperScript Reverse Transcription kit. 500 ng - 2 µg RNA were mixed with 1 µl Oligo(dT) and 1 µl dNTPs (10 mM) to a final volume of 13 µl and incubated at 65 °C for 5 minutes. This was followed by the addition of 4 µl reverse transcriptase buffer, 1 µl DTT, 1 µl RNAse OUT^{TM} and 1 µl Superscript III reverse transcriptase. cDNA synthesis was carried out at 50°C for one hour followed by heat inactivation at 70°C for 15 minutes.

2.2.2.16. Quantitative real-time PCR

Gene expression was monitored by quantitative real-time PCR using SYBR GreenER qPCR SuperMix (Invitrogen) in an ABI Prism 7900 (Applied Biosystems). The SYBR

GreenER qPCR SuperMix allows normalization with ROX reference dye which adjusts for non-PCR-related fluctuations in fluorescence between reactions. Each individual analysis was performed in triplicates. The Ct (cycle threshold) value defines the number of cycles required for the fluorescence signal to exceed the background. These values are proportional to the amount of DNA. Expression values were normalized to the mean of housekeeper Hprt or Gapdh.

Table 3: Quantitative real-time PCR reagent mix

Reagent	Volume
cDNA	1.5 µl
10 mM Primer mix (forward and reverse)	2 µl
SYBR GreenER qPCR SuperMix	5 µl
DEPC-treated water	ad 10 µl

Table 4: Quantitative real-time PCR cycling conditions

Cycling step	temperature	time	# of cycles
UDG incubation	50°C	2 min	1
UDG inactivation/ DNA polymerase activation	95°C	10 min	1
Denaturation	95°C	15 sec	40
Annealing	60°C	1 min	40

UDG: uracil DNA glycosylase

Melting curve analysis was performed for each set of primers to avoid primer dimer formation.

2.2.2.17. Statistical methods

Statistical significance was calculated using the students' t-test. A p-value less than 0.05 was considered to be significant. (* = $p < 0.05$; ** = $p < 0.005$; *** = $p < 0.0005$)

2.2.2.18. Sequencing

DNA was sequenced according to Sanger and performed by Entelechon (Regensburg). DNA sequences were evaluated using the sequence alignment tool HUSAR (Heidelberg UNIX Sequence Analysis Resources) provided by the DKFZ (Heidelberg), the data bases NCBI (www.ncbi.nlm.nih.gov/), and Ensembl (www.ensembl.org/index.html).

2.2.2.19. Affymetrix microarray procedures

RNA of 15 Ap-2δ-/- and wild-type E15 posterior midbrains was purified using the RNeasyMini-kit from Qiagen. 2.5 µg RNA was transcribed into biotinylated cRNA according to the Affymetrix standard protocol version 2. After purification and fragmentation, cRNA was hybridized to Affimetrix GeneChip Mouse Genome xY 2. = ArraysHG-U133Plus_2.0 microarrays (Affymetrix Inc.). The microarray data have been released into the GEO-database (Accession Number GSE27296).

2.2.3. Biochemistry

2.2.3.1. Preparation of protein samples from adherent cells

Cells were washed and scraped off in ice cold PBS. Cells were pelleted by centrifugation at 3,000 rpm for 3 minutes at 4°C and lysed with RIPA buffer or coimmunoprecipitation buffer on ice for 30 min in the presence of protease inhibitor. The lysates were cleared by centrifugation for 15 minutes at 12,000 rpm.

2.2.3.2. Protein quantification

Protein was quantified using the Bradford dye assay employing coomassie blue and a BSA (bovine serum albumine) standard comprising five concentrations (0.25 µg, 1.25 µg, 2.5 µg, 5 µg and 7.5 µg). Absorption measurements were determined photometrically by an ELISA reader. Protein concentrations were calculated from plotted standard curve.

2.2.3.3. SDS-PAGE/Western Blot

SDS-PAGE separates proteins based on their weight and electrical properties as they migrate through a polyacrylamide gel. Denatured cell extracts as well as a prestained molecular weight marker were loaded onto a polyacrylamide gel and separated by electrophoresis at 45-65 mA in 1x Laemmli running buffer.
Proteins were then immobilized on a polyvinylidene fluoride (PVDF) membrane with the semi-dry blotting method in western transfer buffer by applying an electrical field (11 V for 1,25 hours). In order to reduce non-specific protein interactions between the membrane and the antibody, free binding sites were blocked with 5% non-fat dry milk in PBST for 1-3h. Proteins were detected by incubation with specific antibodies

in 5% non-fat dry milk in PBST overnight at 4°C and with secondary HRP conjugated antibodies in PBST for 1 hour at room temperature. Bound antibodies were visualized with the help of chemiluminescence and autoradiography films according to the manufacturer's protocol.

2.2.3.4. Protein staining with Coomassie Brilliant Blue R250

The PVDF membrane was stained with Coomasie Blue for 2 minutes and then incubated with Destain solution for approximately 15 minutes, until the background was reduced and blue bands were clearly visible.

2.2.3.5. Immunofluorescence

Transfected cells were fixed with 4% paraformaldehyde for 10 minutes at room temperature. Permeabilization was achieved with 0.2% Triton-X in PBS for 5 minutes. Free binding sites were blocked with 1.5% BSA in PBS for 1 hour. Anti-Nfatc2 and anti-Ap-2δ antibodies were diluted 1:400 in PBS containing 1.5% BSA and incubated overnight at 4°C. Unbound antibody was washed away with PBS. Proteins were detected with Alexa Fluor 488- and Alexa Fluor 595-conjugated antibodies diluted 1:400 in PBS containing 1.5% BSA for 1 hour at room temperature. Cell nuclei were stained with Hoechst 33342 diluted 1:500 in PBS containing 1.5% BSA for 5 minutes. Analysis of immunofluorescence was performed with a fluorescence microscope.

2.2.4. Functional studies

2.2.4.1. Luciferase assay

Neuro2a cells were co-transfected with the reporter plasmids pGl3-Pou4f3 -2.8 kb, pGl3-Bhlhb4 -6 kb, pGl3-Bhlhb4 -0.5 kb and the expression plasmid pSG5-Ap-2δ. Cells were lysed 48 hours later for 5 minutes in lysis buffer. After sedimentation, 10 µl of the supernatant were transferred to a white luminometer 96-well plate.
Luciferase (LUC) activity was assayed with 50 µl assay buffer for 1 second as recommended by the manufacturer in the Luminometer Centro LB 960. Relative light units were normalized to protein concentration using the Bradford dye assay. All experiments were repeated at least five times.

2.2.4.2. Chromatin immunoprecipitation (ChIP)

Expression plasmid transfected Neuro2a cells were grown 48 hours before harvesting for ChIP. Aliquots of $2x10^6$ cells were cross-linked with 1% formaldehyde for 7 minutes and incubated with 0.1 M glycine for 5 minutes at room temperature with intensive shaking in a thermomixer (1100rpm). After two rounds of washing with 1 ml cold PBS, cells were resuspended in 200 µl SDS Lysis Buffer and sonicated for 3 cycles consisting of 7.5 minutes (30 seconds "ON"/30 seconds "OFF"). Immunoprecipitation mix contained 50 µg sonicated DNA, 2 µg salmon sperm DNA, and protease inhibitors in ChIP dilution buffer in a final volume of 400 µl. Specific antibodies against Ap-2δ, Nfatc2, HA and IgG as a negative control were added to the probes and incubated for 2-4 hours at 4°C at constant rotation. After that, 25 µl of each protein A and protein G coupled Dynabeads® (Invitrogen, Karlsruhe, Germany) were washed with dilution buffer and added to the probes for overnight incubation. On the next day, protein/DNA complexes were washed three times with 500 µl wash buffer, eluted for 1-2 hours using 100 µl elution buffer, reverse crosslinked and Proteinase K digested under the following conditions:

Table 5: Reverse crosslink

Temperature	Time
55°C	2 hours
65°C	6 hours
75°C	2 hours
4°C	infinite

Purified DNA specimens were subjected to real-time PCR using SYBR GreenER qPCR SuperMix as indicated above (qRT-PCR). Amplicons were normalized to the DNA immunoprecipitated with antibody to histone H3 (Abcam, Cambridge, UK). Values were displayed as percent H3 with H3 occupancy arbitrarily set to 100%.

2.2.4.3. Annealing of oligonucleotides for EMSA

Double-stranded oligonucleotides were prepared by incubating 30 µg of single-stranded, complementary olidonucleotides with 1x NEB buffer 1 in a final volume of 100 µl at 85°C for 10 minutes and slowly cooled down to room temperature. Annealed oligonucleotides were precipitated with 4 volumes 100% ethanol, 0.1 volume 3 M NaAc and 1 M $MgCl_2$ for at least 30 minutes at -80°C followed by

centrifugation at 13000 rpm for 30 minutes at 4°C. Pellets were resuspended in 60 µl water.

2.2.4.4. Radioactive labeling of oligonucleotides

100 ng of double-stranded oligonucleotides were 5'-labeled by Klenow with 50 µCi [α-^{32}P] CTP. Labeling reactions were incubated at 30°C for 30 minutes. ProbeQuant G-50 Micro Columns were used according to the manufacturer's instructions to remove unincorporated [α-^{32}P] CTP.

2.2.4.5. EMSA

The TNT-coupled reticulocyte extract (Promega) was employed to generate *in vitro* translated Ap-2δ protein. Protein was diluted in EMSA binding buffer and incubated with approximately 0.8 ng of the ^{32}P-labeled oligonucleotide probe in at room temperature for 20 min. Separation of complexes was achieved on 5% nondenaturing polyacrylamide gels in 0.25 × TBE running buffer at room temperature. After electrophoresis, gels were dried and subjected to autoradiography at −80°C. To demonstrate the presence of Ap-2δ in the shifted complexes, samples were incubated with α-Ap-2δ and rabbit α-IgG antibodies. 80-fold excess of unlabeled oligo served as a competitor.

2.2.4.6. Expression and purification of recombinant GST fusion proteins in E. coli BL21

Chemically competent *E. coli BL21* were transformed with a plasmid coding for a N-terminal glutathione-S-transferase fused to the Ap-2δ transactivation domain. One colony was used to inoculate 40 ml of LB medium containing ampicillin. This overnight culture was diluted 1:10 and grown to an OD 600 of 0.7. The expression of the fusion protein was induced by adding 1 mM isopropyl-1-thio-β-D-galactopyranoside (IPTG). For control reasons, samples were collected before and after IPTG addition. After 2-3 hours, the bacteria were pelleted and resuspended in 10 ml lysis buffer. Lysis was achieved upon 3 repeated freeze-thaw cycles. Lysed bacteria were pelleted and supernatant containing recombinant protein was aliquoted and stored at -20°C. Again, a control sample was drawn from the supernatant.

Efficiency of protein expression and purification was analyzed by subjecting control samples to SDS-PAGE.

2.2.4.7. GST Pulldown

Glutathione Sepharose was precleared by washing 3 times with PBS. 50 µl of the precleared sepharose were combined with 15 µl GST alone or 250 µl GST-Ap-2δ, respectively, and incubated for one hour. The sepharose was washed three times with 1 ml pulldown interaction buffer and resuspended in 500 µl of the same buffer. To this sample, 5 µl of *in vitro* translated Ap-2δ protein was added and binding was facilitated by incubating for 1 hour at room temperature under constant rotation. After three washing steps with 1 ml interaction buffer, sepharose was resuspended in 20 µl Roti®-load, boiled at 95°C for five minutes and electrophoresed in a 15% polyacylamide gel.

2.2.4.8. Co-immunoprecipitation

Cells were transiently transfected with pCMX-Ap-2δ and pCMX-Nfatc2 and harvested after 48 hours in Co-IP lysis buffer. Immunoprecipitation was performed overnight with 100 – 300 µg protein lysate, 3 µl of anti-Ap-2δ antibody and either 40 µl immunoprecipitation matrix (Exacta Cruz B^{TM}, Santa Cruz, Heidelberg) or 25 µl of each protein A and protein G coupled Dynabeads®. After three washing steps with Co-IP lysis buffer, the pellet was resuspended in 2x Roti®-load and boiled for five minutes. The supernatant was electrophoresed and immunoblotted as described above using anti-HA.11 or anti-Nfatc2 antibody in a 1:5000 dilution. The HRP-conjugated Exacta Cruz B detection reagents or conventional HRP-conjugated antibodies were used as secondary antibodies.

3. Results

The following work was carried out in collaboration with PD Dr. Markus Moser (Martinsried). The results of project 3.1 have been published in PlosOne. “Ap-2δ is a crucial transcriptional regulator of the posterior midbrain” (Hesse et al., 2011).
A manuscript for publication on the findings of project 3.2 is currently in preparation. “Transcription factors Ap-2δ and Nfatc2 interact to synergistically regulate target gene transcription”.

3.1. Ap-2δ is a crucial transcriptional regulator of the posterior midbrain

3.1.1. Loss of colliculus inferior in Ap-2δ-deficient mice

In an effort to elucidate the role of Ap-2δ *in vivo*, the *Tcfap2d* gene was inactivated in mice by Markus Moser (MPI Martinsried). Owing to the brain-specific expression of Ap-2δ, embryonic lethality of the mice was not expected and thus, we did not choose to construct an inducible null-allele. The constitutive *Tcfap2d*-deficient mice were generated by gene targeting. The first exon of the *Tcfap2d* gene was deleted by insertion of a β-galactosidase-neomycin cassette. Heterozygous Ap-2δ mice (*Tcfap2d* +/-) did not exhibit an overt phenotype and produced offspring. In contrast to other established *Tcfap2* knockouts (Eckert et al., 2005) (except for *Tcfap2e*), Ap-2δ-deficient mice (*Tcfap2d*-/-) completed embryogenesis and were vital.
Further analysis of these mice addressed the question of whether loss of *Tcfap2d* affects brain morphology. As already comprehensively described in the introduction, Ap-2δ expression is mainly restricted to the brain, and to a lesser extent to retina and myocardium. The brains of 6 weeks old *Tcfap2d*-/- mice had developed into a normally organized forebrain and hindbrain. However, analysis of sagittal brain

sections of Ap-2δ mutant mice revealed the absence of a structure of the posterior midbrain, the colliculus inferior (Fig. 5a, b).

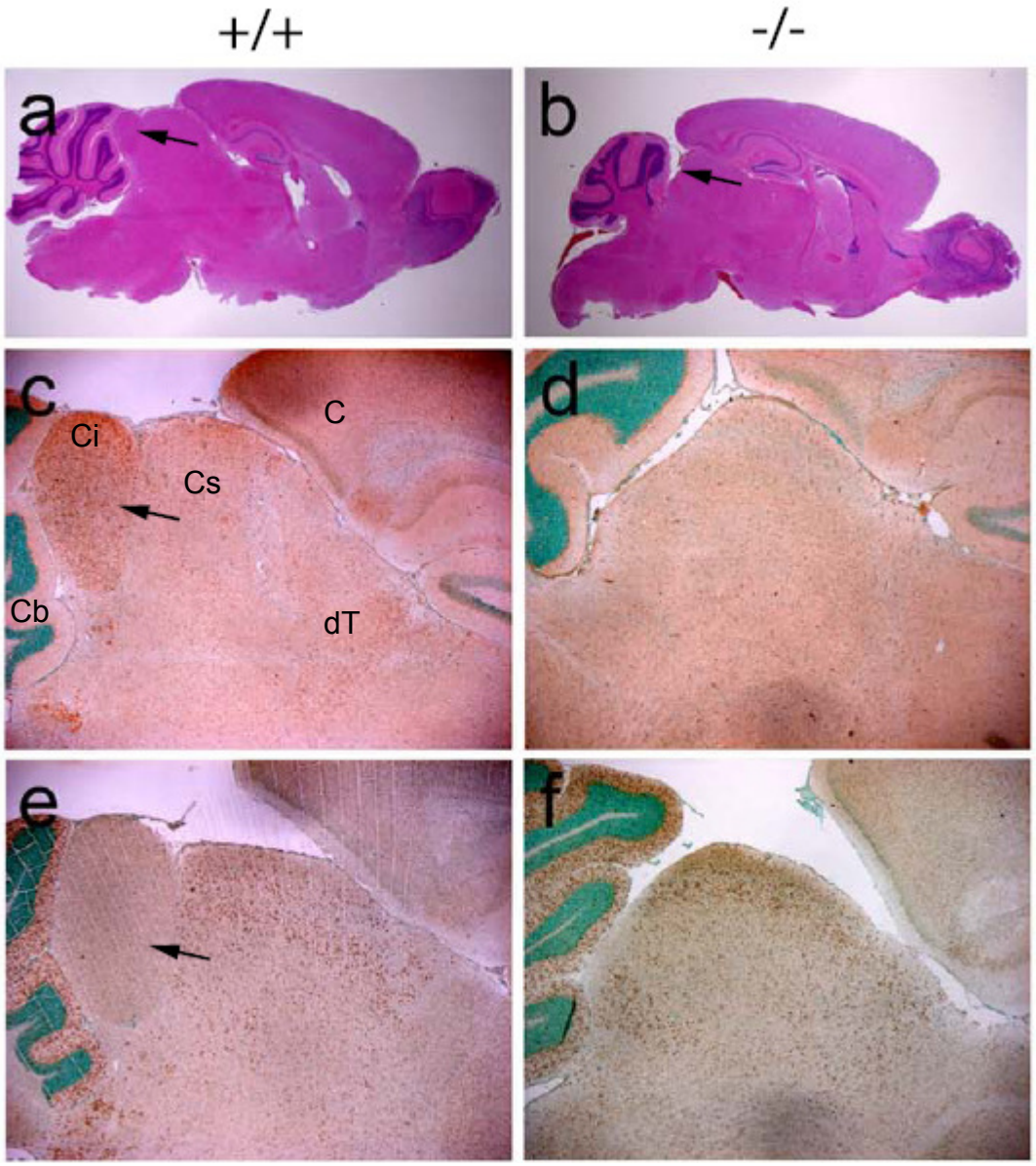

Markus Moser (Hesse et al., 2011)

Figure 5: Histological differences between wild-type (+/+) and Ap-2δ-deficient (-/-) posterior midbrains (a, b) Midbrain paraffin sections of 1.5 months old mice were stained with hematoxylin-eosin. The colliculus inferior (Ci) is missing in Ap-2δ-deficient mice (arrow). (c-f) Labeling of Ap-2 expression with Ap-2δ (c, d) and Ap-2α (e, f) -specific antibodies on sagittal sections from 3 weeks old mice midbrains. Ap-2δ antibody reactivity is concentrated in the colliculus inferior. The colliculus superior (Cs) and the dorsal thalamus (dT) also stain positive for Ap-2δ. Ap-2α expression can be detected in the colliculus superior and the cerebellum (Cb) of wild-type animals. In Ap-2δ-deficient brains that lack the colliculus inferior, Ap-2α is expressed throughout the entire mesencephalon. C = cortex

Ap-2δ expression was visualized with the help of an isoform-specific Ap-2δ rabbit antiserum kindly provided by PD Dr. Markus Moser. In adult wild-type brains, Ap-2δ

is expressed in the colliculus inferior and, to a lesser extent, the dorsal thalamus and the colliculus superior (Fig. 5c). Immunostaining of sagittal brain sections from *Tcfap2d*-/- mice with the Ap-2δ antibody did not produce any signal indicating the absence of Ap-2δ protein (Fig. 5d). Ap-2α is strongly expressed in the colliculus superior and the cerebellum which are structures of the anterior dorsal midbrain. Ap-2α is not co-expressed with Ap-2δ in the colliculus inferior (Fig. 5e). Of note, Ap-2α expression extends throughout the entire mesencephalon of *Tcfap2d*-/- mice substantiating the complete absence of the colliculus inferior (Fig. 5f).

3.1.2. Ap-2δ-deficient mice lack colliculus inferior as a result of apoptosis

Ap-2 transcription factors are involved in programming cell survival during embryogenesis since disruption of Ap-2 function leads to massive apoptosis (Moser et al., 1997). Therefore, it was analyzed if the colliculus inferior was lost as a result of increased cell death in the developing brain. The expression of the apoptotic marker activated caspase 3 was immunohistochemically investigated in embryonic brains between E13 and E17. Wild-type and Ap-2δ-deficient brains showed no signs of apoptosis at E13. At E15, however, first apoptotic cells stained positive for activated caspase 3 in the posterior midbrain of Ap-2δ-deficient mice. The number of cells undergoing apoptosis was dramatically increased by E17 in the posterior midbrain of Ap-2δ mutants. Control embryos did not experience enhanced apoptosis at neither developmental stage (Fig. 6, middle and right column). Labeling of consecutive wild-type sections with Ap-2δ antibody mapped Ap-2δ expression to the same region of the posterior midbrain where apoptotic cell death was observed in Ap-2 mutant mice (Fig. 6, right and left column). These data demonstrate that Ap-2δ deficiency leads to a dramatic increase in apoptosis and subsequent degradation of the posterior

midbrain and assign a role for Ap-2δ in cell survival and maturation of the posterior midbrain.

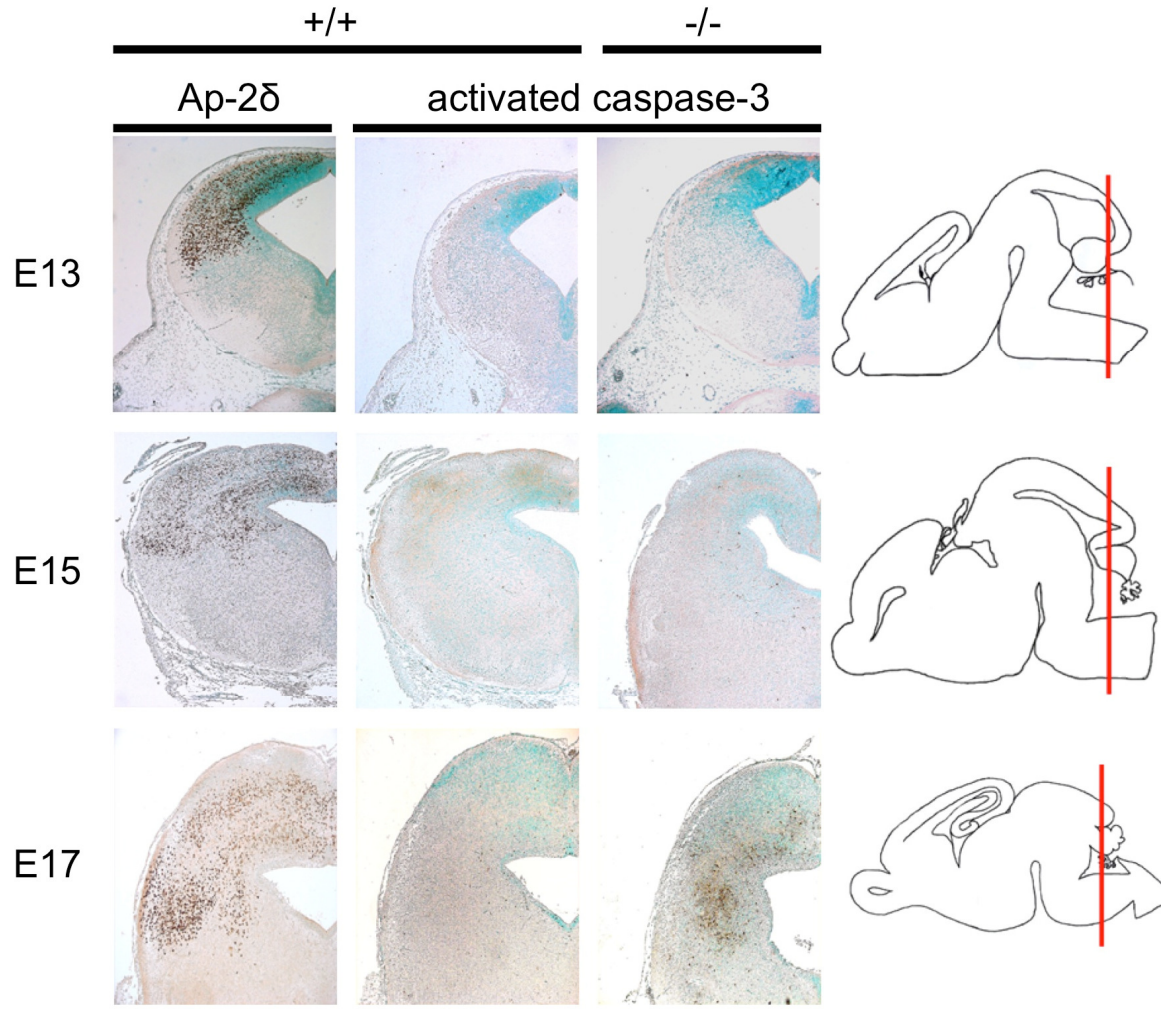

Markus Moser (Hesse et al., 2011)

Figure 6: Ap-2δ-deficiency leads to enhanced apoptosis in the posterior midbrain. (a) Using immunolabeling on coronal sections of embryonic brains of different developmental stages (E13-E17), Ap-2δ expression (left column) and apoptosis (middle and right column) were visualized with an Ap-2δ antibody or an activated caspase 3 antibody, respectively. At E15, single apoptotic cells stained positive in the posterior midbrain of Ap-2δ mutant mice (arrows). By E17, the number of apoptotic cells was dramatically increased in Ap-2δ-deficient brains. Very right column: Sectional plane through the brain.

3.1.3. Ap-2δ-regulated genes in the developing posterior midbrain

To dissect the mechanisms that are involved in posterior midbrain development under the control of Ap-2δ, Ap-2δ-specific target genes were identified using microarray analysis. Extraction of RNA was performed on E15.5 before the onset of

massive apoptosis. Fifteen wild-type and fifteen *Tcfap2d*-/- posterior midbrains were used for RNA preparation and pooled for the comparison of expression patterns by microarray analysis. Ap-2δ-deficient posterior midbrains showed a differential expression of 12 genes compared to wild-type expression levels (Table 6).

Table 6: In the posterior midbrain, knockout of *Tcfap2d* resulted in differential expression of 12 genes at E15.5.

No. of hits	Gene Name	Gene	Factor (ko vs. wt signal log ratio)
1	*Tcfap2d*	Transcription factor Ap-2δ	-1.84
4	*Mef2c*	Myocyte enhancer factor 2c	-1.34 -1.33 -1.43 -1.48
1	*Bhlhb4*	Basic helix-loop-helix domain containing, class B4	-1.70
1	*Pou4f3*	POU domain, class 4, transcription factor 3	-2.08
1	*Pitx2*	Paired-like homeodomain transcription factor 2	-1.28
3	*Rgs4*	Regulator of G-protein signaling 4	1.78 1.82 1.99
1	*Myh8*	Myosin, heavy polypeptide 8, skeletal muscle, perinatal	-2.09
1	*Cxcl12*	Chemokine (C-X-C motif) ligand 12	-1.60
1	*Ndst4*	N-deacetylase/N-sulfotransferase (heparin glucosaminyl)4	-1.93
1	*Slap*	Scr-like adaptor protein	-2.09
1	*Rdh9*	Retinol dehydrogenase 9	1.65
1	*Hjurp*	Holliday junction recognition protein	-1.38
1	*Fgf3*	Fibroblast growth factor 3	-1.66

To confirm differential expression detected via microarray analysis, quantitative RT-PCR analysis from total RNA samples isolated from the midbrains of E15.5 embryos was performed. Of the 12 candidate genes, 10 genes showed a reduced expression in Ap-2δ-deficient midbrain compared to wild-type tissue (Fig. 7). Interestingly, the

expression of two genes, *Rdh9* and *Rgs4*, was increased in the absence of Ap-2δ suggesting that Ap-2δ is also involved in transcriptional repression.

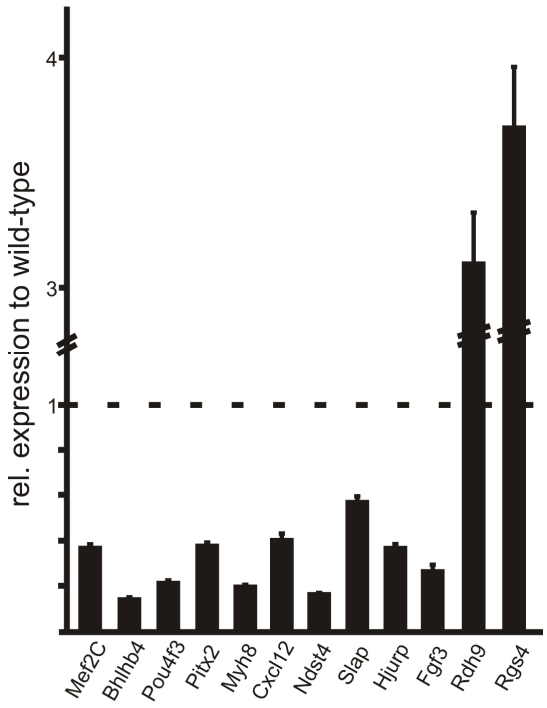

Figure 7: Validation of microarray data by quantitative real-time PCR. RNA samples isolated from the midbrains of E15.5 wildtype and *Tcfap2d*-/- embryos were subjected to qRT-PCR using target-specific primers. Bars are displayed as relative expression of candidates in *Tcfap2d*-/- embryos compared to wildtype embryos (Hesse et al., 2011).

Notably, among the identified putative Ap-2δ target genes were the four transcription factors *Pitx2* (paired-like homeodomain transcription factor 2), *Mef2c* (myocyte enhancer factor 2C), *Bhlhb4* (basic helix-loop-helix domain containing, class B4), and *Pou4f3* (POU domain, class 4, transcription factor 3). These transcription factors play fundamental roles during development (Gage et al., 1999; Lin et al., 1996) in particular the development and survival of sensory neurons (Bramblett et al., 2004; Xiang et al., 1998). Wild-type brains from E15.5 were used to verify expression of those transcription factors in the midbrain using whole mount *in situ* hybridizations (Fig. 8). Ap-2δ deficiency clearly abrogates expression of Pitx2, Mef2c, Bhlhb4 and Pou4f3 specifically in the midbrain, since other brain structures such as the forebrain

and thalamus continue to express *Mef2c* and *Pitx2*, respectively, in the absence of Ap-2δ (Fig. 8).

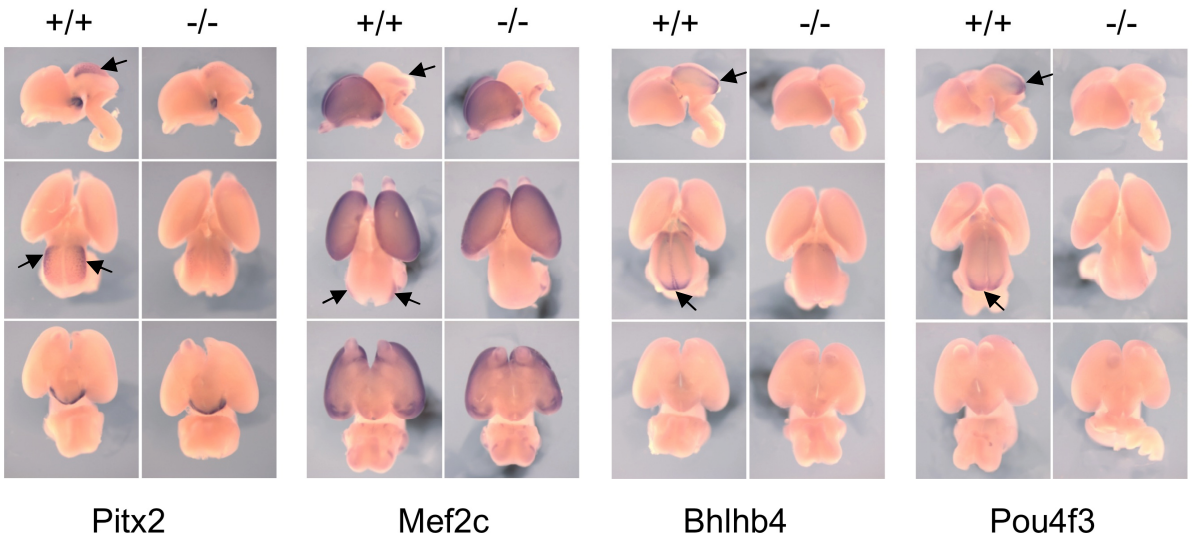

Figure 8: Loss of *Pitx2*, *Mef2c*, *Bhlhb4*, and *Pou4f3* expression in midbrain of *Tcfap2d*-deficient mice. *Pitx2*, *Mef2c*, *Bhlhb4* and *Pou4f3* expression was detected with the help of *in situ* hybridizations. Wild-type (+/+) and *Tcfap2d*-deficient (-/-) brains from E15 were probed with corresponding cDNA probes. The figure displays lateral (top), dorsal (middle) and ventral (below) views. Loss of Ap-2δ abolished expression of candidate targets in midbrain (arrows) (Hesse et al., 2011).

3.1.4. Ap-2δ transactivates Pou4f3 and Bhlhb4 promoter

The regulatory potential of Ap-2δ on the transcription of *Bhlhb4* and *Pou4f3* was investigated with the help of transient transfection experiments using candidate promoter-driven luciferase constructs were conducted. Luciferase reporters were generated containing 6 kb and 500 bp fragments of the *Bhlhb4* promoter (*Bhlhb4* -6kb and *Bhlhb4* -0.5kb, respectively) and a 2.8 kb fragment of the *Pou4f3* promoter (*Pou4f3* -2.8kb) (Fig. 9A) upstream of the firefly luciferase reporter gene.

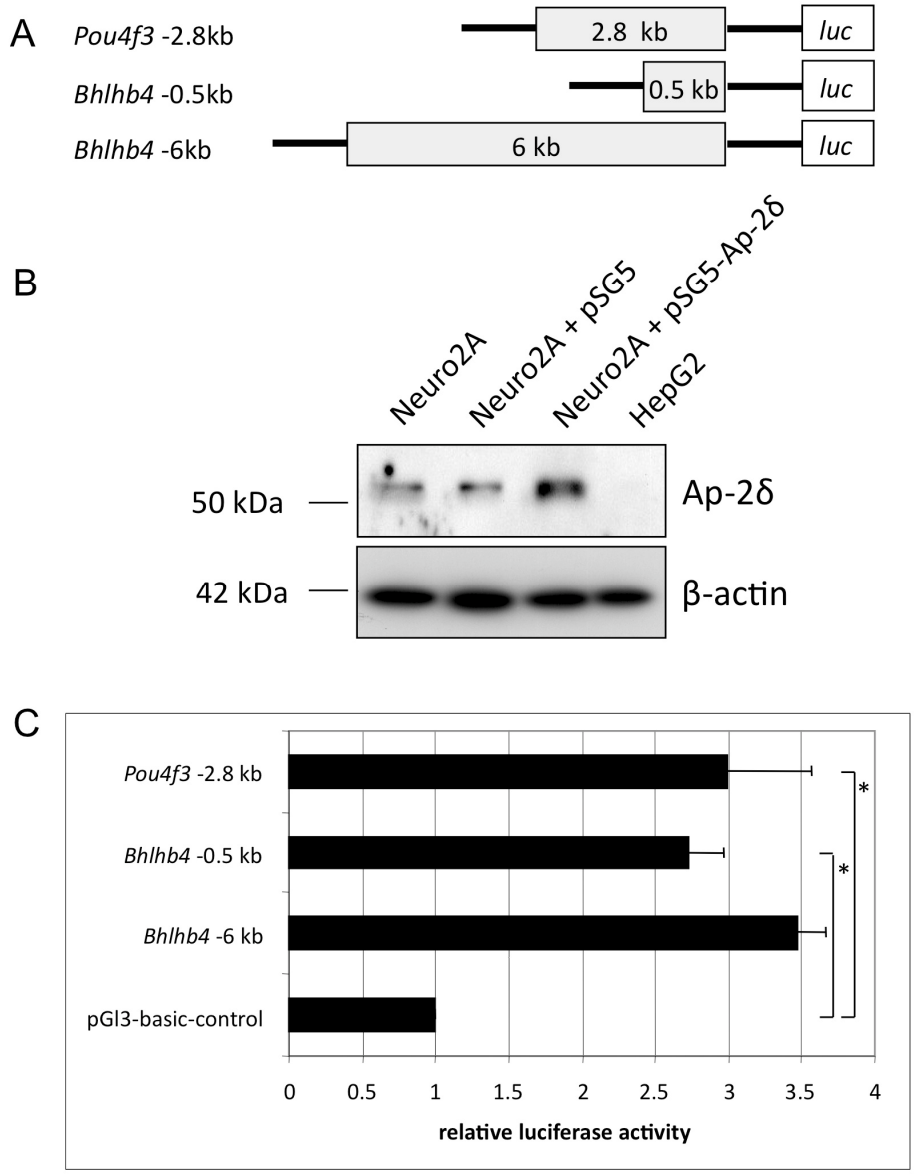

Figure 9: Ap-2δ functions as a transactivator of *Pou4f3* and *Bhlhb4* promoter
(A) Schematic presentation of reporter plasmids containing various lengths of 5'-flanking regions of Ap-2δ candidate target genes placed upstream of a luciferase reporter gene.
(B) Western Blot showing endogenous Ap-2δ expression in Neuro2a cells. Expression could be increased by transfection with the expression plasmid pSG5-Ap-2δ. β-actin was used as a loading control and HepG2 as negative control.
(C) Neuro2a cells were co-transfected with reporter plasmids *Pou4f3*-2.8kb, *Bhlhb4*-6kb, and Bhlhb4-0.5 kb together with an Ap-2δ expression plasmid or the empty plasmid as a control. Luc reporter constructs were activated by Ap-2δ. Luciferase units are displayed relative to total protein and show the mean ± s.e.m. of three independent transfections. Promoter-less pGl3-basic vector-only transfections were set at 1. p-values show significant increase to control plasmid-transfected cells. * = $p < 0.05$ (Hesse et al., 2011).

Transcriptional activation of these reporters was monitored following transfection in Neuro2a cells which endogenously express Ap-2δ. Transfection with an Ap-2δ

expression plasmid further increased expression (Fig. 9B). HepG2 cells do not express Ap-2δ and were used as a control. Cell lysates were collected and luciferase activity was measured 48 hours after transfection. All three reporter constructs were activated for more than 2.5-fold upon co-transfection of an Ap-2δ expression plasmid. This activation lies within the activating potential of Ap-2 proteins (Fig. 9C). The promoter-less pGl3-basic vector was used as a control.

3.1.5. In vivo promoter occupancy of Bhlhb4 and Pou4f3 by Ap-2δ

3.1.5.1. Optimization of ChIP conditions

To determine if Ap-2δ directly binds to and activates *Bhlhb4* and *Pou4f3*, chromatin immunoprecipitation (ChIP) followed by quantitative real-time PCR was performed.

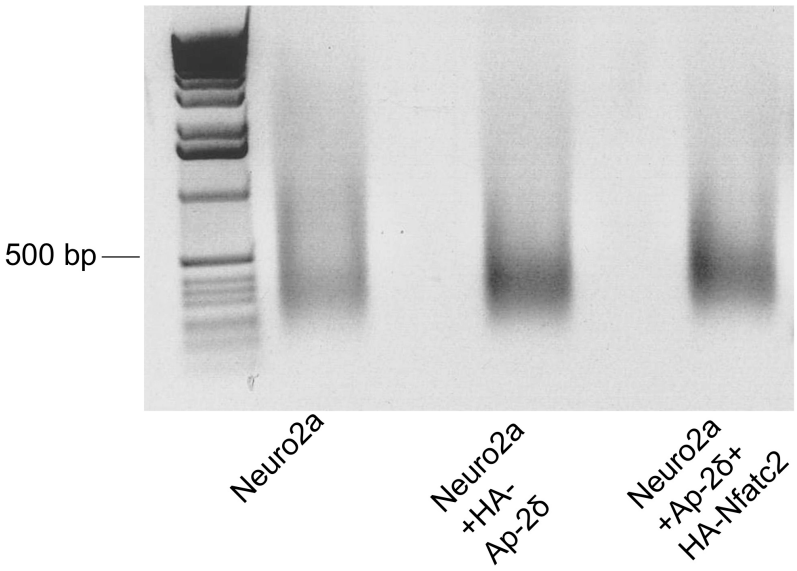

Figure 10: Chromatin fragmentation characterization
Agarose gel analysis of sheared chromatin obtained with the BioruptorTM (Diagenode). DNA and proteins of Neuro2a cells were crosslinked with 1% formaldehyde. Each sample consists of 2 x 10^6 cells in a total volume of 200 µl lysis buffer. Samples were sonicated for 3 cycles consisting of 7.5 minutes (30 seconds "ON"/30 seconds "OFF") and cross-linking was reversed. Lane 1 contains a 1kb DNA ladder.

ChIP is a powerful tool to study if a protein of interest is localized to a specific genomic locus *in vivo*. Sheared chromatin fragments are enriched with antibodies specific for the protein of interest which has been crosslinked to the DNA before. Quantitative real-time PCR is then employed to detect specific DNA sequences in the enriched chromatin.

Chromatin DNA was fragmented to an average apparent size of 200 to 500 bp (Fig. 10). Samples were sonicated for 3 cycles consisting of 7.5 minutes (30 seconds "ON"/30 seconds "OFF") and submitted to cross-linking reversion. Subsequently, chromatin fragmentation was judged by agarose gel electrophoresis (Fig. 10).

With the help of algorithm rVista and manual sequence analysis, potential Ap-2 binding sites were identified on genomic loci of *Bhlhb4* and *Pou4f3* within 3 kb upstream of the transcriptional start site (TSS).

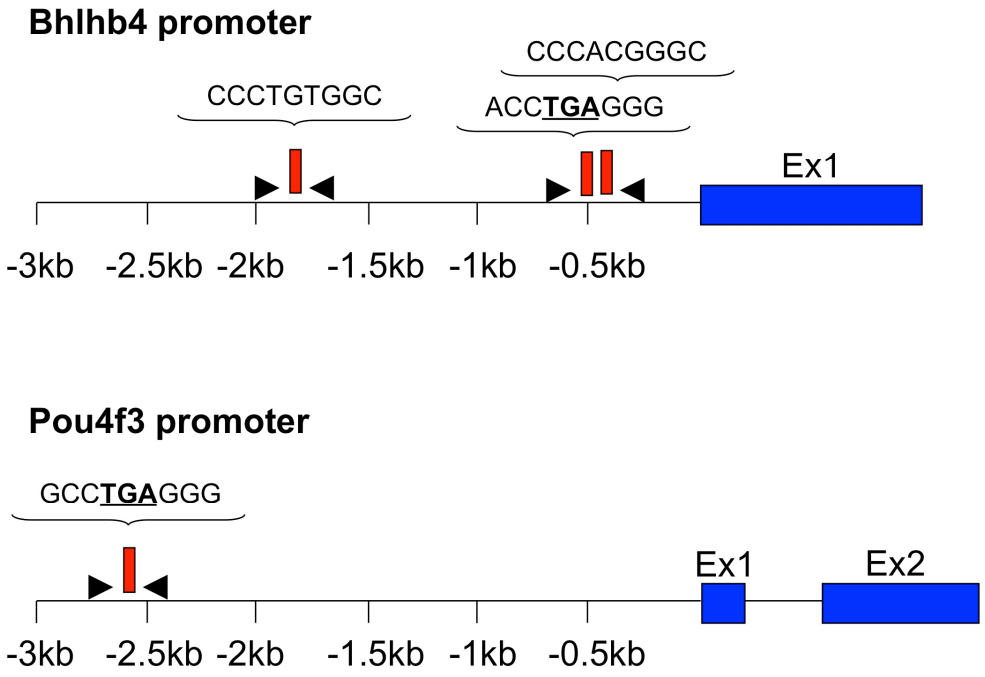

Figure 11: Schematic presentation of *Bhlhb4* and *Pou4f3* genomic loci. With the help of algorithm rVista and manual sequence analysis three potential Ap-2 binding sites were identified in the *Bhlhb4* promoter and one potential binding site in the *Pou4f3* promoter. Binding sites are displayed as red bars, primers are depicted as arrows. Numbers indicate location relative to TSS. Ex = exon

This resulted in the detection of two regions with three putative binding sites in the Bhlhb4 promoter. One sequence in the Pou4f3 promoter was of special interest because it consists of a central TGA spacer flanked by GCC and GGG triplets (Fig. 11). Zhao et al. (Zhao et al., 2003) could show that Ap-2δ specifically binds to a sequence with TGA as the preferred central 3 bp spacer between the palindromic GCC motifs. Primers were designed to specifically amplify those putative binding sites.

3.1.5.2. Ap-2δ associates to Bhlhb4 and Pou4f3 promoters in vivo

Neuro2a cells endogenously express Ap-2δ but showed a strong increase in expression after transfection with an HA-tagged Ap-2δ expression plasmid (Fig. 12A). Chromatin of HA-tagged Ap-2δ-transfected Neuro2a cells or untransfected cells was immunoprecipitated with an α-HA/Ap-2δ antibody or α-IgG antibody as a negative control. The ChIP assay demonstrated a significant level of Ap-2δ binding in the genomic locus of *Bhlhb4* at the two previously identified binding sites located -1.8 kb and -300 bp upstream of the transcriptional start site (TSS) (Fig. 12B/C). Moreover, *Pou4f3* promoter occupancy by Ap-2δ was observed at the conserved recognition sequence 2.6 kb upstream of the TSS (Fig. 12D). In contrast, the association of Ap-2δ to these sites was not evident in untransfected cells or after immunoprecipitation with the control antibody (Fig. 12B-D).

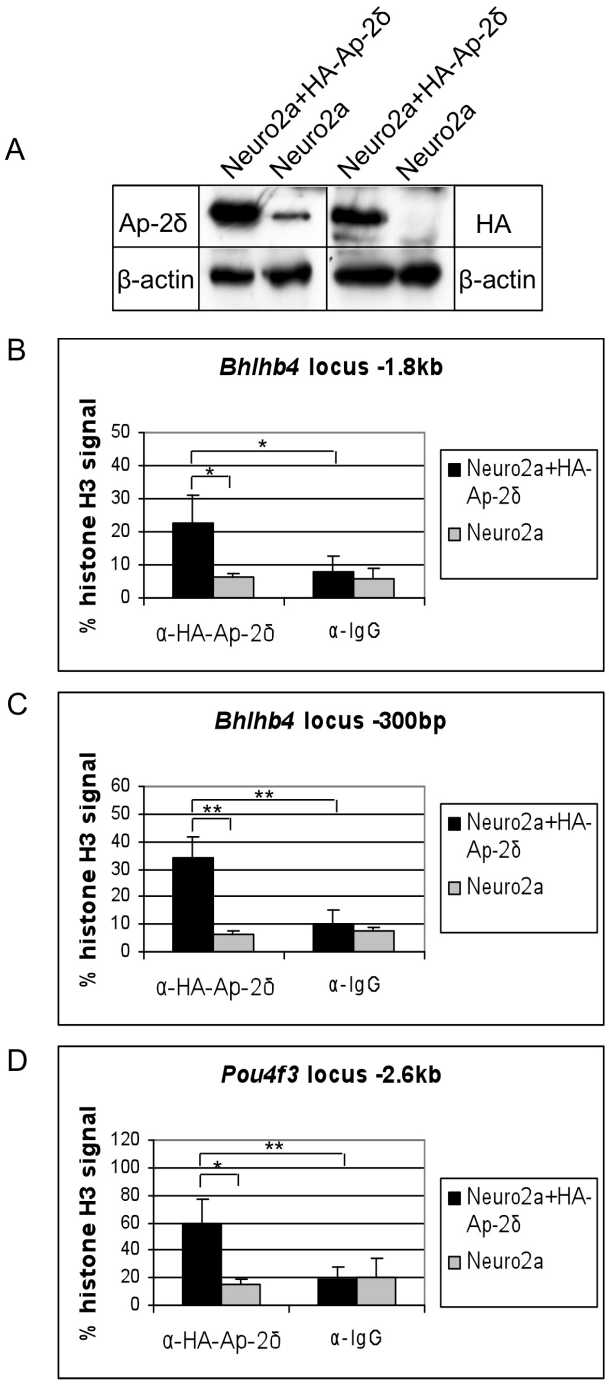

Figure 12: Ap-2δ occupies *Bhlhb4* and *Pou4f3* promoter *in vivo*
(A) Western blot analysis shows Ap-2δ expression and detection of the HA-tag as a control in protein extracts of untreated Neuro2a cells or transfected with an HA-tagged Ap-2δ expression plasmid. β-actin was used as a loading control.
(B/C/D) DNA from untransfected and HA-Ap-2δ transfected Neuro2a cells immunoprecipitated with antibodies to HA or IgG was quantified by real-time PCR using primers flanking the *Bhlhb4* (-1.6 kb and -300 bp) and the *Pou4f3* (-2.6kb) genomic loci upstream of the transcriptional start site (TSS). (B/C) Ap-2δ is associated to specific regions of the *Bhlhb4* promoter. Sites are located 1.8 kb and 300 bp upstream of the TSS. (D) *Pou4f3* promoter is bound by Ap-2δ 2.8 kb upstream of the TSS. Bars display mean abundance ± s.e.m. relative to histone H3 (internal control) from triplicates. P-values indicate significant differences from HA-Ap-2δ transfected Neuro2a cells precipitated with an anti-HA antibody compared to non-transfected Neuro2a cells or IgG treated lysates. ** = $p < 0.005$; * = $p < 0.05$ (Hesse et al., 2011)

3.1.6. Pou4f3 promoter is a direct target of Ap-2δ

Binding and transactivation by Ap-2 proteins is only achieved at recognition sites of the sequence $GCCN_{3/4}GGC$ or $GCCN_{3/4}GGG$. A sequence containing TGA as the preferred central 3 bp spacer which facilitates Ap-2δ binding is present in the *Pou4f3* promoter at the site demonstrated to be occupied by Ap-2δ. Thus, electrophoretic mobility shift assays (EMSA) were conducted to evaluate the direct binding of Ap-2δ to this sequence. This sensitive method is based on the fact that complexes of protein and DNA migrate through a non-denaturing polyacrylamide gel more slowly than free double-stranded oligonucleotides. The expression vector pCMX-Ap-2δ contains a T7 promoter which enables the *in vitro* translation of Ap-2δ. For visualization, the oligonucleotides being composed of the putative binding sites were ^{32}P-labeled. The EMSA assays demonstrated direct binding of Ap-2δ protein (pCMX-Ap-2δ) to both oligonucleotides containing the optimized Ap-2 binding site from Zhao et al. (Zhao probe) as positive control or the native binding site of the *Pou4f3* promoter (Pou wt probe) (Fig. 9A, lanes 2 and 7) (Zhao et al, 2003). The supershift obtained after addition of an α-Ap-2δ antibody but not an unrelated IgG antibody indicates the presence of Ap-2δ protein in the retarded complex (Fig. 13A, lanes 3 and 8; Fig. 13B, lanes 3 and 4). The signal of the Ap-2δ/DNA complex was antagonized by an 80-fold molar excess of unlabeled oligo (Zhao/Pou wt competitor)(Fig. 13A, lanes 4 and 5; 9 and 10).

The specificity of binding was manifested by introduction of mutations in the central 3 nucleotides between the palindromic GCC motifs (core sequence Pou wt: GCC TGA GGG, mutated forms Pou mt1: GCC AGT GGG, Pou mt2: GCC GTT GGG). Ap-2δ binding was abrogated upon mutagenesis of the consensus sequence demonstrating high specificity (Fig. 13B).

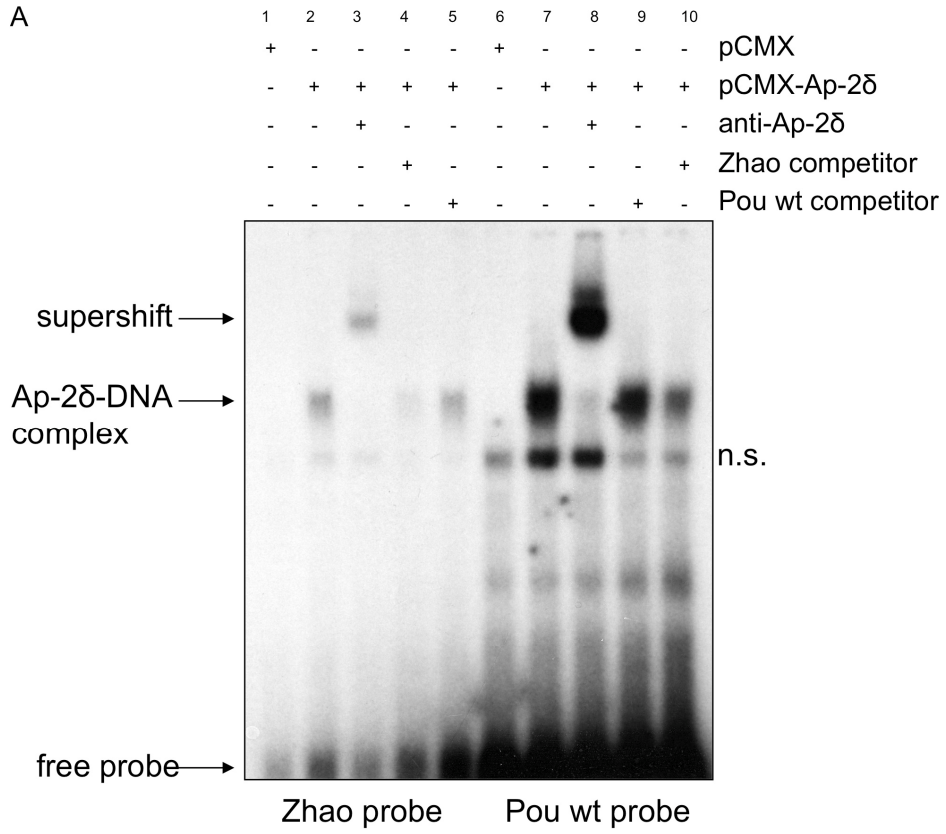
A
1 2 3 4 5 6 7 8 9 10
+ - - - - + - - - - pCMX
- + + + + - + + + + pCMX-Ap-2δ
- - + - - - - + - - anti-Ap-2δ
- - - + - - - - - + Zhao competitor
- - - - + - - - + - Pou wt competitor
supershift
Ap-2δ-DNA complex
n.s.
free probe
Zhao probe
Pou wt probe

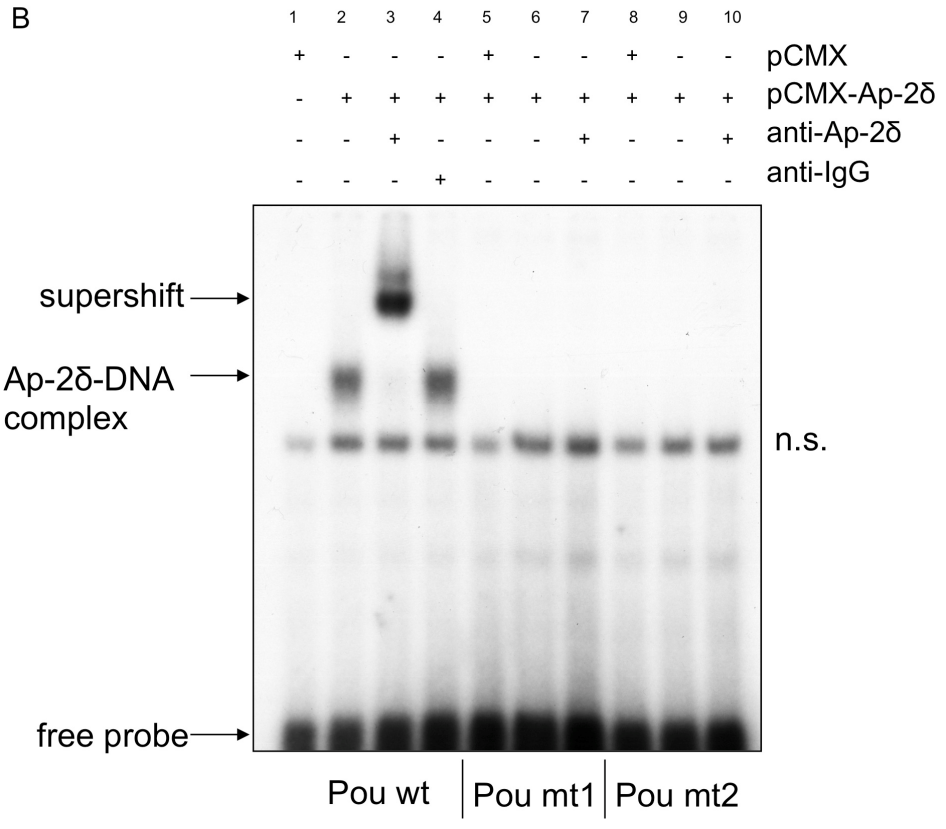
B
1 2 3 4 5 6 7 8 9 10
+ - - - + - - + - - pCMX
- + + + + + + + + + pCMX-Ap-2δ
- - + - - - + - - + anti-Ap-2δ
- - - + - - - - - - anti-IgG
supershift
Ap-2δ-DNA complex
n.s.
free probe
Pou wt
Pou mt1
Pou mt2

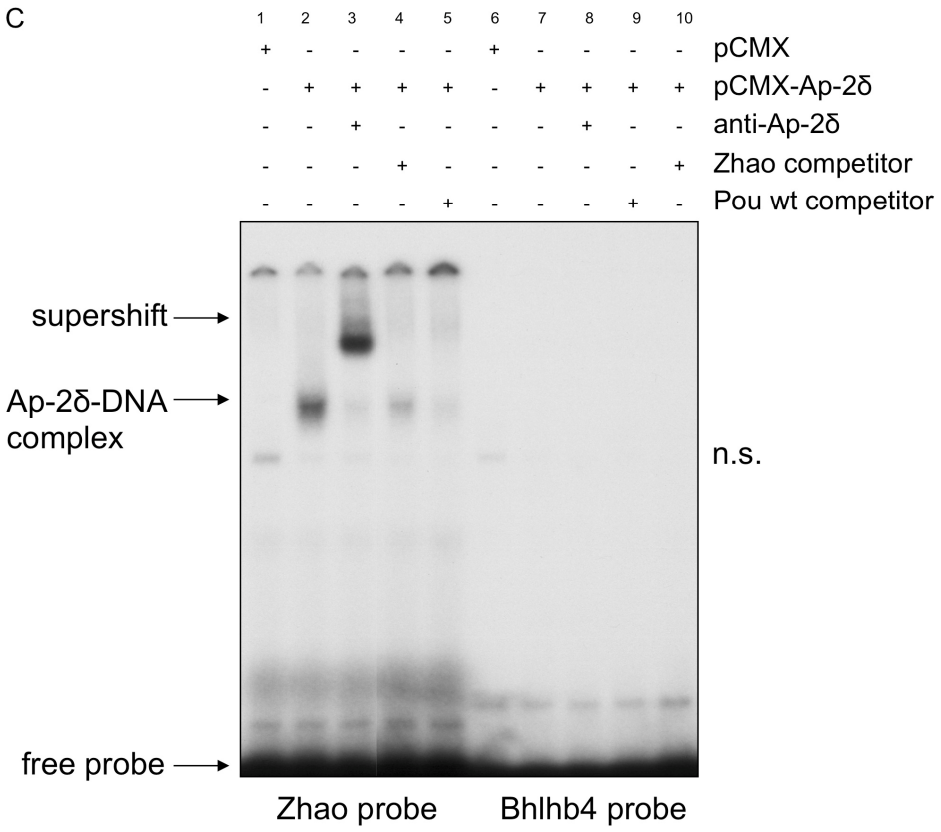

Figure 13: Direct binding of Ap-2δ to specific consensus sequence within *Pou4f3* promoter
(A) EMSA assay with ^{32}P-labeled oligonucleotide containing the specific binding site of the *Pou4f3* promoter (Pou wt) or an optimized Ap-2δ binding site (Zhao) and *in vitro* translated Ap-2δ protein. Addition of an α-Ap-2δ antibody but not an unspecific control antibody produced a supershift. Competition experiments were performed using an 80-fold excess of unlabeled oligonucleotide. pCMX = empty vector (control), pCMX-Ap-2δ = Ap-2δ cDNA; anti-Ap-2δ = Ap-2δ antibody, anti-rIgG = IgG antibody (control), Zhao/Pou wt competitor = unlabeled oligos
(B) EMSA assay with wildtype binding site of the *Pou4f3* promoter (core sequence: GCC TGA GGG) or mutated forms (Pou mt1: GCC AGT GGG, Pou mt2: GCC GTT GGG). Ap-2δ binding was abrogated upon mutagenesis of the consensus sequence (Hesse et al., 2011).
(C) EMSA was performed with an oligonucleotide containing a binding site of the *Bhlhb4* promoter or the optimized Ap-2δ binding site. *In vitro* translated Ap-2δ protein did not bind to the oligonucleotide derived from the Bhlhb4 promoter.
n.s. = not specific

In contrast to that, complex formation between *in vitro* translated Ap-2δ (pCMX-Ap-2δ) and oligonucleotides containing binding sites of the *Bhlhb4* promoter could not be detected. Fig. 13C shows an EMSA with the ACC TGA GGG binding site (*Bhlhb4* -300 bp) as an example. Thus, we assume that Ap-2δ might associate with and activate the *Bhlhb4* promoter through a complex with cofactors and interaction partners.

3.1.7. Pou4f3 target genes are downregulated upon Ap-2δ ablation

The downregulation of *Pou4f3* transcription after *Tcfap2d* knockout was demonstrated with the help of microarray analysis and qRT-PCR (Table 6, Fig.7) Whether Ap-2δ deficiency also had an effect on Pou4f3 target genes was examined next (Clough et al., 2004; Hertzano et al., 2007). Pou4f3 is expressed in a subset of cells of neuronal origin and all hair cells of the inner ear. It has been described to activate the promoter of brain-derived neurotrophic factor (Bdnf; (Clough et al., 2004). This neurotrophin is expressed in sensory hair cells of inner ear epithelia and is essential for normal afferent innervation of the inner ear (Pirvola et al., 1992). Transcript levels of *Bdnf* as well as *Calbindin2* were significantly downregulated in samples of Pou4f3-deficient inner ears compared to wildtype (Hertzano et al., 2007). Calbindin2 is a calcium-binding protein expressed in the cochlear nucleus (Friedland et al., 2006). It may be implicated in auditory processing due to upregulation of expression in aging animals and models of hearing loss (Fuentes-Santamaria et al., 2003; Zettel et al., 1997). The LIM domain transcription factor Lhx3 is a hair cell-specific gene expressed in all hair cells of the auditory and vestibular system. It was identified as an *in vivo* target gene of Pou4f3 by a microarray approach with inner ears of Pou4f3 mutant and wildtype mice (Hertzano et al., 2007).

RNA from posterior midbrain samples of wild-type and *Tcfap2d*-/- mice was subjected to cDNA conversion and subsequent qRT-PCR. In Ap-2δ mutant samples, mRNA levels of *Pou4f3* were reduced for more than 80% compared to control levels. Consistently, the Pou4f3 target gene *Bdnf* was also significantly downregulated and *Calbindin2* expression was slightly reduced. The gene encoding transcription factor *Lhx3*, another Pou4f3 target, was not affected by the absence of Ap-2δ (Fig. 14).

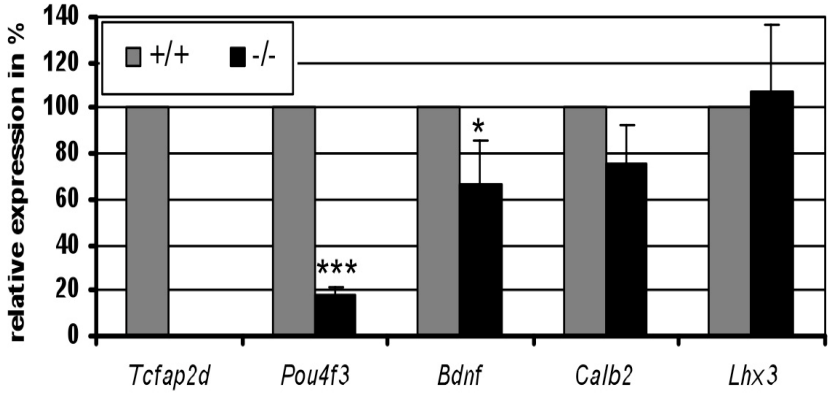

Figure 14: Relative mRNA expression of Pou4f3-regulated genes in Ap-2δ-deficient brains. qRT-PCR on posterior midbrains of wild-type and *Tcfap2d* knockout mice at E15 with 4-6 repetitions. HPRT served as reference gene. p-values indicate significant differences of targets in the posterior midbrains of *Tcfap2d* knockout mice compared to wild-types.*** = $p < 0.0005$; * = $p < 0.05$. Transcript levels of *Bdnf* and *Calbindin2* were reduced, whereas an alteration in expression of *Lhx3* cannot be observed upon Ap-2δ deficiency. Calb2 = Calbindin2 (Hesse et al., 2011)

3.2. Transcription factors Ap-2δ and Nfatc2 interact to synergistically regulate target gene transcription

A preliminary step in understanding protein function is to determine which proteins interact with each other, thereby identifying the relevant biological pathways. Up to date, only one interaction partner for Ap-2δ has been identified. Tan et al. demonstrated in 2008 an interaction between Ap-2δ and Ash2l and showed that these proteins cooperatively activate Hoxc8 (Tan et al., 2008). The identification of other interacting partners could elucidate the functional role of Ap-2δ. The transactivation domain is only poorly conserved among the Ap-2 proteins. A PY motif as well as few conserved residues were described to be essential for transactivation (Wankhade et al., 2000). Interestingly, Ap-2δ lacks those few conserved PY motif and characteristic residues. In an effort to isolate more proteins that interact with Ap-2δ, a yeast two-hybrid screen was conducted using the unique transactivation domain of Ap-2δ as a bait (Markus Moser, Martinsried). Screening of approximately 6 x 10^7 clones revealed 38 clones that (i) showed positive interaction after several rounds of confirmation and (ii) contained the same reading frame as the vector. Of these 38 clones, two clones, Nfatc2 and FoxG1, were especially interesting due to their function as transcription factors and were therefore chosen for further analysis. The calcium-sensitive Nfatc2 is expressed at relatively high levels in many brain compartments including the midbrain and colliculi (Vihma et al., 2008). In neurons, Nfatc2 is implicated in synaptic plasticity, axonal outgrowth and neuronal survival (Benedito et al., 2005; Graef et al., 1999; Groth and Mermelstein, 2003). FoxG1 is expressed in neuronal cells of the telencephalon, in particular the developing dentate gyrus and hippocampus (Murphy et al., 1994). In the mouse embryo, expression was also detected in the eye, foregut, and otic placode (Huh et al., 1999; Pauley et al.,

2006). FoxG1 is essential for proper proliferation of the neuronal progenitor population (Xuan et al., 1995).

3.2.1. Ap-2δ physically interacts with Nfatc2 and FoxG1

The interaction of Nfatc2 and FoxG1 with Ap-2δ determined by the yeast two-hybrid assay needed to be further verified using other independent methods such as the GST pulldown assay. The pull-down assay is an *in vitro* method used to determine a physical interaction between two proteins.

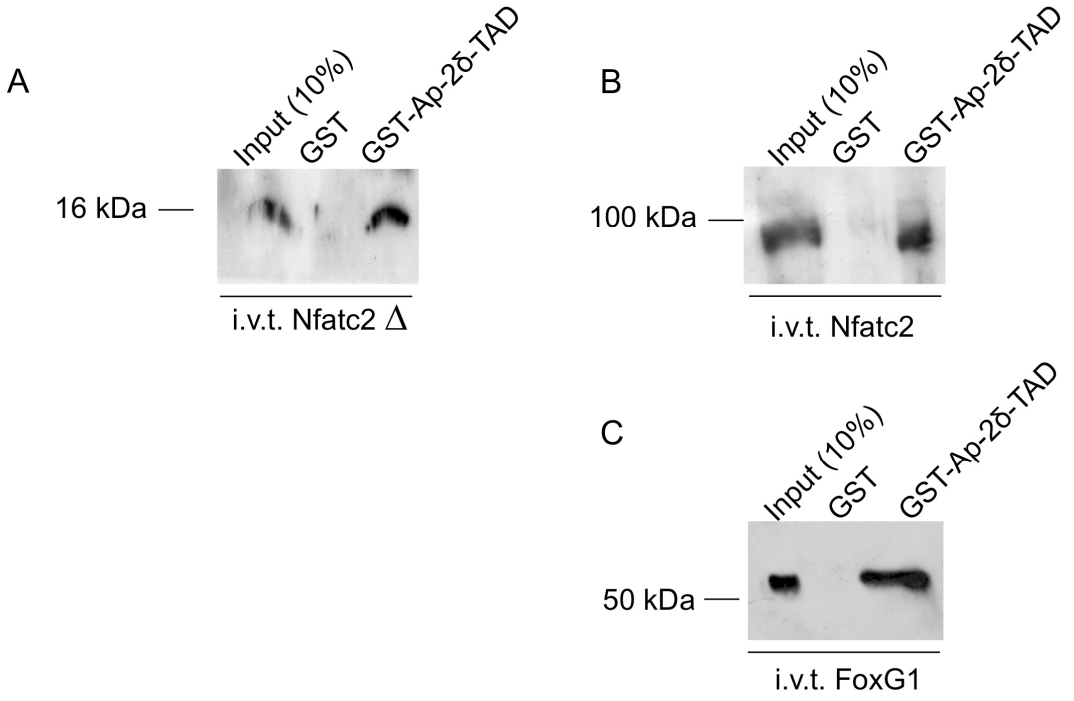

Figure 15: Nfatc2 and FoxG1 physically interact with the transactivation domain of Ap-2δ. GST-Ap-2δ-TAD or GST alone as negative control were probed for interaction with *in vitro* translated (i.v.t.) Nfatc2 and FoxG1. Interaction was detected via α-HA immunoblotting. Partial (A) and full length (B) Nfatc2 as well as full length FoxG1 (C) were retained by GST-Ap-2δ-TAD. Input represent i.v.t. protein and serves as a positive control. 10% of the amount used for immunoprecipitation was used for the direct detection.

Recombinant fusion proteins consisting of the Ap-2δ transactivation domain (TAD) and glutathione S-transferase (GST-Ap-2δ-TAD) or GST control protein (GST) were produced. The partial (Nfatc2Δ) and full length cDNA fragments of the two potential

candidates, Nfatc2 and FoxG1, were N-terminally tagged with an HA epitope and cloned into the expression vector pCMX harboring a T7 promoter. GST-Ap-2δ-TAD and control GST proteins were incubated with *in vitro* translated candidate cDNA fragments and analysed using SDS-PAGE. Proteins were blotted onto PVDF membranes and incubated with α-HA antibody. Partial (Nfatc2Δ) and full length Nfatc2 as well as full length FoxG1 were retained by GST-Ap-2δ-TAD indicating a physical interaction between Ap-2δ and Nfatc2 or FoxG1, respectively (Fig. 15). The protein interaction is specifically elicited by Ap-2δ TAD and not the GST portion of the fusion protein because GST protein alone does not bind to the potential candidates. Nfatc2 was chosen for a more detailed analysis.

With regard to the sequence identified by the yeast two-hybrid screen, 115 residues of Nfatc2 seem to be sufficient for the interaction with the transactivation domain of Ap-2δ. These residues are located at the C-terminus and partially overlap with the conserved Rel homology region that is responsible for DNA binding.

3.2.2. Ap-2δ co-immunoprecipitates with Nfatc2 in vivo

To analyze if Ap-2δ and Nfatc2 also interact in mammalian cells, full-length Ap-2δ and Nfatc2 were transiently expressed in 3T3 cells. Ap-2δ protein was immunoprecipitated with α-Ap-2δ antibody from whole cell extracts coupled to sepharose beads. To rule out unspecific binding of the protein to the antibody, the unrelated GST antibody was also used to immunoprecipitate the co-transfected cell extracts. Immunocomplexes were separated in a polyacrylamide gel and detected via immunoblotting using an α-HA antibody. Immunocomplexes precipitated with the α-Ap-2δ antibody contained Nfatc2, confirming the interaction observed in yeast and the *in vitro* GST pulldown (Fig. 16). In contrast to that, immunoprecipitation with

neither the control antibody GST nor in cells transfected with either cDNA alone resulted in the isolation of Nfatc2.

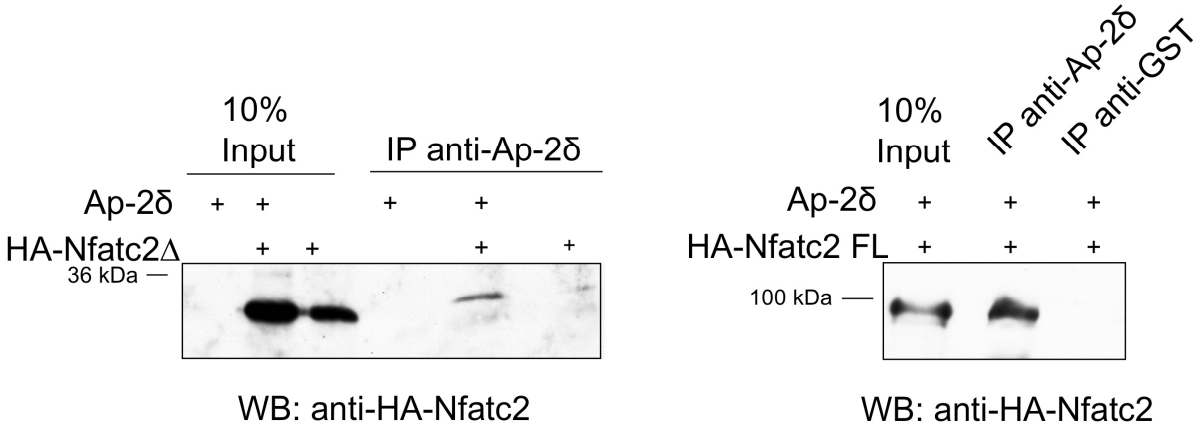

Figure 16: Interaction between Ap-2δ and Nfatc2 in eukaryotic cells. Proteins from transiently transfected 3T3 cells were immunoprecipitated (IP) with α-Ap-2δ antibody and immunoblotted with α-HA antibody. The partial cDNA fragment of Nfatc2 (HA-Nfatc2Δ) was immunoprecipitated with α-Ap-2δ antibody in Ap-2δ and Nfatc2 cotransfected cells but not in cells transfected with either cDNA alone (A). Full length Nfatc2 (HA-Nfatc2 FL) was specifically immunoprecipitated with α-Ap-2δ but not a control α-GST antibody (B). Input represents transfected cells before immunoprecipitation and serves as a positive control. 10% of the amount used for immunoprecipitation was used for the direct detection.

3.2.3. Modulating Nfatc2 activation using Ionomycin and Cyclosporin A

Nfatc2 was shown to be primarily expressed in the cytoplasm in a highly phosphorylated state. Upon several stimuli that raise intracellular calcium levels, the calmodulin-dependent phosphatase calcineurin dephosphorylates Nfatc2, unmasks a conserved nuclear localization signal and thereby promotes nuclear entry and increases DNA binding affinity (Okamura et al., 2000; Okamura et al., 2004). Nfatc2 dephosphorylation can be facilitated by the addtion of the calcium ionophore ionomycin. Ionomycin is produced by the bacterium *Streptomyces conglobatus* and acts as a motile Ca^{2+} carrier and enhances Ca^{2+} influx by direct stimulation of store-regulated cation entry across biological membranes (Morgan and Jacob, 1994). In contrast to that, calcineurin phosphatase activity can be blocked with the help of the cyclic hydrophobic decapeptide Cyclosporin A (CsA) derived from the soil funghi *Tolypocladium inflatum*. It has strong immunosuppressive capacity and inhibits the

dephosphorylation and nuclear entry of Nfatc2. It is highly efficient and displays relatively low toxicity. To analyze if transfected Nfatc2 can be activated and phosphorylation modulated in 3T3 cells, these cells were treated with either ionomycin for 45 minutes or CsA for 5-8 hours. Whole cell or nuclear extracts were subjected to SDS-PAGE and immunoblotted using anti-Nfatc2 antibody. Two bands were observed in samples treated with ionomycin indicating phosphorylated and dephosphorylated Nfatc2. In cells incubated with CsA, only phosphorylated Nfatc2 can be detected (Fig. 17) indicating a physiological response of the transfected Nfatc2 towards the modulating agents.

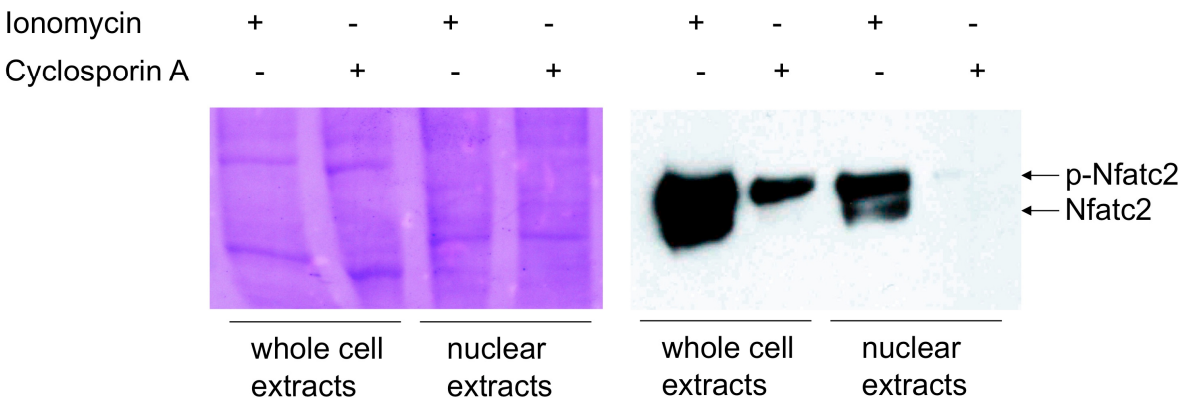

Figure 17: Activation of transfected Nfatc2 in 3T3 cells. Whole cell extracts or nuclear extracts were prepared from 3T3 cells expressing Nfatc2 and Ap-2δ and stimulated with 0.75 µM ionomycin for 1 hour or incubated with the calcineurin inhibitor CsA. Phosphorylation state of Nfatc2 was analyzed by western blotting using anti-Nfatc2 antibody. Coomassie stained membrane indicates equal loading. p-Nfatc2= phosphorylated Nfatc2.

3.2.4. Ap-2δ and Nfatc2 co-localize in mammalian cells

Given that Ap-2δ and Nfatc2 interact in *in vitro* as well as *in vivo* experiments, the the subcellular distribution of Ap-2δ and Nfatc2 in 3T3 cells was investigated. Under the assumption that Ap-2δ and Nfatc2 interact to cooporatively regulate transcription, Nfatc2 needs to be present in the nucleus. The subcellular localization

of the two proteins was visualized by immunocytochemistry 48 hours after transient transfection with full length Ap-2δ and HA-Nfatc2. Under normal growth conditions, Ap-2δ was located mainly nuclear whereas Nfatc2 was confined to the cytoplasm (Fig. 18, upper panel, DMEM).

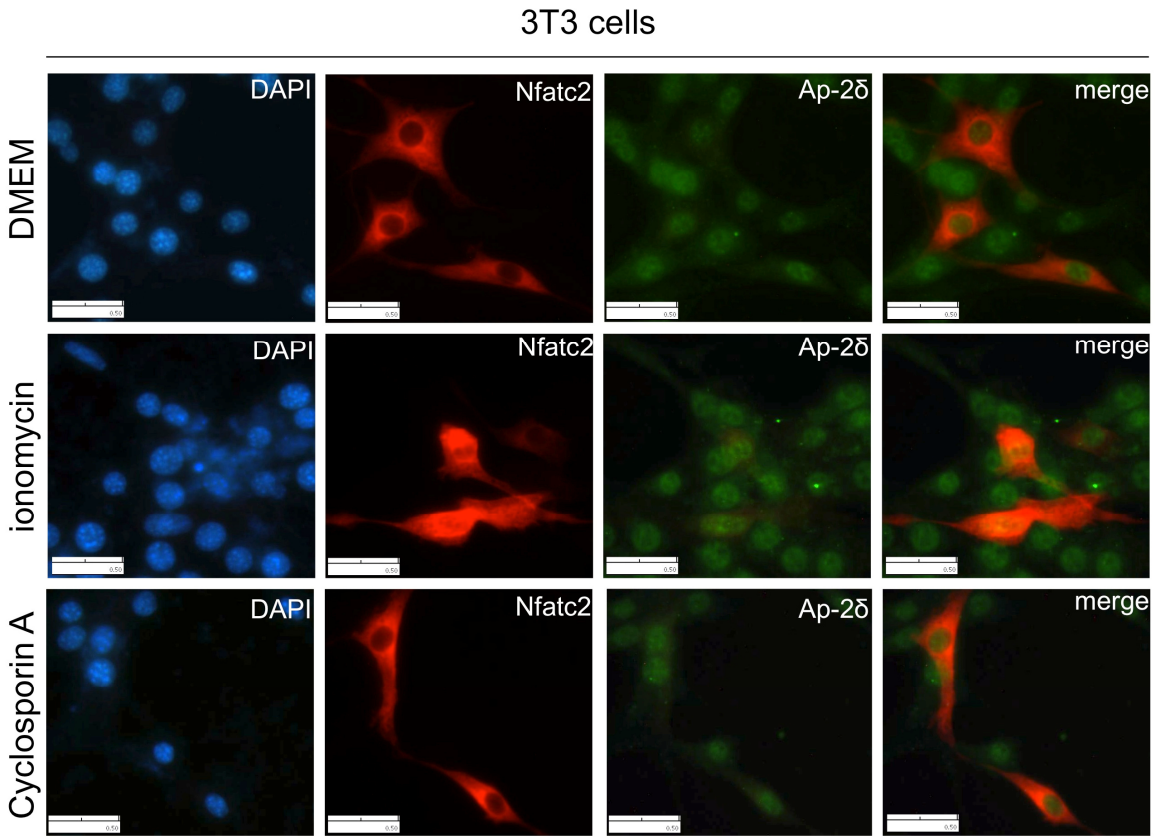

Figure 18: Co-localization of Ap-2δ and Nfatc2 in 3T3 cells. Expression vector-transfected cells were incubated with ionomycin or CsA and visualized by immunofluorescence microscopy after double-staining with Ap-2δ and HA antibody and the corresponding secondary antibodies Alexa Fluor 488 and Alexa Fluor 594, respectively. Scale bar: 50 µm

To modulate Nfatc2 subcellular localization, cells were treated with the calcium ionophore ionomycin and the calcineurin inhibitor cyclosporin A (CsA). Ionomycin treatment promoted the nuclear entry of Nfatc2 since antibody staining showed an even distribution of Nfatc2 throughout the whole cell (Fig. 18, middle panel, ionomycin). The inducible nuclear translocation of Nfatc2 was completely abrogated by CsA (Fig. 18 bottom panel, Cyclosporin A).

3.2.5. Identification of target genes regulated by Ap-2δ and Nfatc2

To gain insights into relevant target genes of both Ap-2δ and Nfatc2, mRNA expression of candidate targets was analyzed after ectopic expression of Ap-2δ and Nfatc2. *Atm*, *Mtss-1* and *c-Fos* were already identified as Nfatc2 target genes after expression profile analysis of ionomycin-stimulated 8988t pancreas carcinoma cells (Manuela Malsy, dissertation, 2009). Atm (ataxia telangiectasia mutated) is a nuclear protein that is involved in cell division and DNA repair. Mutations in the *Atm* gene can cause ataxia-telangiectasia, an autosomal recessive disorder, and increase the susceptibility to cancer (Lavin and Shiloh, 1996; Thompson et al., 2005). Mtss1 (metastasis suppressor protein 1) has been reported to play a role as a metastasis suppressor in prostate and bladder cancer (Lee et al., 2002; Loberg et al., 2005). C-Fos is a member of a family of immediate early gene (IEG) transcription factors which were also identified as proto-oncogenes. The nuclear phosphoprotein functions as a transcriptional regulator of cell proliferation, differentiation, and transformation (Piechaczyk and Blanchard, 1994). *Egr3* was proposed to be regulated by Nfat proteins after the identification of an Nfat regulatory element in the *Egr3* promoter (Mages et al., 1998). This transcriptional regulator belongs to the EGR family of C2H2-type zinc-finger proteins and plays a role in processes including muscle development, endothelial cell growth and migration, and neuronal development (Kumbrink et al., 2011).

Nfat proteins are known to interact with other transcription factors that extensively determine the selection and regulation of Nfat-controlled genes. Whether these Nfat target genes are cooperatively regulated by Nfatc2 and Ap-2δ was investigated by qRT-PCR. RNA from Neuro2a cells that were transfected with expression vectors for

Ap-2δ and Nfatc2 for 48 hours and incubated with ionomycin for 45 minutes analyzed using qRT-PCR on the set of target genes described above.

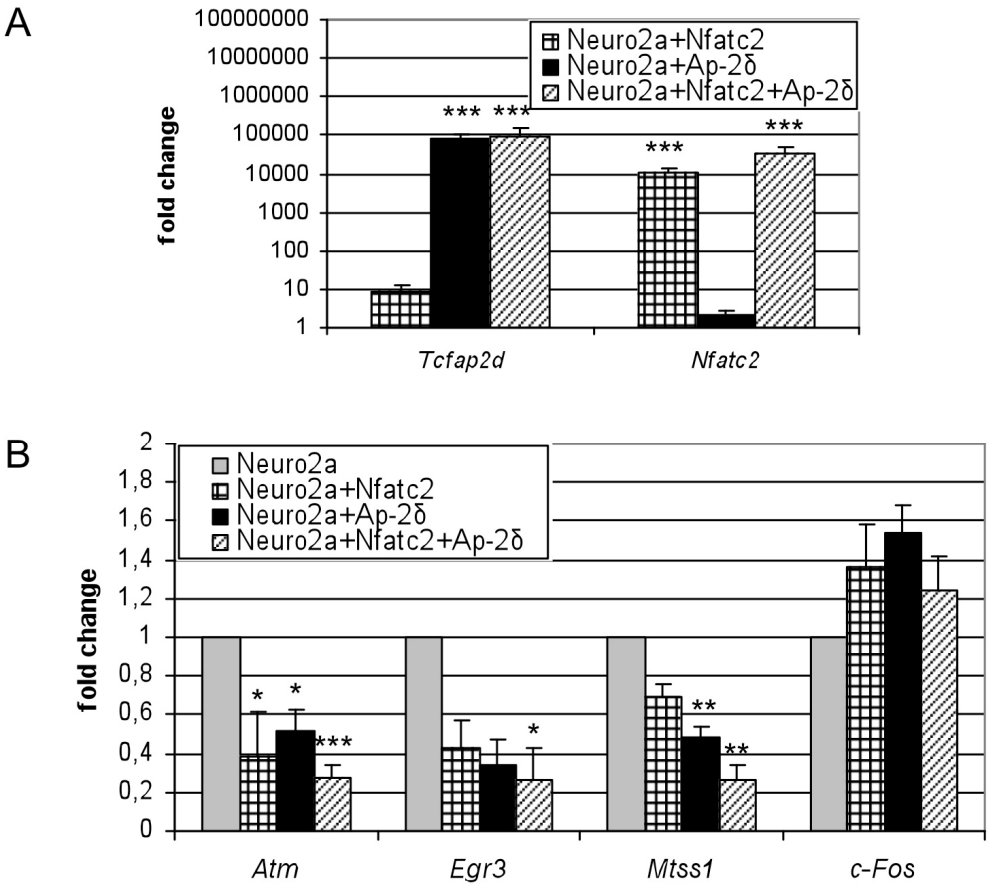

Figure 19: Overexpression of Ap-2δ and Nfatc2 (A) results in reduced expression of target genes. Transcript levels of *Atm*, *Egr3*, *Mtss1* and *c-Fos* where examined by qRT-PCR after transient transfection of Ap-2δ and Nfatc2 expression vectors into Neuro2a cells (B). *Gapdh* was used as an internal control to normalize the expression of each mRNA. Bars are displayed as fold change compared to untreated Neuro2a cells and show the mean ± s.e.m. of three independent experiments.

Overexpression of both transcription factors was shown by a potent fold induction, ranging from 10.000 - 100.000 fold (Fig. 19A). The downstream targets *Atm* and *Egr3* showed residual activity of only 30-40% and *Mtss1* retained 50-70% of wildtype steady-state transcript levels after overexpression of Ap-2δ and Nfatc2. Co-transfection of both Ap-2δ and Nfatc2 further substantiate the repression

(approximately 30% residual activity). The transcription of *c-Fos* is merely affected showing only a slight induction (Fig. 19B).

3.2.6. Transient siRNA knockdown of Tcfap2d results in upregulation of target genes

SiRNA-mediated transient knockdown of endogenous *Tcfap2d* was used to study consequences on target transcript levels after *Tcfap2d* downregulation. In this process, siRNA molecules bind to and transiently break down the *Tcfap2d* mRNA, thereby inhibiting the translation of the Ap-2δ protein. Untreated cells served as a reference for endogenous mRNA and protein levels.

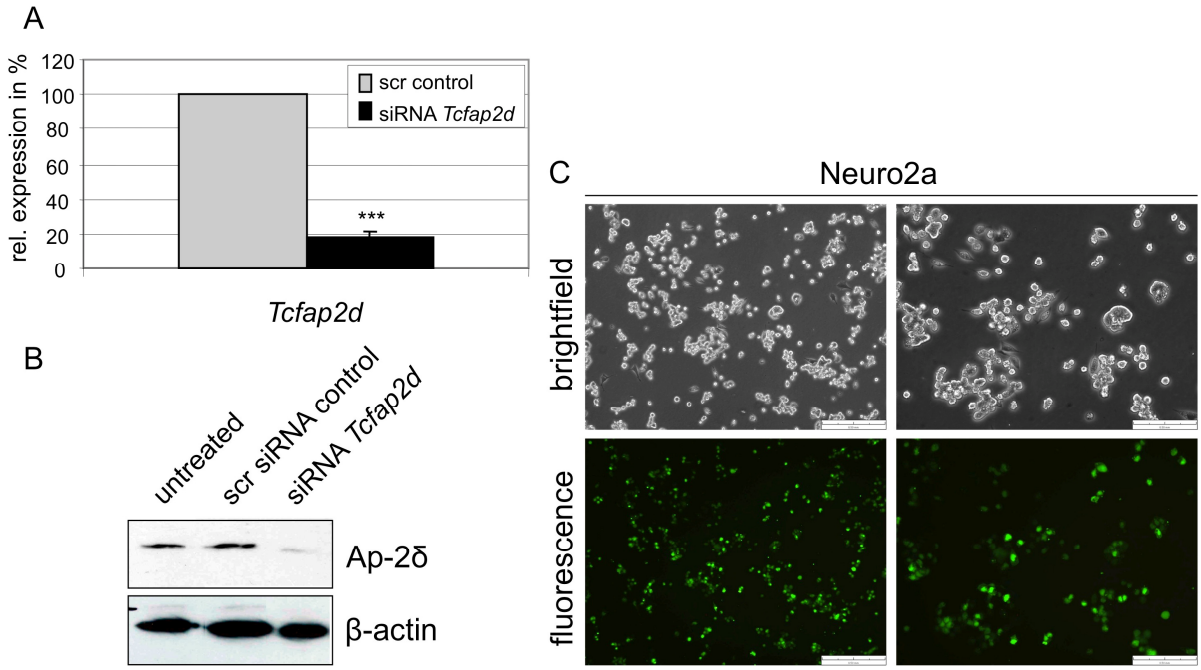

Figure 20: Transient knockdown of *Tcfap2d* in Neuro2a cells. Neuro2a cells were transfected with *Tcfap2d* siRNA or an unspecific scrambled siRNA (scr control) and analyzed 72 hours later. Transcript levels were significantly reduced for 80% in *Tcfap2d* siRNA-treated cells as indicated by qRT-PCR (A). A reduction of Ap-2δ protein was demonstrated by Western blotting. β-actin staining was used as loading control. (B). Transfection efficiency was detected with a fluorescence-labeled siRNA (C). Scale bar: 500 µm left panel, 200 µm right panel

Transfection efficiency was monitored using a fluorescence-labeled siRNA (Fig. 20C). Transfection of Neuro2a cells with siRNA was analyzed 72 hours later. The

nonsense siRNA did not have any consequence on *Tcfap2d* mRNA or protein levels. In contrast to that, *Tcfap2d* mRNA levels were significantly reduced for 80% 72 hours after *Tcfap2d* siRNA transfection (Fig. 20A). This was further evidenced by Western Blot where a strong reduction of Ap-2δ protein was observed (Fig. 20B). These data demonstrate the high efficiency of the *Tcfap2d* siRNA in breaking down mRNA levels and preventing protein translation.

The four genes that had already been analyzed for altered expression after Ap-2δ and Nfatc2 overexpression were also examined for expression changes upon *Tcfap2d* knockdown. After *Tcfap2d* siRNA transfection for 72 hours, RNA was collected and cDNA was subjected to qRT-PCR.

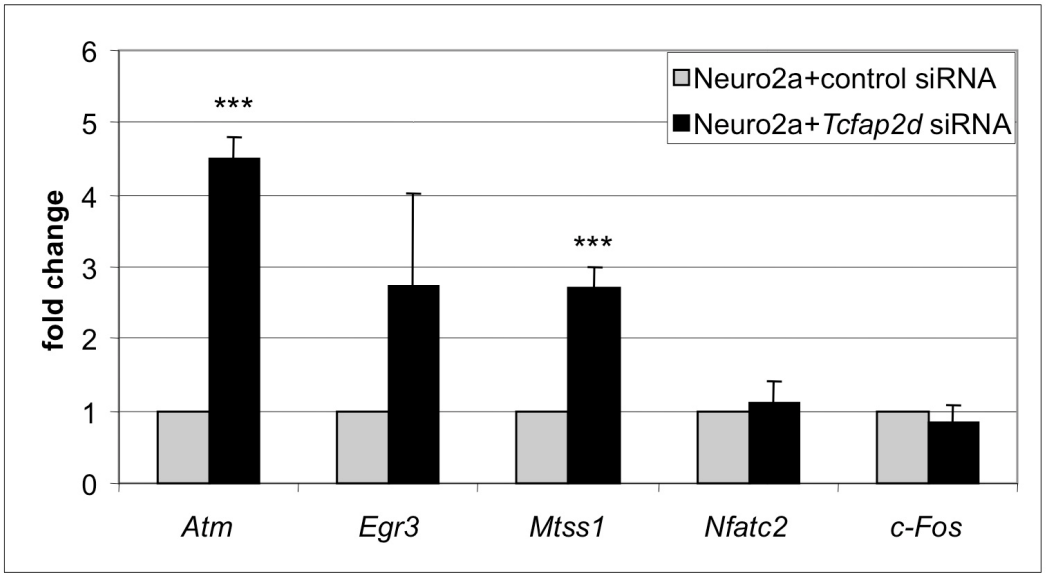

Figure 21: Quantitative real-time PCR analysis on candidate target genes after transient knockdown of *Tcfap2d* in Neuro2a cells. RNA from control or *Tcfap2d* siRNA analyzed for altered expression of potential target genes using qRT-PCR. Expression levels were normalized to *Gapdh*. Bars represent fold change of *Tcfap2d* siRNA-treated samples compared to control siRNA-treated samples and show the mean ± s.e.m. of three to six independent experiments.

Atm mRNA was upregulated for more than 4-fold and *Egr3* and *Mtss1* transcript levels were increased 2-3 fold after downregulation of *Tcfap2d* (Fig. 21). Again, *c-*

Fos expression was not altered upon *Tcfap2d* siRNA transfection. Notably, transcript levels of *Nfatc2* were also not affected by the downregulation of *Tcfap2d*.

3.2.7. Atm, Egr3 and Mtss1 are direct targets of Ap-2δ and Nfatc2

To determine if the observed effects on gene regulation after knockdown or exogenous expression of Ap-2δ and Nfatc2 were due to direct binding of these transcription factors to the promoters of the candidate target genes, we performed chromatin immunoprecipitation in combination with qRT-PCR. This allows mapping of the *in vivo* distribution of chromatin-associated Ap-2δ and Nfatc2. The genomic loci of the potential target genes were screened for Ap-2 and Nfat binding sites using rVista algorithm (Fig. 22).

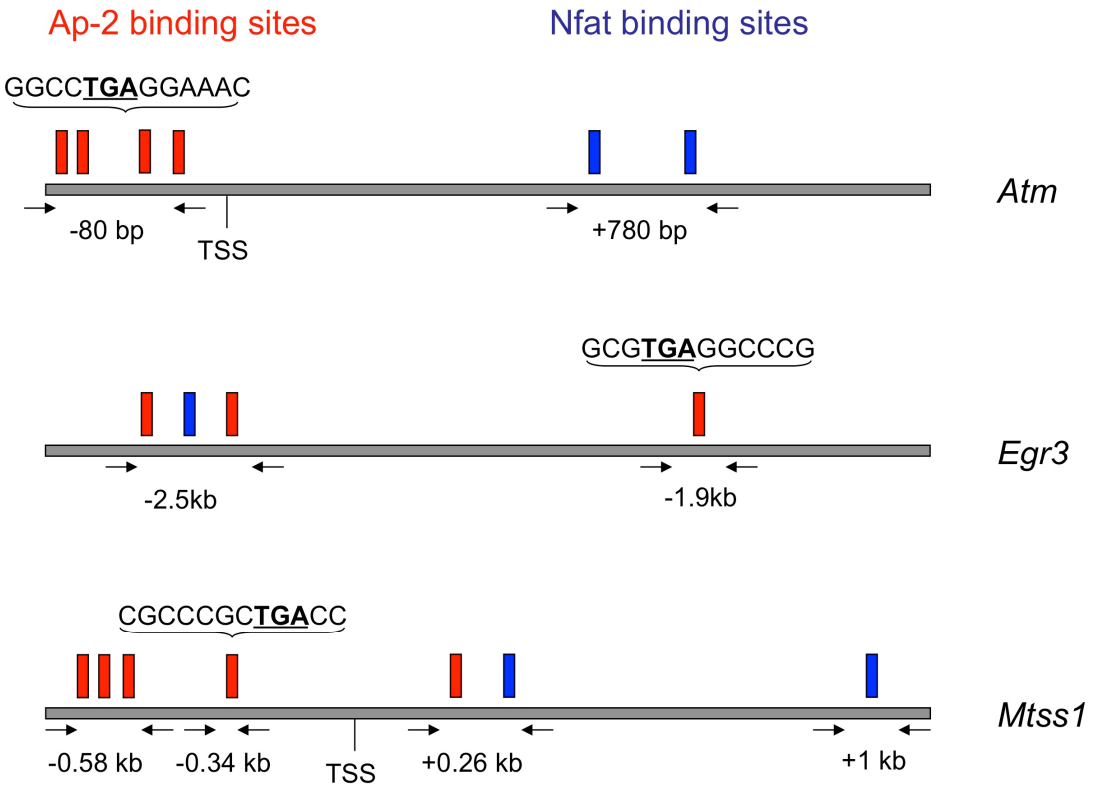

Figure 22: Schematic presentation of candidate target genomic loci. Potential target genes were screened for Ap-2 and Nfat binding sites using rVista algorithm. Ap-2 binding sites are displayed as red bars, Nfatc2 binding sites as blue bars. Primers are depicted as arrows. Numbers indicate distance relative to TSS.

Two regions containing binding sites for either one of the transcription factors or for both (*Egr3*, -2.5 kb) were found in each of the *Atm* and *Egr3* promoters. In the genomic locus of *Mtss1*, four potential sites for the binding of Ap-2δ and Nfatc2 were identified (Fig. 22). For all of the eight regions within the three promoters, primers were designed to specifically amplify those putative binding sites. Formaldehyde-fixed chromatin fragments from cotransfected and ionomycin-stimulated Neuro2a cells were enriched with antibodies against Ap-2δ and Nfatc2. Immunoprecipitated DNA was amplified by qRT-PCR using primer sets flanking the potential Ap-2δ and Nfatc2 binding sites.

The ChIP assay revealed that Ap-2δ occupied the *Atm* promoter at the two previously identified regions. These regions included the sites 80 bp upstream and 780 bp downstream of the transcriptional start site. In contrast to that, Nfatc2 was only enriched at the +780 bp binding site (Fig. 23A). It did not significantly bind to the -80 bp region which is only composed of predicted Ap-2 binding sites. Interestingly, although the +780 bp locus solely contains Nfat binding sites, Ap-2δ was found to be present in this promoter region suggesting physical interaction with Nfatc2. Moreover, immunoprecipitation with anti-Ap-2δ antibody revealed high levels of Ap-2δ at -2.5 kb and -1.9 kb of the *Egr3* promoter. Like Ap-2δ, immunoprecipitation with the Nfatc2 antibody revealed that Nfatc2 was also associated to both sites (Fig. 23B). Whereas Nfatc2 did not bind to a region only containing Ap-2 binding sites in the *Atm* promoter, Nfatc2 presence was observed at the -1.9 kb locus of the *Egr3* promoter which only harbors one putative Ap-2 binding site.

ChIP was also subjected to fragmented chromatin using Ap-2δ and Nfatc2 antibodies to enrich for either of the four putative binding sites predicted for the

Mtss1 promoter. The assay demonstrated a significant level of Ap-2δ binding at all of the four sites present in the genomic locus of *Mtss1*.

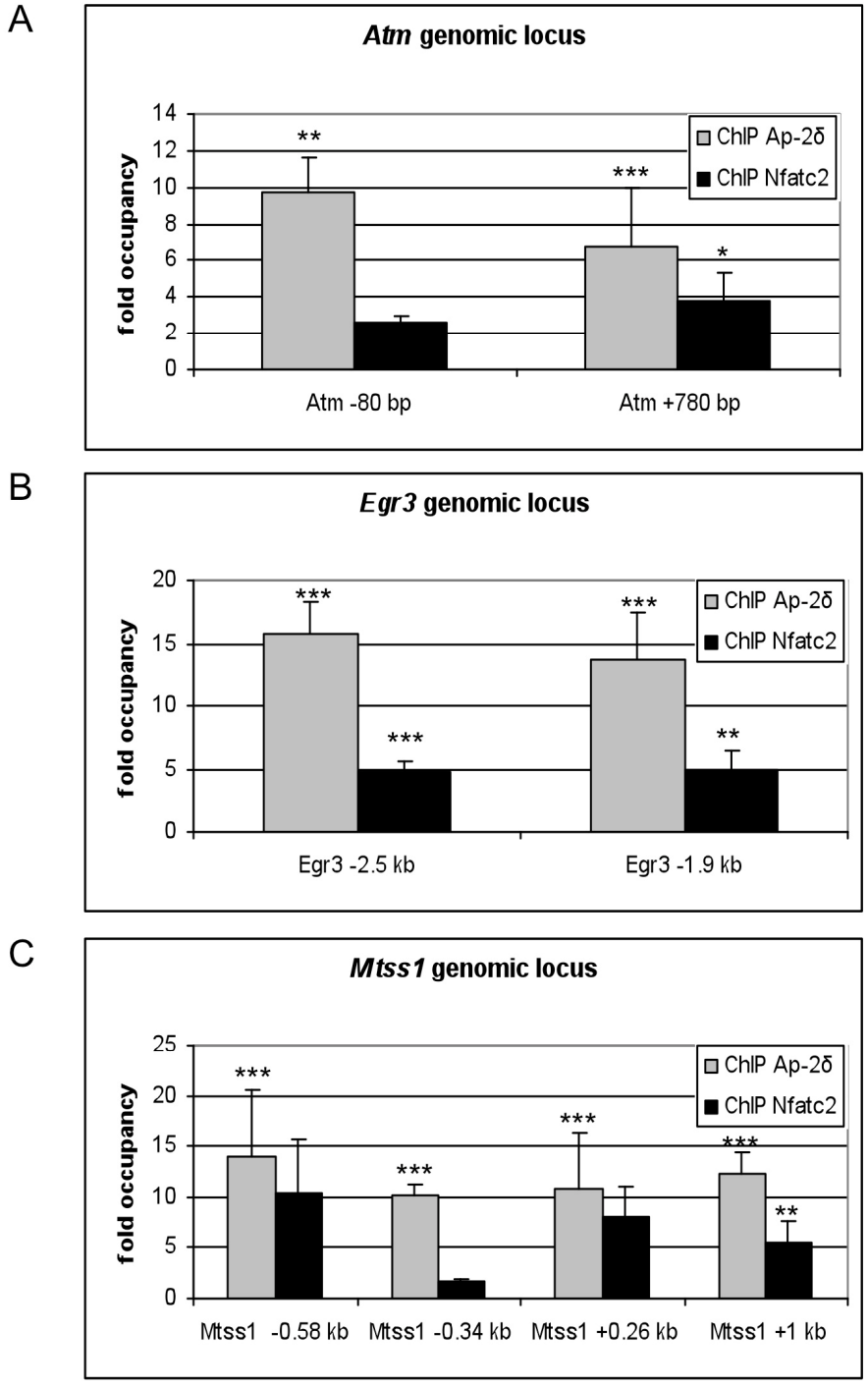

Figure 23: *In vivo* occupancy of Ap-2δ and Nfatc2 at target genomic loci. ChIP/qPCR assays of Ap-2δ and Nfatc2-transfected Neuro2a cells. DNA immunoprecipitated with antibodies against Ap-2δ and Nfatc2, along with histone H3 or IgG as positive and negative controls was quantified by real-time PCR using primers flanking candidate genomic loci. Values were normalized against H3 and presented as fold occupancy relative to the negative control IgG. Bars represent fold occupancy ± s.e.m. relative to IgG as determined from 4-6 independent experiments.

Two of theses sites are located upstream of the TSS (-0.58 kb and -0.34 kb) whereas the other two regions were found downstream of the TSS (+0.26 kb and +1 kb). After DNA fragment enrichment with the Nfatc2 antibody, a substantial Nfatc2 occupancy could also be observed at regions -0.58 kb, +0.26 kb and +1kb of the *Mtss1* promoter. Notably, the potential binding site -0.34 kb was not enriched after immunoprecipitation with anti-Nfatc2 antibody (Fig. 23C). In the *Mtss1* promoter, both transcription factors were found to occupy regions which contain potential binding sites for both factors (+0.26 kb) as well as regions that only contain binding sites for one factor (-0.58 kb and +1kb).

3.2.8. Knockdown of Tcfap2d and withdrawal of Nfatc2 abolish promoter occupancy

To further confirm the promoter occupancy of Ap-2δ and Nfatc2 observed for *Atm*, *Egr3* and *Mtss1*, ChIP was performed on Neuro2a cells that were either depleted of Ap-2δ by siRNA or not transfected with an Nfatc2 expression construct. Since Ap-2δ and Nfatc2 protein levels are reduced or absent in these cells, respectively, binding to the promoter regions of their targets should be reduced. Chromatin fragments of these cells were enriched with antibodies against Ap-2δ and Nfatc2. Indeed, knockdown of *Tcfap2d* abolished promoter occupancy at the -80 bp site in the *Atm* promoter and the -1.9 kb site in the *Egr3* promoter. Also, enrichment of Ap-2δ at the +0.26 kb and +1 kb sites of the *Mtss1* promoter was markedly diminished in *Tcfap2d* siRNA-treated cells (Fig. 24 upper panel).

Notably, Ap-2δ binding to the -2.5 kb region of the *Egr3* promoter is only slightly reduced in *Tcfap2d* siRNA-transfected cells indicating unspecific binding to this site.

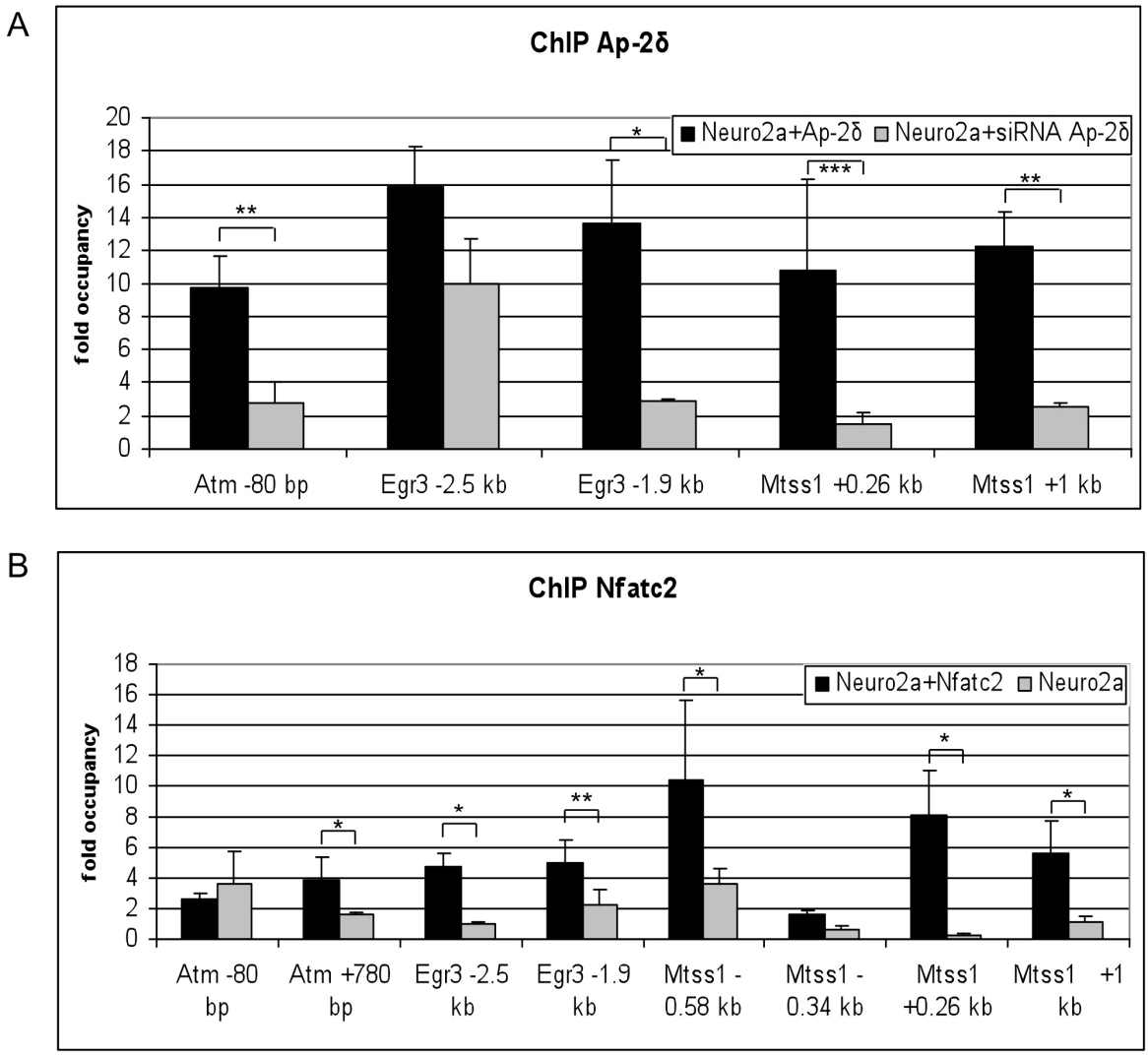

Fig. 24: Knockdown of Ap-2δ and withdrawal of Nfatc2 abolish promoter occupancy. ChIP assay and subsequent qRT-PCR of siRNA-transfected (upper panel) or untreated Neuro2a cells (lower panel). Immunoprecipitation was performed with Ap-2δ, Nfatc2, H3 and IgG antibodies. Values were normalized against H3 and presented as fold occupancy relative to the negative control IgG. Bars represent fold occupancy ± s.e.m. relative to IgG as determined from 3 independent experiments.

Immunoprecipitation of chromatin fragments from untransfected Neuro2a cells compared to Nfatc2-transfected cells with an Nfatc2 antibody revealed smaller amounts of enriched DNA from untransfected cells. This was observed at all analyzed promoter sites except for the region -80 bp of the *Atm* promoter (Fig. 24 lower panel). This is in line with the ChIP assay performed with Nfatc2-transfected cells where Nfatc2 binding to this region was not detected (Fig. 23A). In conclusion,

the relatively low signals obtained from this site do not seem to be specific and may represent background.

As the -80 bp region of the *Atm* promoter does not contain any predicted Nfatc2 binding site but only Ap-2δ binding sites, promoter occupancy by Nfatc2 through physical association with Ap-2δ does not seem to occur at this locus.

In summary, Ap-2δ and Nfatc2 were associated to the gene loci of *Atm*, *Egr3* and *Mtss1*. The differential expression pattern of the target genes upon overexpression or downregulation of the transcription factors can therefore be attributed to a direct effect exerted by Ap-2δ and Nfatc2.

4. Discussion

4.1. Ap-2δ is a crucial transcriptional regulator of the posterior midbrain

To investigate the role of Ap-2δ *in vivo*, *Tcfap2d*-/- mice were generated by homologous recombination. New Ap-2δ target genes were identified with the help of microarray analysis on brain tissue from control and Ap-2δ-deficient mice.

Members of the Ap-2 transcription factor family have multiple roles in controlling normal growth and differentiation during development. Despite the widespread expression of Ap-2α to γ proteins in a variety of different tissues, Ap-2δ expression is mainly restricted to the central nervous system, particular to the posterior midbrain. The other Ap-2 family members are also co-expressed in the roof of the midbrain. However, during embryogenesis, Ap-2δ expression decreases in the anterior mesencephalon, becomes enriched in the posterior mesencephalon and concentrates in the colliculus inferior. Such a dynamic expression pattern has not yet been described for other Ap-2 proteins. Furthermore, expression of the other Ap-2 isoforms is restricted to the dorsal part of the midbrain leaving Ap-2δ as the only expressed isoform in the posterior midbrain at the newborn stage. Thus, Ap-2δ seems to be a crucial regulator within this brain structure. Accordingly, ablation of Ap-2δ in the posterior midbrain results in the complete absence of the Ap-2δ-expressing structure of the posterior midbrain, the colliculus inferior, in adult mice. Marker analysis of the midbrain/hindbrain region revealed a normal initial organization into mid- and hindbrain in Ap-2δ mutant mice although Ap-2δ is already expressed during development of this structure (Hesse et al., 2011). These results indicate that midbrain/hindbrain organization is controlled either independent from Ap-2δ or due to functional redundancy, possibly through compensation by the expression of the other

Ap-2 isoforms. However, loss of Ap-2δ in the colliculus inferior of Ap-2δ-deficient mice cannot be compensated by other Ap-2 isoforms evidenced by massive apoptotic processes on embryonic day E17.

This phenomenon is in line with other Ap-2 knockout models. All knockout phenotypes included apoptotic processes at the main expression sites when compensation by other AP-2 proteins was not given indicating their impact on the cell survival and maintenance. Ap-2α mutant mice experienced severe cell loss in neural structures such as the midbrain, anterior hindbrain and the proximal mesenchyme of the first branchial arch (Schorle et al., 1996). The study of Ap-2β-deficient mice revealed that downregulation of the anti-apoptotic genes *bcl-X*$_L$, *bcl-w* and *bcl-2* occured parallel to massive apoptosis in kidneys of these mice (Moser et al., 1997). Finally, inner cell mass outgrowths of Ap-2γ-deficient blastocyst cultures underwent differentiation and apototic processes (Werling and Schorle, 2002). A possible mechanism for Ap-2-suppressed cell death was proposed by Gaubatz et al. (Gaubatz et al., 1995) who demonstrated in an *in vitro* approach that AP-2 acts as a negative regulator of Myc function. AP-2 inhibited Myc transactivation by a direct competition for DNA binding and by formation of a ternary Myc/Max/Ap-2 complex which impaired DNA binding activity of the Myc/Max complex (Gaubatz et al., 1995). Also, AP-2 can modulate apoptosis directly since cotransfection of AP-2α or AP-2β suppressed nucleosome release induced by transiently transfected c-myc (Moser et al., 1997). These data define a role for AP-2 in negatively controlling myc-induced programmed cell death.

Ap-2 family members are also involved in cell differentiation by influencing target genes transcription. Regulation of the *keratin 3* gene transcription by Ap-2 and Sp-1 determines the differentiation state of rabbit corneal epithelial cells. Differentiation and activation of the differentiation-related *K3* gene coincided with downregulation of

Ap-2 (Chen et al., 1997). Similarly, in a study by Pfisterer et al., Ap-2α was shown to repress *Klf4* which is implicated in induction of terminal differentiation. *Klf4* was prematurely expressed in Ap-2α mutant mice and fibroblasts lacking Ap-2α and consistently, expressing *Klf4* resulted in growth retardation, suggesting that Ap-2α is required for cell proliferation by suppression of genes inducing differentiation (Pfisterer et al., 2002).

4.1.1. Identification of Ap-2δ target genes in the posterior midbrain

Since Ap-2δ is essential for the development of the posterior midbrain, this study also aimed at the determination of new target genes employing microarray analysis. Using this approach, 12 potential downstream targets including four transcription factors with a differential expression after Ap-2δ knockout were identified. The expression of *Pitx2*, *Mef2c*, *Bhlhb4* and *Pou4f3* in the midbrain was validated with whole mount in situ hybridization of wild-type mice. Intriguingly, deletion of *Tcfap2d* resulted in the complete absence of these molecules in this brain structure. These data demonstrate that neuronal differentiation is accomplished by expression of several transcription factors under the control of Ap-2δ.

Two genes, *Rdh9* and *Rgs4*, were also upregulated in the absence of Ap-2δ suggesting a role for Ap-2δ in gene repression. However, whether Ap-2δ directly represses these genes remains to be investigated. Further circumstantial evidence for a repressor function of Ap-2 genes comes from reports on Ap-2α-γ repression of rat serum amyloid A1 (*SAA1*) transcription, D(1A) dopamine receptor gene transcription and manganese superoxide dismutase (*Mn-SOD*) expression in a cell-specific mechanism (Ren and Liao, 2001; Takeuchi et al., 1999; Zhu et al., 2001).

Primary target genes identified in this study are involved in a number of different biological functions including immunoregulation (*Slap*) and possibly cell migration

(*Cxcl12*). The absence of Ap-2δ furthermore affected genes controlling muscle development and contraction (*Mef2c*, *Myh8*), signal transduction (*Rgs4*) and metabolism (*Ndst4*, *Rdh9*). Interestingly, Pitx2 was found among the genes that showed a significant downregulation in the posterior midbrain. Another isoform of Pitx2, Pitx2c, is activated by Cited2 and Ap-2α in transient transfections in a hepatoma cell line. Moreover, Cited2 and Ap-2α are present at the Pitx2c promoter in the heart (Bamforth et al., 2004). Thus, Ap-2α controls Pitx2c expression in the heart whereas any Pitx2 isoform may represent a candidate target for Ap-2δ in the brain.

An important objective of this target gene analysis was to use posterior midbrain samples of Ap-2δ-deficient animals representing *in vivo* expression patterns. This is in contrast to previously published work examining Ap-2δ target gene expression after exogenous expression or siRNA-mediated knockdown of Ap-2δ in the human embryonic kidney cell line AD293 or the neuroblastoma cell line Neuro2a (Sun et al., 2007; Tan et al., 2009). The approach used here better reflects the *in vivo* situation by avoiding exogenous transfections, however, it is limited to genes expressed in the posterior midbrain. Nevertheless, all genes identified on the microarrays were validated by qRT-PCR and in situ hybridization.

4.1.2. Transactivation of Bhlhb4 and Pou4f3 by Ap-2δ

The present study suggests two different mechanisms for Ap-2δ transactivation and occupancy of the promoters of *Bhlhb4* and *Pou4f3.* Bhlhb4 is a basic helix-loop-helix (bHLH) protein that is expressed in a highly regionalized fashion in the nervous system and retina during development and adulthood (Bramblett et al., 2002). Loss of Bhlhb4 leads to abolishment of the retinal rod bipolar (RB) cell population. This in turn results in disrupted rod signalling and profound retinal dysfunction resembling human congenital stationary night blindness (CSNB) (Bramblett et al., 2004).

We could not detect a direct binding of Ap-2δ to the Ap-2 binding sites derived from the *Bhlhb4* promoter. One mechanism for Ap-2δ transactivation would be that Ap-2δ associates with and activates the *Bhlhb4* promoter through a complex with cofactors and interaction partners. Ap-2 proteins have been reported to functionally interact with several proteins. Bamforth et al. (Bamforth et al., 2001) showed that Ap-2 proteins interact with CBP/p300 and mediate Cited2-dependent coactivation. Protein interactions of Ap-2 isoforms with other transcription factors were demonstrated for c-myc, rBP, and p53 (Batsche et al., 1998a; Decary et al., 2002; McPherson et al., 2002). Recently, Tan et al. provided evidence for a new complex that included Ap-2δ associated with Ash2l and Alr which mediated H3K4 trimethylation and gene activation of the *Hoxc8* locus. It remains to be investigated in which protein complex Ap-2δ elicits transactivation of *Bhlhb4*.

Pou4f3 is a class IV POU domain transcription factor that is weakly expressed in the midbrain, in particular in the inferior colliculus and superior colliculus, and in ganglion cells of the retina (Xiang et al., 1995). The expression patterns of *Bhlhb4* and *Pou4f3* are almost identical to that of Ap-2δ, supporting our idea that *Bhlhb4* and *Pou4f3* are Ap-2δ target genes. This idea is further substantiated by direct binding of Ap-2δ to a defined sequence of the Pou4f3 promoter in a highly specific manner indicated by abrogated binding after mutagenesis of the binding site.

4.1.3. Ap-2δ deficiency might result in hearing impairment via Pou4f3

Pou4f3 is a pivotal regulator of sensorineural development and survival, in particular auditory system development. Expression can first be detected in all hair cells of the inner ear as soon as they exit cell cycle between E12 and E15 (Xiang et al., 1998). *Pou4f3-/-* inner ears encounter hair cell degeneration resulting in hearing loss. In Pou4f3-deficient mice, hair cells initially start to differentiate but undergo apoptosis at

embryonic day 17 (Xiang et al., 1998; Xiang et al., 2003). Autosomal dominant mutations in the *POU4F3* gene have been associated with non-syndromic hearing loss DFNA15 in humans (Collin et al., 2008). Since absence of Ap-2δ results in loss of the inferior colliculus which is the principal nucleus of the auditory pathway and receives input from peripheral brain stem nuclei in the auditory pathway as well as from the auditory cortex, it is likely that loss of Ap-2δ leads to a hearing impairment. As Ap-2δ expression has not yet been detected in inner ear hair cells, Ap-2δ-deficient mice are currently investigated for Ap-2δ expression in the ear and a concomitant hearing defect.

Sound is transmitted from the inner ear through the cochlear nuclei and superior olivary complex of the brainstem towards the inferior colliculus. In the inferior colliculus, sound information is integrated and then transferred to the medial geniculate nucleus (MGB) of the thalamus. It acts as a thalamic relay station that further processes auditory signals before they are received by the auditory cortex.

Interestingly, mice already harbor these auditory connections before acquiring hearing. This suggests that formation of auditory connections is genetically anchored (Gurung and Fritzsch, 2004). First results from electrophysiological recordings of neocortical neurons suggest that Ap-2δ mutant mice are indeed able to respond to sound indicated by tone-evoked neuronal responses at the neocortical level (Hesse et al., 2011). Therefore, a compensatory mechanism seems to have evolved that overcomes the need for a colliculus inferior and adopts its function. An alternative pathway omitting the inferior colliculus was identified in bats and cats (Casseday et al., 1989). Fibers originating in the nucleus of the central acoustic tract (NCAT) travelled ventral to the inferior colliculus and medial and ventral to the brachium of the colliculus inferior. Via these pathways, auditory information can reach the deep

superior colliculus and the suprageniculate nucleus along cortical and subcortical routes bypassing the colliculus inferior (Casseday et al., 1989; Kobler et al., 1987). This proposed pathway may provide a route for individual tones that arouse cortical neuronal activity in Ap-2δ-deficient mice. It is therefore interesting to analyze the response to more complex processing tasks in the absence of the inferior colliculus. Accordingly, auditory discrimination learning tests should be employed to investigate learning performance. Preliminary data of this kind of test revealed that mice lacking Ap-2δ were able to to learn the discrimination of tones and showed a significant performance level. Nevertheless, learning speed was much slower and took five days longer to reach significant discrimination compared to a large sample of normal hearing NMRI mice (Kurt & Ehret, unpublished data). Thus it seems that at least some auditory discrimination capability is preserved in Ap-2δ-/- mice despite absence of a functional inferior colliculus. Further studies will be necessary to contribute to clarification of these mechanisms (Kurt and Ehret, in progess).

Ap-2δ-mediated acvtivation of *Pou4f3* can also occur in the midbrain or the retina, but the function of *Pou4f3* in the midbrain is not clear to date. A prominent phenotype of reduced *Pou4f3* expression due to loss of Ap-2δ in the retina is not very likely since targeted *Pou4f3* disruption does not cause retinal defects probably due to a functional compensation by *Pou4f2* (Erkman et al., 1996; McEvilly et al., 1996; Xiang et al., 1997).

In summary, this study demonstrates that Ap-2δ is a central, higher-order transcription factor that establishes the survival and maintenance of posterior midbrain cells by suppressing apoptosis. Ap-2δ ablation results in massive apoptotic processes eventually leading to the loss of the colliculus inferior. Control of midbrain development by Ap-2δ can further be substantiated by the identification of *Bhlhb4*

and *Pou4f3* along with a set of other candidates from the posterior midbrain as de novo Ap-2δ target genes. Thus, the data presented here provide new insights into the molecular mechanisms underlying posterior midbrain development governed by Ap-2δ.

4.2. Transcription factors Ap-2δ and Nfatc2 interact to synergistically regulate target gene transcription

4.2.1. Identification of FoxG1 and Nfatc2 as binding partners for Ap-2δ

In a previous study, potential interacting partners of Ap-2δ were isolated using the yeast two-hybrid system to gain insights into the biological function of Ap-2δ. The Ap-2δ transactivation domain served as a bait protein that was screened against an adult mouse brain cDNA library (prey). After verification by retransformation, X-gal filter assays, autoactivity screens, and sequencing of the cDNAs, the number potential interactors was narrowed down to 38 candidates. FoxG1 and Nfatc2 were of special interest due to their function as transcription factors because Ap-2 proteins have been reported to exert their function by interaction with other transcription factors (Wu and Lee, 2001). In this study, verification of the yeast two-hybrid assay was initially performed with both candidates. FoxG1 is a winged helix transcription factor expressed in the telencephalon, retina, optic stalks, otic placode, and superior colliculus (Hebert and McConnell, 2000; Xuan et al., 1995). FoxG1-Cre mice that express Cre under the control of FoxG1 regulatory elements also confer recombination in the ear, olfactory epithelium, the mid-hindbrain junction, and facial and head ectoderm (Hebert and McConnell, 2000).

Since the partial FoxG1 fragment obtained from the screen was not retained by GST-Ap-2δ-TAD in the GST pulldown assay, the interaction between Nfatc2 and Ap-2δ was examined in more detail.

The *in vitro* GST pulldown assay demonstrated that the Ap-2δ-Nfatc2 interaction is mediated via the TAD of Ap-2δ and the DNA binding and C-terminal regions of Nfatc2. Co-immunoprecipitation assays furthermore showed that the interaction occured *in vivo* and also confirmed interaction in mammalian cells. The physiological

basis of this interaction was demonstrated by co-localization of both proteins in the nucleus after activation of Nfatc2.

Nfatc2 is a member of the Nfat family that are expressed at relatively high levels in many brain compartments (Vihma et al., 2008). Expression increases during postnatal development and is most abundant in the colliculi, cerebellum, medulla, olfactory bulb and striatum. Interestingly, *Nfatc2* is the predominantly expressed isoform in the mouse brain. Its mRNA is widely expressed at high or moderate levels in most cells of the thalamus, hypothalamus, and midbrain. In contrast, Nfatc1, Nfatc3, and Nfatc4 are not significantly expressed in these brain structures. This partially overlapping expression pattern of Nfatc2 with Ap-2δ constitutes a prerequisite for the physiological interaction.

4.2.2. Interaction of Ap-2δ and Nfatc2 in regulation of target genes

In neurons, Nfat is implicated in synaptic plasticity, axonal outgrowth and neuronal survival (Benedito et al., 2005; Graef et al., 1999; Groth and Mermelstein, 2003). It is believed that different neuronal subtypes may use distinct Nfat transcriptional complexes to elicit morphogenic or pro-survival signals.

Nfat function is orchestrated by the formation of regulatory complexes with other transcription factors (Macian, 2005). Those complexes are not only characterized by their functional synergy but also by cooperative physical interaction between two or more transcription factors that bind to DNA. The cooperative regulation of *Atm*, *Egr3*, and *Mtss1* by Ap-2δ and Nfatc2 was analyzed by qRT-PCR and ChIP assays and demonstrates that Ap-2δ and Nfatc2 negatively regulate these targets by binding to their promoters *in vivo*. Various binding sites for Ap-2 and Nfat in the promoters of the candidate targets were proposed by the algorithm rVista. These binding sites were neither overlapping nor in close proximity to each other, thereby excluding the

mechanism of physical interaction after binding to the factor-specific sites reported in the above mentioned studies. Here, Ap-2δ and Nfatc2 did not only bind to their specific putative binding sites but were also found at promoter regions only containing binding sites for the interaction partner (Fig. 25).

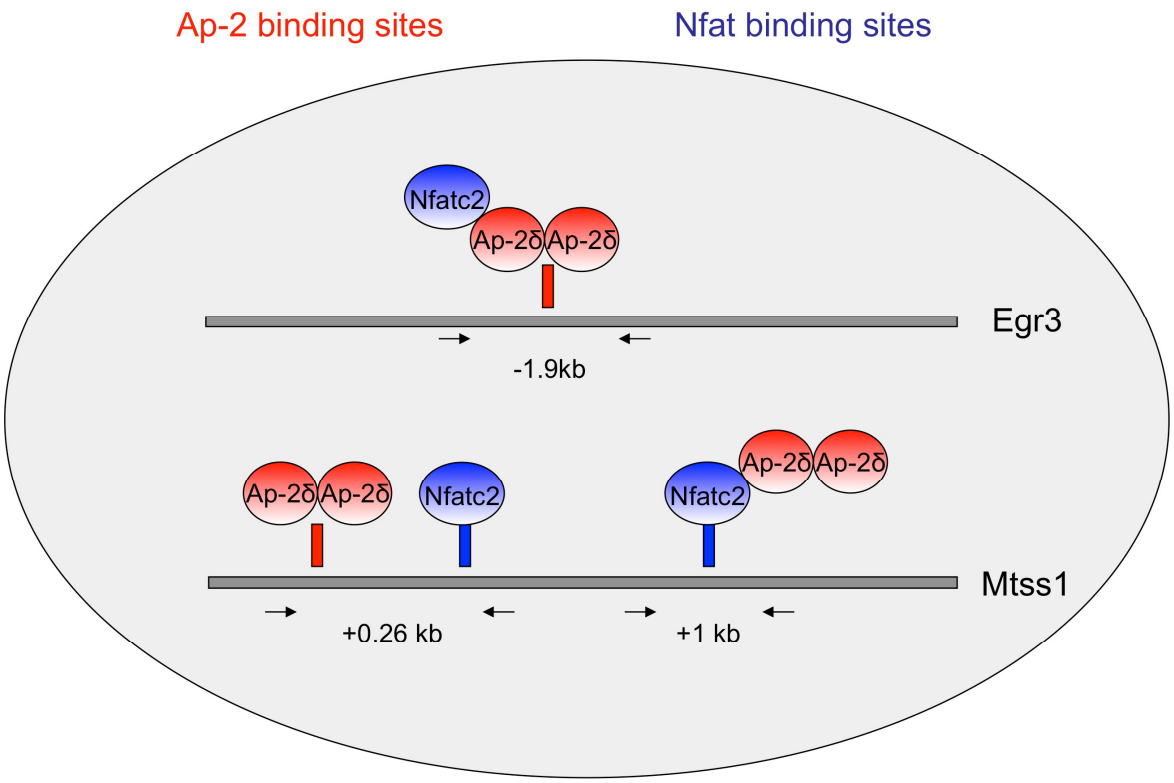

Fig. 25: Model for promoter occupancy of Ap-2δ and Nfatc2. Ap-2δ and Nfatc2 can either bind to their own specific putative binding sites (Mtss1 +0.26kb) or they occupy genomic loci containing only binding sites for one of the two factors by physical interaction (Egr3 -1.9kb and Mtss1 +1kb).

Therefore, Ap-2δ and Nfatc2 are able to exert their regulatory potential by occupancy at the target promoter through physical interaction with their partner. This has already been reported for AP-2α as well as for NFATc2. The interaction of AP-2α and YY1 in the hamster histone *H3.2* gene occurs through binding to sequences specific for each factor as well as through binding in a complex to only AP-2 specific sites (Wu and Lee, 2001). The idea that direct binding of NFAT to DNA might be dispensable and can be replaced by interaction with other transcription factors was proposed in

studies with SP-1 and NFATc2. Calcineurin upregulates SP-1-dependent transcription of *p21* promoter activity by association of NFAT with SP-1 (Santini et al., 2001).

4.2.3. Ap-2δ and Nfat2c-regulated genes in the nervous system

Since target genes of Nfat proteins have been primarily determined outside the nervous system, only little is known about genes under the control of the calcineurin-Nfat-signaling in the nervous system. *IP_3R1*, *Bdnf*, *CCR2* and *Cox-2* are genes that have been described to be regulated by Nfat proteins in the nervous system. (Graef et al., 1999; Groth et al., 2007; Groth and Mermelstein, 2003; Jung and Miller, 2008).

This study demonstrates for the first time new target genes of the nervous system that are regulated by both Ap-2δ and Nfatc2. The findings presented here provide evidence that the widely expressed Nfatc2 transcription factor interacts with the highly restricted and neuronal-specific transcription factor Ap-2δ thereby involving Nfatc2 in the regulation of neuronal target gene transcription. This interaction may direct Nfat-dependent gene expression in neurons and achieve specificity of Nfat proteins despite their almost ubiquitous expression pattern. Moreover, the results of this study implicate that Ap-2δ and Nfatc2 combinatorially regulate gene expression in a negative manner (Fig. 22). *Atm*, *Egr3*, and *Mtts1* were downregulated upon overexpression of Ap-2δ or exogenous expression of Nfatc2 in Neuro2a cells. Owing to the concerted interaction, this effect was enhanced when expression plasmids of both transcription factors were transfected. Accordingly, knockdown of Ap-2δ by siRNA resulted in increased target mRNA transcripts.

This is the first work demonstrating a repressive function for the transcription factor Ap-2δ. It was suggested before that Ap-2δ might utilize an alternative mechanism for transactivation or might act as a repressor due to its divergent TAD (Zhao et al.,

2001). Moreover, the microarray performed in the first part of this study identified the two genes *Rdh9* and *Rgs4* that were upregulated in the absence of Ap-2δ, already suggesting a role for Ap-2δ in gene repression (see page 84). This study now provides evidence that Ap-2δ indeed has the potential to repress target gene transcription. The repressive effect is not only elicited by interaction with Nfatc2 since overexpression of Ap-2δ alone already confers reduced transcript levels of target genes.

4.2.4. The serine/threonine protein kinase Atm

Atm participates in orchestrating cell cycle in response to DNA damage and oxidative stress (Rotman and Shiloh, 1997a, 1997b; Watters, 2003). Mutational loss of *Atm* contributes to ataxia-telangiectasia (A-T), a disease characterized by progressive neurodegeneration, radiosensitivity, cell-cycle checkpoint defects, genome instability, and a predisposition to cancer (Kastan and Lim, 2000; Lavin and Shiloh, 1996). One of the earliest cellular phenotypes discovered was a defect in cell cycle control. The efficient induction of the tumor suppressor p53 in the G1/S cell cycle checkpoint following irradiation depends on Atm (Kastan et al., 1992). Atm phosphorylates p53 and its interactors MDM2 and Chk2, thereby allowing p53 to activate its target genes, particularly the cyclin-dependent kinase (CDK) inhibitor p21 which results in the inhibition of cyclin-E/CDK2 complex and inhibition of progression from G1 into S-phase (Kastan and Lim, 2000).

The downregulation of a DNA repair and cell cycle checkpoint protein does not seem to be desirable during development in a highly proliferative environment in which mutations can have a major impact. On the other hand, high amounts of Atm result in cell cycle arrest and eventually cell death. The Ap-2δ and Nfatc2-mediated downregulation of Atm could reduce phosphorylation of p53 and downstream targets

to promote cellular proliferation. A recent study reported that Atm-depletion in a human neural stem cell line ihNSC did not affect growth rate, DNA replication or chromosomal stability (Carlessi et al., 2009). However, it attenuated the response to IR-induced DNA damage. When Atm-depleted ihNSCs were subjected to differentiation, similar numbers of neurons and astrocytes were found in control and shATM cells. The number of oligodendrocytes was mildly reduced. These data suggest a dispensable role for Atm during differentiation of ihNSCs toward the neuron and astrocyte lineage. Interestingly, the authors observed a substantial increase in apoptotic markers such as cleaved caspase 3 and 9 and an accumulation of p53 and $p21^{waf1}$ accompanying the differentiation of ihNSCs. This apoptotic activity was less pronounced in Atm-depleted cells (Carlessi et al., 2009). Maric et al. (Maric et al., 2007) already reported that during early neurogenesis, neural stem cells encounter both lineage differentiation and apopotosis. Ap-2δ and Nfatc2-conferred downregulation of Atm might therefore repress apoptotic activity. This is in line with the phenotype of Ap-2δ-/- mice described in the first part of this work. Knockout of Ap-2δ resulted in increased apoptosis of posterior midbrains. The absence of Ap-2δ could relieve Atm repression which in turn could activate p53 and downstream signaling to elicit cell death. This hypothesis is supported by the finding presented in this study that knockdown of Ap-2δ in Neuro2a cells led to upregulation of Atm transcription. Further work is needed to analyze phosphorylation states of Atm, p53 and downstream targets like p21 in Ap-2δ-/- mice to confirm this hypothesis.

Controversial data were reported by Kim and Wong (Kim and Wong, 2009). Owing to the progressive neurodegeneration as one of the main phenotypes of A-T, the authors investigated the effects of Atm loss on murine neural stem cells (NSC). Cultured subventricular zone neurospheres from Atm-deficient mice showed impaired proliferation. Several signaling pathways seemed to be affected as Akt and Erk1/2

pathways were disrupted and the p38 mitogen-activated protein kinase (MAPK) activity was enhanced. These findings suggest that Atm plays a crucial role in NSC proliferation by activating Akt and Erk1/2 pathways and suppressing p38 MAPK signaling (Kim and Wong, 2009). Whether these pathways are also affected after Ap-2δ and Nfatc2-mediated repression of Atm stills needs to be investigated.

4.2.5. The early growth response transcription factor Egr3

Early growth response (Egr) transcription factors belong to the regulatory immediate early genes that are expressed in response to neuronal activity coupled to MAPK-Erk signaling. Egr1 and Egr3 are the most abundant Egr proteins upregulated by synaptic activity in the brain (Li et al., 2005; O'Donovan and Baraban, 1999). These NMDA receptor/MAPK-Erk signaling molecules may modulate target gene expression required for long-term structural and physiological synaptic changes associated with learning and memory. In support of this, CA-1 hippocampal neurons of Egr-deficient mice show abnormal long-term potentiation. Accordingly, Egr-/- mice display profound impairments in context and cued-associated learning and short-term and long-term objective recognition memory (Li et al., 2007).

Studies on the molecular basis of learning and memory have highlighted the impact of calcium-regulated pathways (reviewed in Platenik et al., 2000). Nfatc4 has also been implicated in learning and memory as it regulates *IP_3R1* expression in hippocampal neurons. This regulation may be important for synaptic plasticity and long-term depression (Graef et al., 1999). Further evidence for a role of Nfat in memory was given by de la Fuente (de la Fuente et al., 2011). Hippocampal calcineurin induced nuclear Nfat translocation after a prolonged re-exposure to the training context of fear conditioning. This activation resulted in memory extinction. Also, TNF-a was described to be activated by calcineurin/Nfat signaling. TNF-a has

been proposed to be involved in the pathogenesis of neurodegenerative diseases related to memory (Elliott, 2001; Ghezzi et al., 1998) and TNF-a knockout mice display deficits in spatial learning and memory (Golan et al., 2004). These findings assign a role for calcineurin/nfat signaling in learning and memory. The observation that Ap-2δ and Nfatc2 regulate Egr3 expression may further contribute to the understanding of the molecular basis of learning and memory. Interestingly, Ap-2δ-deficient mice subjected to auditory discrimination learning tests showed a delayed learning behavior compared to normal-hearing mice, indicating that Ap-2δ downstream signaling is indeed involved in learning and memory.

4.2.6. The metastasis suppressor protein Mtss1

The metastasis suppressor protein 1 (Mtss1; also called “missing in metastasis” (MIM)) was originally identified as a potential metastasis suppressor as the transcript was missing in metastatic bladder and prostate cancer (Lee et al., 2002). It is suggested to have a scaffolding function although its *in vivo* role is not yet fully understood. Mtss1 was identified as a transcriptional co-factor in association with the sonic hedgehog (Shh) signaling pathway. Mtss1 cooperates with and co-activates the transcription factor Gli-1 and Gli-2 to potentiate the activation of the Shh transcriptional pathway in epidermal cells. The identification of conserved nuclear localization signals and a nuclear export signal emphasizes the dual role of Mtss1 in cytoskeleton remodelling and transcriptional regulation (Glassmann et al., 2007).

Mtss1 has been observed to be downregulated or missing in several cancer cells compared to normal tissue. *Mtss1* transcript levels were found to be downregulated in prostate cancer cell lines such as PC-3, Du145 and LNCap cells as well as in patient samples of benign prostate hyperplasia, localized prostate cancer and metastatic prostate cancer (Loberg et al., 2005). Accordingly, overexpression of

Mtss1 suppressed growth of transformed and cancer cell lines (Utikal et al., 2006). These findings, together with the implication in Shh signaling, indicate an important role for Mtss1 in tumor development.

In a very recent study, Mtss1 was reported to be required for neural fold elevation and anterior neural tube closure in *Xenopus laevis*. Mtss1 depletion inhibited anterior neural fold closure without affecting anterior gene expression. In particular, Mtss1 specifically binds to Daam1 and mediates non-canonical Wnt signaling. Thus, Mtss1 provides a link between non-canonical Wnt signaling and the remodeling of the actin cytoskeleton and changes in membrane dynamics required for neural tube closure (Liu et al.). Similarly, Ap-2α knockout mice also suffer from a failure in neural tube closure (Schorle et al., 1996; Zhang et al., 1996). These data together with the findings of this work that Ap-2δ and Nfatc2 influence Mtss1 transcription support the idea that Ap-2 proteins and Mtss1 may eventually converge upon the same developmental regulatory pathways.

In summary, this work demonstrates that Ap-2δ and Nfatc2 specifically interact with each other. The physical interaction is mediated via the TAD of Ap-2δ and the DNA binding and C-terminal region of Nfatc2. This interaction augments in synergistically regulating expression of the newly identified targets *Atm*, *Egr3*, and *Mtss1*. Furthermore, this study for the first time provides evidence for a repressive function of Ap-2δ. *Atm*, *Egr3*, and *Mtss1* were shown to be repressed by Ap-2δ and Nfatc2 (Fig. 26). Thus, these data provide insights into the complex transcriptional network in neurons in which Ap-2δ and Nfatc2 participate.

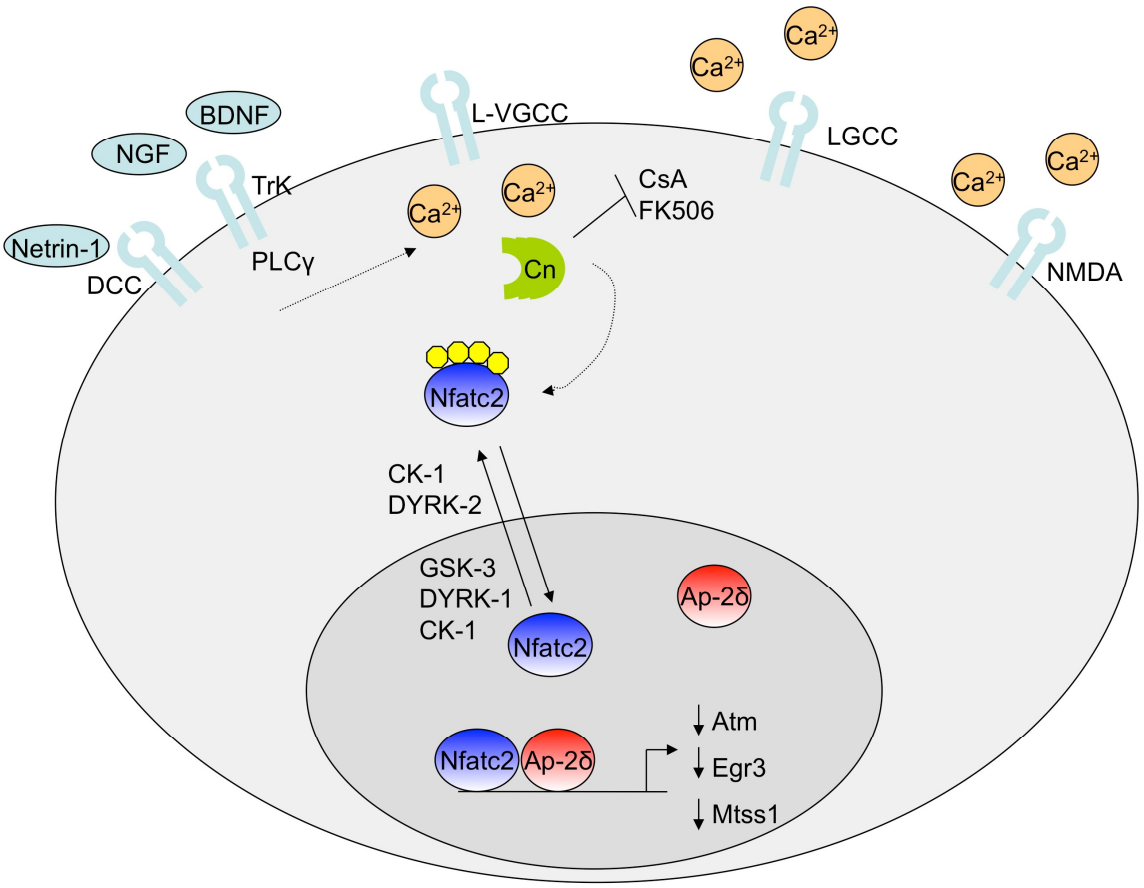

Figure 26: Model for target gene regulation by Ap-2δ and Nfatc2 in neurons. Nfat nuclear translocation in neurons can be elicited by a number of stimuli. Membrane depolarization opens L-type voltage gated calcium channels (L-VGCC). An initial Ca^{2+} release can also be triggered by L-type calcium channels (LGCC), NMDA receptors, neurotrophin binding to TrK receptors, and netrin/DCC signaling. Upon dephosphorylation by calcineurin (Cn), Nfat enters the nucleus and associates with binding partners. Nuclear entry is counteracted by a number of kinases including GSK-3, CK-1, DYRK1, and DYRK2 and calcineurin inhibitors CsA and FK506. This study demonstrates that Nfatc2 interacts with Ap-2δ to synergistically regulate target genes. *Atm*, *Egr3*, and *Mtss1* were identified as new target genes negatively regulated by both transcription factors.

4.3. Outlook

The function of transcription factor Ap-2δ is only poorly understood. In an effort to elucidate the role of Ap-2δ, the *Tcfap2d* gene was inactivated in mice. Knockout of *Tcfap2d* resulted in loss of the colliculus inferior, the principal nucleus for auditory input. Thus, Ap-2δ null mice serve as a model system to study hearing. First evidence from electrophysiological recordings suggest that Ap-2δ-deficient mice are able to respond to sound but show delayed learning behavior. Therefore, Ap-2δ expression in the ear and hearing ability of Ap-2δ mutant mice should be analyzed in depth. Experiments such as electrophysiological recordings as well as tracing studies have to be performed in order to analyze how auditory information reaches the neocortex in these animals. Emphasis should be put on more complex processing tasks involving learning and memory such as auditory discrimination learning tests.

In this context, involvement of regulation of *Egr3* transcription by Ap-2δ and Nfatc2 should also be taken into account. Since both Egr3 and Nfatc2 have been reported to play important roles during learning and memory processes, the contribution of these two factors to the delayed learning process in Ap-2δ mutant mice should be considered.

Another interesting approach would be the investigation of Ap-2δ in the diencephalon. Expression analysis revealed that the main expression locus of Ap-2δ is the posterior midbrain. Nevertheless, the transcription factor is also expressed in the diencephalon, possibly the medial geniculate body (MGB), at moderate levels. As described before, the MGB receives input from the inferior colliculus and sends projections to the auditory cortex. It would therefore be attractive to study thalamocortical connections in Ap-2δ knockout mice using tracing experiments.

The interaction and regulation of target genes by Ap-2δ and Nfatc2 were demonstrated in this study. To gain further insights into the mode of interaction between these two transcription factors, the influence of interaction can be investigated using luciferase assays on co-transfected cells. With the help of these assays, the impact of Ap-2δ or Nfatc2 to increase the regulatory potential of its interacting partner can be elucidated. Furthermore, other isoforms of Ap-2 and Nfat proteins can be tested for their ability to interact. This might determine whether Ap-2 proteins are general binding partners for Nfat proteins or whether Ap-2δ and Nfatc2 interact specifically. In this context, mutants of both proteins might identify the exact interaction domain.

To identify other target genes synergistically activated or repressed by Ap-2δ and Nfatc2, a microarray approach would be useful. The microarray could be performed with RNA from cells overexpressing Ap-2δ and Nfatc2 or alternatively, with RNA depleted of both transcription factors by a siRNA approach.

To further understand the regulatory mechanism exerted by Ap-2δ and Nfatc2, the signaling cascade elicited after repression of the here identified target genes could be investigated. For example, Atm is repsonsible for the activation of p53, MDM2 and Chk2. Therefore, the phosphorylation states of Atm, p53 and other downstream targets like p21 should be analyzed in Ap-2δ-/- mice. Moreover, Atm-deficient NSCs showed impaired proliferation due to disrupted Akt and Erk1/2 pathways and enhanced p38 MAPK signaling (Kim and Wong, 2009). It would be interesting to find out whether these pathways are also affected in cells with reduced *Atm* transcript levels mediated by Ap-2δ and Nfatc2.

5. Literature

Amasaki, Y., Adachi, S., Ishida, Y., Iwata, M., Arai, N., Arai, K., Miyatake, S., 2002. A constitutively nuclear form of NFATx shows efficient transactivation activity and induces differentiation of CD4(+)CD8(+) T cells. J Biol Chem 277, 25640-25648.

Bakkenist, C. J., Kastan, M. B., 2003. DNA damage activates ATM through intermolecular autophosphorylation and dimer dissociation. Nature 421, 499-506.

Bamforth, S. D., Braganca, J., Eloranta, J. J., Murdoch, J. N., Marques, F. I., Kranc, K. R., Farza, H., Henderson, D. J., Hurst, H. C., Bhattacharya, S., 2001. Cardiac malformations, adrenal agenesis, neural crest defects and exencephaly in mice lacking Cited2, a new Tfap2 co-activator. Nat Genet 29, 469-474.

Bamforth, S. D., Braganca, J., Farthing, C. R., Schneider, J. E., Broadbent, C., Michell, A. C., Clarke, K., Neubauer, S., Norris, D., Brown, N. A., Anderson, R. H., Bhattacharya, S., 2004. Cited2 controls left-right patterning and heart development through a Nodal-Pitx2c pathway. Nat Genet 36, 1189-1196.

Batsche, E., Muchardt, C., Behrens, J., Hurst, H. C., Cremisi, C., 1998a. RB and c-Myc activate expression of the E-cadherin gene in epithelial cells through interaction with transcription factor AP-2. Mol Cell Biol 18, 3647-3658.

Batsche, E., Muchardt, C., Behrens, J., Hurst, H. C., Cremisi, C., 1998b. RB and c-Myc activate expression of the E-cadherin gene in epithelial cells through interaction with transcription factor AP-2. Mol Cell Biol 18, 3647-3658.

Bauer, R., Imhof, A., Pscherer, A., Kopp, H., Moser, M., Seegers, S., Kerscher, M., Tainsky, M. A., Hofstaedter, F., Buettner, R., 1994. The genomic structure of the human AP-2 transcription factor. Nucleic Acids Res 22, 1413-1420.

Beals, C. R., Clipstone, N. A., Ho, S. N., Crabtree, G. R., 1997. Nuclear localization of NF-ATc by a calcineurin-dependent, cyclosporin-sensitive intramolecular interaction. Genes Dev 11, 824-834.

Beier, U. H., Gorogh, T., 2005. Implications of galactocerebrosidase and galactosylcerebroside metabolism in cancer cells. Int J Cancer 115, 6-10.

Benedito, A. B., Lehtinen, M., Massol, R., Lopes, U. G., Kirchhausen, T., Rao, A., Bonni, A., 2005. The transcription factor NFAT3 mediates neuronal survival. J Biol Chem 280, 2818-2825.

Bosher, J. M., Totty, N. F., Hsuan, J. J., Williams, T., Hurst, H. C., 1996. A family of AP-2 proteins regulates c-erbB-2 expression in mammary carcinoma. Oncogene 13, 1701-1707.

Braganca, J., Eloranta, J. J., Bamforth, S. D., Ibbitt, J. C., Hurst, H. C., Bhattacharya, S., 2003. Physical and functional interactions among AP-2 transcription factors, p300/CREB-binding protein, and CITED2. J Biol Chem 278, 16021-16029.

Braganca, J., Swingler, T., Marques, F. I., Jones, T., Eloranta, J. J., Hurst, H. C., Shioda, T., Bhattacharya, S., 2002. Human CREB-binding protein/p300-interacting transactivator with ED-rich tail (CITED) 4, a new member of the CITED family, functions as a co-activator for transcription factor AP-2. J Biol Chem 277, 8559-8565.

Bramblett, D. E., Copeland, N. G., Jenkins, N. A., Tsai, M. J., 2002. BHLHB4 is a bHLH transcriptional regulator in pancreas and brain that marks the dimesencephalic boundary. Genomics 79, 402-412.

Bramblett, D. E., Pennesi, M. E., Wu, S. M., Tsai, M. J., 2004. The transcription factor Bhlhb4 is required for rod bipolar cell maturation. Neuron 43, 779-793.

Carlessi, L., De Filippis, L., Lecis, D., Vescovi, A., Delia, D., 2009. DNA-damage response, survival and differentiation in vitro of a human neural stem cell line in relation to ATM expression. Cell Death Differ 16, 795-806.

Casseday, J. H., Kobler, J. B., Isbey, S. F., Covey, E., 1989. Central acoustic tract in an echolocating bat: an extralemniscal auditory pathway to the thalamus. J Comp Neurol 287, 247-259.

Chazaud, C., Oulad-Abdelghani, M., Bouillet, P., Decimo, D., Chambon, P., Dolle, P., 1996. AP-2.2, a novel gene related to AP-2, is expressed in the forebrain, limbs and face during mouse embryogenesis. Mech Dev 54, 83-94.

Chen, T. T., Wu, R. L., Castro-Munozledo, F., Sun, T. T., 1997. Regulation of K3 keratin gene transcription by Sp1 and AP-2 in differentiating rabbit corneal epithelial cells. Mol Cell Biol 17, 3056-3064.

Clipstone, N. A., Crabtree, G. R., 1992. Identification of calcineurin as a key signalling enzyme in T-lymphocyte activation. Nature 357, 695-697.

Clough, R. L., Sud, R., Davis-Silberman, N., Hertzano, R., Avraham, K. B., Holley, M., Dawson, S. J., 2004. Brn-3c (POU4F3) regulates BDNF and NT-3 promoter activity. Biochem Biophys Res Commun 324, 372-381.

Collin, R. W., Chellappa, R., Pauw, R. J., Vriend, G., Oostrik, J., van Drunen, W., Huygen, P. L., Admiraal, R., Hoefsloot, L. H., Cremers, F. P., Xiang, M., Cremers, C. W., Kremer, H., 2008. Missense mutations in POU4F3 cause autosomal dominant hearing impairment DFNA15 and affect subcellular localization and DNA binding. Hum Mutat 29, 545-554.

Courtois, S. J., Lafontaine, D. A., Lemaigre, F. P., Durviaux, S. M., Rousseau, G. G., 1990. Nuclear factor-I and activator protein-2 bind in a mutually exclusive way to overlapping promoter sequences and trans-activate the human growth hormone gene. Nucleic Acids Res 18, 57-64.

Crabtree, G. R., Olson, E. N., 2002. NFAT signaling: choreographing the social lives of cells. Cell 109 Suppl, S67-79.

de la Fuente, V., Freudenthal, R., Romano, A., Reconsolidation or extinction: transcription factor switch in the determination of memory course after retrieval. J Neurosci 31, 5562-5573.

de la Pompa, J. L., Timmerman, L. A., Takimoto, H., Yoshida, H., Elia, A. J., Samper, E., Potter, J., Wakeham, A., Marengere, L., Langille, B. L., Crabtree, G. R., Mak, T. W., 1998. Role of the NF-ATc transcription factor in morphogenesis of cardiac valves and septum. Nature 392, 182-186.

Decary, S., Decesse, J. T., Ogryzko, V., Reed, J. C., Naguibneva, I., Harel-Bellan, A., Cremisi, C. E., 2002. The retinoblastoma protein binds the promoter of the survival gene bcl-2 and regulates its transcription in epithelial cells through transcription factor AP-2. Mol Cell Biol 22, 7877-7888.

Ding, X., Luo, C., Zhou, J., Zhong, Y., Hu, X., Zhou, F., Ren, K., Gan, L., He, A., Zhu, J., Gao, X., Zhang, J., 2009. The interaction of KCTD1 with transcription factor AP-2alpha inhibits its transactivation. J Cell Biochem 106, 285-295.

Eckert, D., Buhl, S., Weber, S., Jager, R., Schorle, H., 2005. The AP-2 family of transcription factors. Genome Biol 6, 246.

Elliott, J. L., 2001. Cytokine upregulation in a murine model of familial amyotrophic lateral sclerosis. Brain Res Mol Brain Res 95, 172-178.

Eloranta, J. J., Hurst, H. C., 2002. Transcription factor AP-2 interacts with the SUMO-conjugating enzyme UBC9 and is sumolated in vivo. J Biol Chem 277, 30798-30804.

Erkman, L., McEvilly, R. J., Luo, L., Ryan, A. K., Hooshmand, F., O'Connell, S. M., Keithley, E. M., Rapaport, D. H., Ryan, A. F., Rosenfeld, M. G., 1996. Role of transcription factors Brn-3.1 and Brn-3.2 in auditory and visual system development. Nature 381, 603-606.

Feng, W., Simoes-de-Souza, F., Finger, T. E., Restrepo, D., Williams, T., 2009. Disorganized olfactory bulb lamination in mice deficient for transcription factor AP-2epsilon. Mol Cell Neurosci 42, 161-171.

Feng, W., Williams, T., 2003. Cloning and characterization of the mouse AP-2 epsilon gene: a novel family member expressed in the developing olfactory bulb. Mol Cell Neurosci 24, 460-475.

Friedland, D. R., Popper, P., Eernisse, R., Cioffi, J. A., 2006. Differentially expressed genes in the rat cochlear nucleus. Neuroscience 142, 753-768.

Fuentes-Santamaria, V., Alvarado, J. C., Brunso-Bechtold, J. K., Henkel, C. K., 2003. Upregulation of calretinin immunostaining in the ferret inferior colliculus after cochlear ablation. J Comp Neurol 460, 585-596.

Gage, P. J., Suh, H., Camper, S. A., 1999. The bicoid-related Pitx gene family in development. Mamm Genome 10, 197-200.

Garcia, M. A., Campillos, M., Marina, A., Valdivieso, F., Vazquez, J., 1999. Transcription factor AP-2 activity is modulated by protein kinase A-mediated phosphorylation. FEBS Lett 444, 27-31.

Gaubatz, S., Imhof, A., Dosch, R., Werner, O., Mitchell, P., Buettner, R., Eilers, M., 1995. Transcriptional activation by Myc is under negative control by the transcription factor AP-2. Embo J 14, 1508-1519.

Gee, J. M., Robertson, J. F., Ellis, I. O., Nicholson, R. I., Hurst, H. C., 1999. Immunohistochemical analysis reveals a tumour suppressor-like role for the transcription factor AP-2 in invasive breast cancer. J Pathol 189, 514-520.

Ghezzi, P., Bernardini, R., Giuffrida, R., Bellomo, M., Manzoni, C., Comoletti, D., Di Santo, E., Benigni, F., Mennini, T., 1998. Tumor necrosis factor is increased in the spinal cord of an animal model of motor neuron degeneration. Eur Cytokine Netw 9, 139-144.

Glassmann, A., Molly, S., Surchev, L., Nazwar, T. A., Holst, M., Hartmann, W., Baader, S. L., Oberdick, J., Pietsch, T., Schilling, K., 2007. Developmental expression and differentiation-related neuron-specific splicing of metastasis suppressor 1 (Mtss1) in normal and transformed cerebellar cells. BMC Dev Biol 7, 111.

Golan, H., Levav, T., Mendelsohn, A., Huleihel, M., 2004. Involvement of tumor necrosis factor alpha in hippocampal development and function. Cereb Cortex 14, 97-105.

Graef, I. A., Chen, F., Crabtree, G. R., 2001. NFAT signaling in vertebrate development. Curr Opin Genet Dev 11, 505-512.

Graef, I. A., Mermelstein, P. G., Stankunas, K., Neilson, J. R., Deisseroth, K., Tsien, R. W., Crabtree, G. R., 1999. L-type calcium channels and GSK-3 regulate the activity of NF-ATc4 in hippocampal neurons. Nature 401, 703-708.

Groth, R. D., Coicou, L. G., Mermelstein, P. G., Seybold, V. S., 2007. Neurotrophin activation of NFAT-dependent transcription contributes to the regulation of pro-nociceptive genes. J Neurochem 102, 1162-1174.

Groth, R. D., Mermelstein, P. G., 2003. Brain-derived neurotrophic factor activation of NFAT (nuclear factor of activated T-cells)-dependent transcription: a role for the transcription factor NFATc4 in neurotrophin-mediated gene expression. J Neurosci 23, 8125-8134.

Gurung, B., Fritzsch, B., 2004. Time course of embryonic midbrain and thalamic auditory connection development in mice as revealed by carbocyanine dye tracing. J Comp Neurol 479, 309-327.

Gwack, Y., Sharma, S., Nardone, J., Tanasa, B., Iuga, A., Srikanth, S., Okamura, H., Bolton, D., Feske, S., Hogan, P. G., Rao, A., 2006. A genome-wide Drosophila RNAi screen identifies DYRK-family kinases as regulators of NFAT. Nature 441, 646-650.

Harbour, J. W., Dean, D. C., 2000. Rb function in cell-cycle regulation and apoptosis. Nat Cell Biol 2, E65-67.

Hebert, J. M., McConnell, S. K., 2000. Targeting of cre to the Foxg1 (BF-1) locus mediates loxP recombination in the telencephalon and other developing head structures. Dev Biol 222, 296-306.

Hertzano, R., Dror, A. A., Montcouquiol, M., Ahmed, Z. M., Ellsworth, B., Camper, S., Friedman, T. B., Kelley, M. W., Avraham, K. B., 2007. Lhx3, a LIM domain transcription factor, is regulated by Pou4f3 in the auditory but not in the vestibular system. Eur J Neurosci 25, 999-1005.

Hesse, K., Vaupel, K., Kurt, S., Buettner, R., Kirfel, J., Moser, M., 2011. Ap-2δ is a crucial transcriptional regulator of the posterior midbrain. PlosOne

Hogan, P. G., Chen, L., Nardone, J., Rao, A., 2003. Transcriptional regulation by calcium, calcineurin, and NFAT. Genes Dev 17, 2205-2232.

Huh, S., Hatini, V., Marcus, R. C., Li, S. C., Lai, E., 1999. Dorsal-ventral patterning defects in the eye of BF-1-deficient mice associated with a restricted loss of shh expression. Dev Biol 211, 53-63.

Imagawa, M., Chiu, R., Karin, M., 1987. Transcription factor AP-2 mediates induction by two different signal-transduction pathways: protein kinase C and cAMP. Cell 51, 251-260.

Imhof, A., Schuierer, M., Werner, O., Moser, M., Roth, C., Bauer, R., Buettner, R., 1999. Transcriptional regulation of the AP-2alpha promoter by BTEB-1 and AP-2rep, a novel wt-1/egr-related zinc finger repressor. Mol Cell Biol 19, 194-204.

Jain, J., McCaffrey, P. G., Miner, Z., Kerppola, T. K., Lambert, J. N., Verdine, G. L., Curran, T., Rao, A., 1993. The T-cell transcription factor NFATp is a substrate for calcineurin and interacts with Fos and Jun. Nature 365, 352-355.

Jung, H., Miller, R. J., 2008. Activation of the nuclear factor of activated T-cells (NFAT) mediates upregulation of CCR2 chemokine receptors in dorsal root ganglion (DRG) neurons: a possible mechanism for activity-dependent transcription in DRG neurons in association with neuropathic pain. Mol Cell Neurosci 37, 170-177.

Karjalainen, J. M., Kellokoski, J. K., Eskelinen, M. J., Alhava, E. M., Kosma, V. M., 1998. Downregulation of transcription factor AP-2 predicts poor survival in stage I cutaneous malignant melanoma. J Clin Oncol 16, 3584-3591.

Kastan, M. B., Lim, D. S., 2000. The many substrates and functions of ATM. Nat Rev Mol Cell Biol 1, 179-186.

Kastan, M. B., Zhan, Q., el-Deiry, W. S., Carrier, F., Jacks, T., Walsh, W. V., Plunkett, B. S., Vogelstein, B., Fornace, A. J., Jr., 1992. A mammalian cell cycle checkpoint pathway utilizing p53 and GADD45 is defective in ataxia-telangiectasia. Cell 71, 587-597.

Kiani, A., Rao, A., Aramburu, J., 2000. Manipulating immune responses with immunosuppressive agents that target NFAT. Immunity 12, 359-372.

Kim, J., Wong, P. K., 2009. Loss of ATM impairs proliferation of neural stem cells through oxidative stress-mediated p38 MAPK signaling. Stem Cells 27, 1987-1998.

King, C. R., Kraus, M. H., Aaronson, S. A., 1985. Amplification of a novel v-erbB-related gene in a human mammary carcinoma. Science 229, 974-976.

King, C. R., Swain, S. M., Porter, L., Steinberg, S. M., Lippman, M. E., Gelmann, E. P., 1989. Heterogeneous expression of erbB-2 messenger RNA in human breast cancer. Cancer Res 49, 4185-4191.

Kobler, J. B., Isbey, S. F., Casseday, J. H., 1987. Auditory pathways to the frontal cortex of the mustache bat, Pteronotus parnellii. Science 236, 824-826.

Kumbrink, J., Kirsch, K. H., Johnson, J. P., EGR1, EGR2, and EGR3 activate the expression of their coregulator NAB2 establishing a negative feedback loop in cells of neuroectodermal and epithelial origin. J Cell Biochem 111, 207-217.

Lavin, M. F., Shiloh, Y., 1996. Ataxia-telangiectasia: a multifaceted genetic disorder associated with defective signal transduction. Curr Opin Immunol 8, 459-464.

Lee, M., Park, J., 2006. Regulation of NFAT activation: a potential therapeutic target for immunosuppression. Mol Cells 22, 1-7.

Lee, Y. G., Macoska, J. A., Korenchuk, S., Pienta, K. J., 2002. MIM, a potential metastasis suppressor gene in bladder cancer. Neoplasia 4, 291-294.

Li, L., Carter, J., Gao, X., Whitehead, J., Tourtellotte, W. G., 2005. The neuroplasticity-associated arc gene is a direct transcriptional target of early growth response (Egr) transcription factors. Mol Cell Biol 25, 10286-10300.

Li, L., Yun, S. H., Keblesh, J., Trommer, B. L., Xiong, H., Radulovic, J., Tourtellotte, W. G., 2007. Egr3, a synaptic activity regulated transcription factor that is essential for learning and memory. Mol Cell Neurosci 35, 76-88.

Li, M., Naidu, P., Yu, Y., Berger, N. A., Kannan, P., 2004. Dual regulation of AP-2alpha transcriptional activation by poly(ADP-ribose) polymerase-1. Biochem J 382, 323-329.

Li, M., Wang, Y., Hung, M. C., Kannan, P., 2006. Inefficient proteasomal-degradation pathway stabilizes AP-2alpha and activates HER-2/neu gene in breast cancer. Int J Cancer 118, 802-811.

Lin, X., Shah, S., Bulleit, R. F., 1996. The expression of MEF2 genes is implicated in CNS neuronal differentiation. Brain Res Mol Brain Res 42, 307-316.

Lipinski, M. M., Jacks, T., 1999. The retinoblastoma gene family in differentiation and development. Oncogene 18, 7873-7882.

Liu, J., Farmer, J. D., Jr., Lane, W. S., Friedman, J., Weissman, I., Schreiber, S. L., 1991. Calcineurin is a common target of cyclophilin-cyclosporin A and FKBP-FK506 complexes. Cell 66, 807-815.

Liu, W., Komiya, Y., Mezzacappa, C., Khadka, D. K., Runnels, L., Habas, R., MIM regulates vertebrate neural tube closure. Development 138, 2035-2047.

Loberg, R. D., Neeley, C. K., Adam-Day, L. L., Fridman, Y., St John, L. N., Nixdorf, S., Jackson, P., Kalikin, L. M., Pienta, K. J., 2005. Differential expression analysis of MIM (MTSS1) splice variants and a functional role of MIM in prostate cancer cell biology. Int J Oncol 26, 1699-1705.

Lopez-Rodriguez, C., Aramburu, J., Rakeman, A. S., Rao, A., 1999. NFAT5, a constitutively nuclear NFAT protein that does not cooperate with Fos and Jun. Proc Natl Acad Sci U S A 96, 7214-7219.

Macian, F., 2005. NFAT proteins: key regulators of T-cell development and function. Nat Rev Immunol 5, 472-484.

Mages, H. W., Baag, R., Steiner, B., Kroczek, R. A., 1998. Utilization of an NF-ATp binding promoter element for EGR3 expression in T cells but not fibroblasts

provides a molecular model for the lymphoid cell-specific effect of cyclosporin A. Mol Cell Biol 18, 7157-7165.

Malsy, M.; dissertation 2009. Charakterisierung neuer Interaktionspartner der NFAT-vermittelten Transkription im Pankreaskarzinom. Philipps-Universität Marburg.

Maric, D., Fiorio Pla, A., Chang, Y. H., Barker, J. L., 2007. Self-renewing and differentiating properties of cortical neural stem cells are selectively regulated by basic fibroblast growth factor (FGF) signaling via specific FGF receptors. J Neurosci 27, 1836-1852.

McEvilly, R. J., Erkman, L., Luo, L., Sawchenko, P. E., Ryan, A. F., Rosenfeld, M. G., 1996. Requirement for Brn-3.0 in differentiation and survival of sensory and motor neurons. Nature 384, 574-577.

McPherson, L. A., Loktev, A. V., Weigel, R. J., 2002. Tumor suppressor activity of AP2alpha mediated through a direct interaction with p53. J Biol Chem 277, 45028-45033.

Mercurio, F., Karin, M., 1989. Transcription factors AP-3 and AP-2 interact with the SV40 enhancer in a mutually exclusive manner. Embo J 8, 1455-1460.

Mitchell, P. J., Timmons, P. M., Hebert, J. M., Rigby, P. W., Tjian, R., 1991. Transcription factor AP-2 is expressed in neural crest cell lineages during mouse embryogenesis. Genes Dev 5, 105-119.

Mitchell, P. J., Wang, C., Tjian, R., 1987. Positive and negative regulation of transcription in vitro: enhancer-binding protein AP-2 is inhibited by SV40 T antigen. Cell 50, 847-861.

Mohibullah, N., Donner, A., Ippolito, J. A., Williams, T., 1999. SELEX and missing phosphate contact analyses reveal flexibility within the AP-2[alpha] protein: DNA binding complex. Nucleic Acids Res 27, 2760-2769.

Morgan, A. J., Jacob, R., 1994. Ionomycin enhances Ca2+ influx by stimulating store-regulated cation entry and not by a direct action at the plasma membrane. Biochem J 300 (Pt 3), 665-672.

Moser, M., Imhof, A., Pscherer, A., Bauer, R., Amselgruber, W., Sinowatz, F., Hofstadter, F., Schule, R., Buettner, R., 1995. Cloning and characterization of a second AP-2 transcription factor: AP-2 beta. Development 121, 2779-2788.

Moser, M., Pscherer, A., Roth, C., Becker, J., Mucher, G., Zerres, K., Dixkens, C., Weis, J., Guay-Woodford, L., Buettner, R., Fassler, R., 1997. Enhanced apoptotic cell death of renal epithelial cells in mice lacking transcription factor AP-2beta. Genes Dev 11, 1938-1948.

Muller, S., Hoege, C., Pyrowolakis, G., Jentsch, S., 2001. SUMO, ubiquitin's mysterious cousin. Nat Rev Mol Cell Biol 2, 202-210.

Murphy, D. B., Wiese, S., Burfeind, P., Schmundt, D., Mattei, M. G., Schulz-Schaeffer, W., Thies, U., 1994. Human brain factor 1, a new member of the fork head gene family. Genomics 21, 551-557.

Nayak, A., Glockner-Pagel, J., Vaeth, M., Schumann, J. E., Buttmann, M., Bopp, T., Schmitt, E., Serfling, E., Berberich-Siebelt, F., 2009. Sumoylation of the transcription factor NFATc1 leads to its subnuclear relocalization and interleukin-2 repression by histone deacetylase. J Biol Chem 284, 10935-10946.

Neal, J. W., Clipstone, N. A., 2001. Glycogen synthase kinase-3 inhibits the DNA binding activity of NFATc. J Biol Chem 276, 3666-3673.

Nyormoi, O., Wang, Z., Doan, D., Ruiz, M., McConkey, D., Bar-Eli, M., 2001. Transcription factor AP-2alpha is preferentially cleaved by caspase 6 and degraded by proteasome during tumor necrosis factor alpha-induced apoptosis in breast cancer cells. Mol Cell Biol 21, 4856-4867.

O'Donovan, K. J., Baraban, J. M., 1999. Major Egr3 isoforms are generated via alternate translation start sites and differ in their abilities to activate transcription. Mol Cell Biol 19, 4711-4718.

Okamura, H., Aramburu, J., Garcia-Rodriguez, C., Viola, J. P., Raghavan, A., Tahiliani, M., Zhang, X., Qin, J., Hogan, P. G., Rao, A., 2000. Concerted dephosphorylation of the transcription factor NFAT1 induces a conformational switch that regulates transcriptional activity. Mol Cell 6, 539-550.

Okamura, H., Garcia-Rodriguez, C., Martinson, H., Qin, J., Virshup, D. M., Rao, A., 2004. A conserved docking motif for CK1 binding controls the nuclear localization of NFAT1. Mol Cell Biol 24, 4184-4195.

Oukka, M., Ho, I. C., de la Brousse, F. C., Hoey, T., Grusby, M. J., Glimcher, L. H., 1998. The transcription factor NFAT4 is involved in the generation and survival of T cells. Immunity 9, 295-304.

Oulad-Abdelghani, M., Bouillet, P., Chazaud, C., Dolle, P., Chambon, P., 1996. AP-2.2: a novel AP-2-related transcription factor induced by retinoic acid during differentiation of P19 embryonal carcinoma cells. Exp Cell Res 225, 338-347.

Park, K., Kim, K. H., 1993. The site of cAMP action in the insulin induction of gene expression of acetyl-CoA carboxylase is AP-2. J Biol Chem 268, 17811-17819.

Pauley, S., Lai, E., Fritzsch, B., 2006. Foxg1 is required for morphogenesis and histogenesis of the mammalian inner ear. Dev Dyn 235, 2470-2482.

Peng, S. L., Gerth, A. J., Ranger, A. M., Glimcher, L. H., 2001. NFATc1 and NFATc2 together control both T and B cell activation and differentiation. Immunity 14, 13-20.

Pfisterer, P., Ehlermann, J., Hegen, M., Schorle, H., 2002. A subtractive gene expression screen suggests a role of transcription factor AP-2 alpha in control of proliferation and differentiation. J Biol Chem 277, 6637-6644.

Piechaczyk, M., Blanchard, J. M., 1994. c-fos proto-oncogene regulation and function. Crit Rev Oncol Hematol 17, 93-131.

Pirvola, U., Ylikoski, J., Palgi, J., Lehtonen, E., Arumae, U., Saarma, M., 1992. Brain-derived neurotrophic factor and neurotrophin 3 mRNAs in the peripheral target fields of developing inner ear ganglia. Proc Natl Acad Sci U S A 89, 9915-9919.

Platenik, J., Kuramoto, N., Yoneda, Y., 2000. Molecular mechanisms associated with long-term consolidation of the NMDA signals. Life Sci 67, 335-364.

Ranger, A. M., Oukka, M., Rengarajan, J., Glimcher, L. H., 1998. Inhibitory function of two NFAT family members in lymphoid homeostasis and Th2 development. Immunity 9, 627-635.

Rao, A., Luo, C., Hogan, P. G., 1997. Transcription factors of the NFAT family: regulation and function. Annu Rev Immunol 15, 707-747.

Ren, Y., Liao, W. S., 2001. Transcription factor AP-2 functions as a repressor that contributes to the liver-specific expression of serum amyloid A1 gene. J Biol Chem 276, 17770-17778.

Ropponen, K. M., Kellokoski, J. K., Pirinen, R. T., Moisio, K. I., Eskelinen, M. J., Alhava, E. M., Kosma, V. M., 2001. Expression of transcription factor AP-2 in colorectal adenomas and adenocarcinomas; comparison of immunohistochemistry and in situ hybridisation. J Clin Pathol 54, 533-538.

Rotman, G., Shiloh, Y., 1997a. Ataxia-telangiectasia: is ATM a sensor of oxidative damage and stress? Bioessays 19, 911-917.

Rotman, G., Shiloh, Y., 1997b. The ATM gene and protein: possible roles in genome surveillance, checkpoint controls and cellular defence against oxidative stress. Cancer Surv 29, 285-304.

Santini, M. P., Talora, C., Seki, T., Bolgan, L., Dotto, G. P., 2001. Cross talk among calcineurin, Sp1/Sp3, and NFAT in control of p21(WAF1/CIP1) expression in keratinocyte differentiation. Proc Natl Acad Sci U S A 98, 9575-9580.

Satoda, M., Zhao, F., Diaz, G. A., Burn, J., Goodship, J., Davidson, H. R., Pierpont, M. E., Gelb, B. D., 2000. Mutations in TFAP2B cause Char syndrome, a familial form of patent ductus arteriosus. Nat Genet 25, 42-46.

Schorle, H., Meier, P., Buchert, M., Jaenisch, R., Mitchell, P. J., 1996. Transcription factor AP-2 essential for cranial closure and craniofacial development. Nature 381, 235-238.

Serfling, E., Berberich-Siebelt, F., Avots, A., Chuvpilo, S., Klein-Hessling, S., Jha, M. K., Kondo, E., Pagel, P., Schulze-Luehrmann, J., Palmetshofer, A., 2004. NFAT and NF-kappaB factors-the distant relatives. Int J Biochem Cell Biol 36, 1166-1170.

Sun, L., Huang, S., Wu, Q., Gu, S., Fu, X., Yu, K., Lu, F., Ji, C., Feng, C., Sun, R., Xie, Y., Mao, Y., 2007. Identification of genes differentially regulated by transcription factor, AP-2delta. Front Biosci 12, 1699-1706.

Takeuchi, S., Imafuku, I., Waragai, M., Roth, C., Kanazawa, I., Buettner, R., Mouradian, M. M., Okazawa, H., 1999. AP-2beta represses D(1A) dopamine receptor gene transcription in neuro2a cells. Brain Res Mol Brain Res 74, 208-216.

Tan, C. C., Sindhu, K. V., Li, S., Nishio, H., Stoller, J. Z., Oishi, K., Puttreddy, S., Lee, T. J., Epstein, J. A., Walsh, M. J., Gelb, B. D., 2008. Transcription factor Ap2delta associates with Ash2l and ALR, a trithorax family histone methyltransferase, to activate Hoxc8 transcription. Proc Natl Acad Sci U S A 105, 7472-7477.

Tan, C. C., Walsh, M. J., Gelb, B. D., 2009. Fgfr3 is a transcriptional target of Ap2delta and Ash2l-containing histone methyltransferase complexes. PLoS One 4, e8535.

Terui, Y., Saad, N., Jia, S., McKeon, F., Yuan, J., 2004. Dual role of sumoylation in the nuclear localization and transcriptional activation of NFAT1. J Biol Chem 279, 28257-28265.

Thompson, D., Duedal, S., Kirner, J., McGuffog, L., Last, J., Reiman, A., Byrd, P., Taylor, M., Easton, D. F., 2005. Cancer risks and mortality in heterozygous ATM mutation carriers. J Natl Cancer Inst 97, 813-822.

Utikal, J., Gratchev, A., Muller-Molinet, I., Oerther, S., Kzhyshkowska, J., Arens, N., Grobholz, R., Kannookadan, S., Goerdt, S., 2006. The expression of metastasis suppressor MIM/MTSS1 is regulated by DNA methylation. Int J Cancer 119, 2287-2293.

Vernimmen, D., Begon, D., Salvador, C., Gofflot, S., Grooteclaes, M., Winkler, R., 2003. Identification of HTF (HER2 transcription factor) as an AP-2 (activator protein-2) transcription factor and contribution of the HTF binding site to ERBB2 gene overexpression. Biochem J 370, 323-329.

Vihma, H., Pruunsild, P., Timmusk, T., 2008. Alternative splicing and expression of human and mouse NFAT genes. Genomics 92, 279-291.

Viola, J. P., Carvalho, L. D., Fonseca, B. P., Teixeira, L. K., 2005. NFAT transcription factors: from cell cycle to tumor development. Braz J Med Biol Res 38, 335-344.

Wajapeyee, N., Britto, R., Ravishankar, H. M., Somasundaram, K., 2006. Apoptosis induction by activator protein 2alpha involves transcriptional repression of Bcl-2. J Biol Chem 281, 16207-16219.

Wang, H. V., Vaupel, K., Buettner, R., Bosserhoff, A. K., Moser, M., 2004. Identification and embryonic expression of a new AP-2 transcription factor, AP-2 epsilon. Dev Dyn 231, 128-135.

Wang, J. Y., 1997. Retinoblastoma protein in growth suppression and death protection. Curr Opin Genet Dev 7, 39-45.

Wankhade, S., Yu, Y., Weinberg, J., Tainsky, M. A., Kannan, P., 2000. Characterization of the activation domains of AP-2 family transcription factors. J Biol Chem 275, 29701-29708.

Watters, D. J., 2003. Oxidative stress in ataxia telangiectasia. Redox Rep 8, 23-29.

Weber, S., Eckert, D., Nettersheim, D., Gillis, A. J., Schafer, S., Kuckenberg, P., Ehlermann, J., Werling, U., Biermann, K., Looijenga, L. H., Schorle, H., Critical function of AP-2 gamma/TCFAP2C in mouse embryonic germ cell maintenance. Biol Reprod 82, 214-223.

Werling, U., Schorle, H., 2002. Transcription factor gene AP-2 gamma essential for early murine development. Mol Cell Biol 22, 3149-3156.

Williams, T., Admon, A., Luscher, B., Tjian, R., 1988. Cloning and expression of AP-2, a cell-type-specific transcription factor that activates inducible enhancer elements. Genes Dev 2, 1557-1569.

Williams, T., Tjian, R., 1991a. Analysis of the DNA-binding and activation properties of the human transcription factor AP-2. Genes Dev 5, 670-682.

Williams, T., Tjian, R., 1991b. Characterization of a dimerization motif in AP-2 and its function in heterologous DNA-binding proteins. Science 251, 1067-1071.

Wu, F., Lee, A. S., 2001. YY1 as a regulator of replication-dependent hamster histone H3.2 promoter and an interactive partner of AP-2. J Biol Chem 276, 28-34.

Xanthoudakis, S., Viola, J. P., Shaw, K. T., Luo, C., Wallace, J. D., Bozza, P. T., Luk, D. C., Curran, T., Rao, A., 1996. An enhanced immune response in mice lacking the transcription factor NFAT1. Science 272, 892-895.

Xiang, M., Gan, L., Li, D., Zhou, L., Chen, Z. Y., Wagner, D., O'Malley, B. W., Jr., Klein, W., Nathans, J., 1997. Role of the Brn-3 family of POU-domain genes in the development of the auditory/vestibular, somatosensory, and visual systems. Cold Spring Harb Symp Quant Biol 62, 325-336.

Xiang, M., Gao, W. Q., Hasson, T., Shin, J. J., 1998. Requirement for Brn-3c in maturation and survival, but not in fate determination of inner ear hair cells. Development 125, 3935-3946.

Xiang, M., Maklad, A., Pirvola, U., Fritzsch, B., 2003. Brn3c null mutant mice show long-term, incomplete retention of some afferent inner ear innervation. BMC Neurosci 4, 2.

Xiang, M., Zhou, L., Macke, J. P., Yoshioka, T., Hendry, S. H., Eddy, R. L., Shows, T. B., Nathans, J., 1995. The Brn-3 family of POU-domain factors: primary structure, binding specificity, and expression in subsets of retinal ganglion cells and somatosensory neurons. J Neurosci 15, 4762-4785.

Xiao, S., Matsui, K., Fine, A., Zhu, B., Marshak-Rothstein, A., Widom, R. L., Ju, S. T., 1999. FasL promoter activation by IL-2 through SP1 and NFAT but not Egr-2 and Egr-3. Eur J Immunol 29, 3456-3465.

Xuan, S., Baptista, C. A., Balas, G., Tao, W., Soares, V. C., Lai, E., 1995. Winged helix transcription factor BF-1 is essential for the development of the cerebral hemispheres. Neuron 14, 1141-1152.

Yoeli-Lerner, M., Yiu, G. K., Rabinovitz, I., Erhardt, P., Jauliac, S., Toker, A., 2005. Akt blocks breast cancer cell motility and invasion through the transcription factor NFAT. Mol Cell 20, 539-550.

Zettel, M. L., Frisina, R. D., Haider, S. E., O'Neill, W. E., 1997. Age-related changes in calbindin D-28k and calretinin immunoreactivity in the inferior colliculus of CBA/CaJ and C57Bl/6 mice. J Comp Neurol 386, 92-110.

Zhang, J., Hagopian-Donaldson, S., Serbedzija, G., Elsemore, J., Plehn-Dujowich, D., McMahon, A. P., Flavell, R. A., Williams, T., 1996. Neural tube, skeletal and body wall defects in mice lacking transcription factor AP-2. Nature 381, 238-241.

Zhao, F., Lufkin, T., Gelb, B. D., 2003. Expression of Tfap2d, the gene encoding the transcription factor Ap-2 delta, during mouse embryogenesis. Gene Expr Patterns 3, 213-217.

Zhao, F., Satoda, M., Licht, J. D., Hayashizaki, Y., Gelb, B. D., 2001. Cloning and characterization of a novel mouse AP-2 transcription factor, AP-2delta, with unique DNA binding and transactivation properties. J Biol Chem 276, 40755-40760.

Zhu, C. H., Huang, Y., Oberley, L. W., Domann, F. E., 2001. A family of AP-2 proteins down-regulate manganese superoxide dismutase expression. J Biol Chem 276, 14407-14413.

Zhu, J., McKeon, F., 1999. NF-AT activation requires suppression of Crm1-dependent export by calcineurin. Nature 398, 256-260.